UNIVERSITÀ DEGLI STUDI DI NAPOLI "FEDERICO II"

SCUOLA DI DOTTORATO "SCIENZE DELLA TERRA"
"Giuseppe De Lorenzo"

Dottorato in Scienze ed Ingegneria del Mare

in consorzio con
SECONDA UNIVERSITÀ DI NAPOLI
UNIVERSITÀ "PARTHENOPE" NAPOLI
in convenzione con
ISTITUTO PER L'AMBIENTE MARINO COSTIERO – C.N.R.
STAZIONE ZOOLOGICA "ANTON DOHRN"

XXIII ciclo

Tesi di Dottorato

Copepod swimming behaviour: from 3D small-scale patterns to species-specific adaptive traits

Candidato:
Giuseppe Bianco

Tutor:
Dr Maurizio Ribera d'Alcalà

Co-Tutor:
Dr Maria Grazia Mazzocchi

Il Coordinatore del Dottorato: Prof. Alberto Incoronato

ANNO 2010

To my parents

Contents

List of Figures

LIST OF FIGURES

List of Tables

LIST OF TABLES

Chapter 1

Introduction

The marine ecosystem has always attracted the attention of the human communities because of the great food reservoir and the important economical resources. A key element of marine ecosystem is the plankton, which includes primary producers (phytoplankton) and consumers (zooplankton) that interplay into complex trophic webs. Each planktonic group comprises populations of species composed of individuals that interact with one another and with the environment (Kiørboe, 2008a).

Among zooplankton, copepods represent a dominant component. They play a key role in the functioning of pelagic systems by linking phytoplankton, on which they graze, to larger consumers by which they are preyed. Copepods are food for small fish, whales, sea birds, chaetognath and medusae. Apart their key role in the marine food webs, copepods significantly contribute to the biological pump (Longhurst and Glen Harrison, 1989; Ducklow *et al.*, 2001) and the geochemical cycles in the oceans.

Copepods are small (*i.e.*, few millimetres in length (Mauchline *et al.*, 1998)), ubiquitous crustaceans that numerically dominate the zooplankton communities (Huys and Boxshall, 1991). About 2,492 species of pelagic copepods have been recorded up to now and the order Calanoida (43 families) is the most numerically abundant (Razouls *et al.*, 2005-2010). Copepods successfully colonized the whole water column in the worlds ocean, both oligotrophic and eutrophic environment (Huys and Boxshall, 1991).

Copepods have a transparent armoured exoskeleton, formed through several moults during the development of the copepod. The life cycle of a copepod begins with the egg after the sexual reproduction between adult female and male. The eggs are carried by the female in one or two sacs attached to the abdomen or freed into the water (Mauchline *et al.*, 1998). The eggs hatch into a first naupliar stage, which develops though other five stages (NI to NVI). The last moult gives rise to a copepodid juvenile which tend to resemble to the adult but with less complex structure. There are five copepodid stages before the copepod mature into one of the two adult genders. The life cycle from egg to adult can span from a week to a year or more according to species and latitudes (Peterson, 2001).

The body of an adult calanoid is composed of: (1) the head that carries the antennulae and is fused or not with the first thoracic segment, (2) the thoracic segments that possess limbs and mouth appendages used for feeding, (3) the abdomen, which together with the furca form the thorax (Boxshall and Halsey, 2004).

1.1 Perceiving and exploring the planktonic environment

Planktonic copepods live all their life-cycle and behave in a three-dimensional world, suspended in the water column. Their behavior is affected by the physical, chemical and biological properties of their surrounding environment. They present a richness of behavioral responses, closely related to the existence of a sensory system, composed by mechano- and chemo-sensor (Friedman and Strickler, 1975; Barrientos, 1980; Legier-Visser *et al.*, 1986), which responds to environmental cues (Bundy *et al.*, 1998).

The mechano-sensors are located over the copepod body and are located in antennae, hairs and setae (Viitasalo *et al.*, 1998; Mauchline *et al.*, 1998). This fluid mechanism perception plays an important role in copepod feeding, sensing, swarming, mating and predator avoidance (Jiang and Osborn, 2004). It allows the rapid detection of potential prey (Kiørboe *et al.*, 1999; Strickler and Balazsi,

2007; Jiang and Paffenhöfer, 2008), predator and mates (Buskey *et al.*, 2002; Alcaraz *et al.*, 2007; Goetze, 2008).

The chemo-sensors are involved in food and mate recognition (Doall *et al.*, 1998; Kiørboe *et al.*, 2005). Thanks to this chemosensor the copepod can detect the female trail and follow it (Yen *et al.*, 1998; Bagoien and Kiørboe, 2005a). However, in some species, both females and males are able to release trails (Doall *et al.*, 1998; Kiørboe *et al.*, 2005) and in rare cases, males can also pursue other males (Doall *et al.*, 1998) or tracking heterospecific females (Goetze, 2008; Goetze and Kiørboe, 2008).

1.2 Swimming behaviour

Swimming is essential for copepods to survive and operate in suspension in a three-dimensional environment. Copepods can not travel along wide distance, although some species can perform vertical migration (Alcaraz *et al.*, 2007), and can not contrast the oceanic currents. However, they move at small scales in search for food and mates, and for escaping predators (Kiørboe, 2008a). Copepod searching efficency depends of swimming pattern and perceiving ability (Bundy *et al.*, 1993).

Most of the copepods are 1–2 mm long and move at few body length per seconds, hence they live at the interface between laminar and turbulent regimes, with Reynolds numbers (Re) that vary over 5 orders of magnitude (from 10^{-2} to 10^{3}) (Yen, 2000). When swimming, the copepod is displaced in the water and is subjected to the physical constraints imposed by both viscous and inertial realms (Bundy and Paffenhöfer, 1996). When at $Re < 1$ the copepod concentrates its forces to swim, at Re from 2 to 100, the copepod is subject to high inertial forces and viscous frictions (van Duren and Videler, 2003).

Copepods swimming behaviour differ among species (Mauchline *et al.*, 1998) depending for example on: feeding habits (Kiørboe, 2010), development stages (van Duren and Videler, 1995; Titelman, 2001; Titelman and Kiørboe, 2003a,b; Takahashi and Tiselius, 2005), gender Doall *et al.* (1998); Kiørboe and Bagoien (2005), food quality and quantity (Paffenhöfer and Vansant, 1985; Jakobsen *et al.*,

2005), salinity concentration (Seuront, 2006; Michalec *et al.*, 2010) and the presence of predators (Kiørboe and Visser, 1999; Hwang and Strickler, 2001; Waggett and Buskey, 2007).

The mate-finding behaviour of pelagic copepod is gender-specific. The female produces a continuous trail of pheromones (Doall *et al.*, 1998; Bagoien and Kiørboe, 2005a) that acts as a recognition signal and is dependent of the swimming behaviour of the female. The male performs active mate searching (Kiørboe, 2008b) and once the male odours the trail, especially fresh one (Kiørboe, 2008b), he begins to follow it increasing speed and form a zigzag-like pattern (like a dance). Often, during the track, the male takes the wrong direction and performs several shifts before identifying the right one (Kiørboe, 2008b; Goetze and Kiørboe, 2008). The species *Temora longicornis* is able to detect a trail up to at least 10 seconds old trail (Doall *et al.*, 1998). The persistence of the trail quality is dependent of the fluid characteristic, the borne odour signal and the hydro-dynamism (Doall *et al.*, 1998). The pheromones increase the probabilities of encounter between the genders and individuals. *Acartia tonsa* appears to depend on hydro-mechanical signals in the detection of mate (Bagoien and Kiørboe, 2005b).

To balance gain and losses of energy, copepods have to select the best feeding strategy in function of the environment and their specific traits of adaptation and plasticity (Alcaraz *et al.*, 2007). The general mode of copepod feeding does not vary much across the species. The basic steps of the feeding process are: (i) capture of the food particle by alternate movements of the cephalic appendages, (ii) ingestion into the mouth, (iii) digestion though the gut and (iv) release of faecal pellets (Strickler, 1982).

However, differences exist among the strategies utilized to find the food particles before they are captured. Three main types of strategies have been identified in copepods: (1) cruising while searching for prey; (2) generating a feeding current and intercept, retain and extract from the current the desired prey; (3) using ambush feeding strategy, capturing motile prey when they enter the copepod radius of perception (Kiørboe, 2010). Cruisers are the fast swimmers; filter feeders are the slow swimmers, and the ambush feeder stay motionless in the water (Tiselius and Jonsson, 1990).

1.3 Observing and analysing copepod behaviour

Copepod behaviour has to be analysed at the microscopic scales (*i.e.*, millimeters and submillimeters, seconds and milliseconds) proper to these small pelagic organisms and this implies the use of particular optical systems (Strickler and Hwang, 1999). Three techniques are commonly used to analysed copepod swimming behaviour: (i) two-dimensional (2D) video recording, (ii) high speed cinematography, and (iii) three-dimensional (3D) video recording.

Two-dimensional observation under microscope is the most ancient technique use to monitor copepod species: their presence, their taxonomy. This instrumentation have a limited field of view that allow to follow swimming copepods in limited water volumes. To overcome this problem, in Paffenhöfer and Mazzocchi (2002) were used the Crittercam® that allow to follow one single individual in a bigger water volume. The limitation of the 2D images remained.

The high speed cinematography is used to monitor movement of appendages in copepod species. The technique allows the observation of food ingestion by cope- pod and the monitored of the way how copepods handle the food (Strickler, 1985). This technique also permits the study of the movement of copepod appendages when feeding, capturing preys (Cowles and Strickler, 1983; van Duren and Videler, 2003; Kiørboe *et al.*, 2009) and escaping (Buskey *et al.*, 2002; Buskey and Hartline, 2003). But also it figures out the interactions between copepod body and appendages and the surrounding fluid. High speed cinematography does not allow recordings longer than few seconds.

The 3D digital video recording allows analysing the swimming activity of copepods in the dimensional volume space (*i.e., x, y, z* environmental coordinates). The 3D recordings was applied relatively recently to the zooplankton behaviour (Young and Getty, 1987; Yen, 1988) and received a notable advancement through the work of Strickler (1998) that used laser cinematographic techniques to evaluate zooplankton swimming patterns. Ramcharan and Sprules (1989) introduced a optic mirror system to allow the stereoscopy for the reconstruction of 3D swimming path. In the last 20 years, the papers studying 3D swimming behaviour increased bu mostly in recent years (Yen *et al.*, 2008; Michalec *et al.*, 2010)[*e.g.*,].

In this thesis new digital recording facilities and especially automated images processing allowed a considerable new exploring approach, allowing to follow more individuals per time. It was possible to build up the bigger bigger database on copepod 3D swimming behaviour.

1.4 Target species

Five calanoid species have been selected in the present study to investigate the specific diversity of copepod swimming behaviour: *Centropages typicus*, *Acartia clausi*, *Temora stylifera*, *Paracalanus parvus* and *Clausocalanus furcatus*. Those species are very abundant in Mediterranean waters and in many other seas Razouls *et al.* (2005-2010). The first four species are characteristic of coastal regions and only *C. furcatus* extends its distribution in open waters (Frost and Fleminger, 1968). *Clausocalanus furcatus* occurs in both environments (Peralba and Mazzocchi, 2004; Mazzocchi and Ribera d'Alcalà, 1995) but become relatively more important offshore.

***Centropages typicus* (Kröyer, 1849)**

Centropages typicus is an omnivorous and fast swimming species whose mouthpart movement is alternated by active (55 Hz, 36.5 Hz for the limbs) / inactive periods with a frequency of 0.1 to 10 seconds in function of the food supply (Cowles and Strickler, 1983; Poulet and Gill, 1988; Tiselius and Jonsson, 1990) and generated a feeding current of 12 cm s^{-1}. This current allows the capture of prey in less than 14 ms (Cowles and Strickler, 1983). Total female length $\sim$ 1.4 mm.

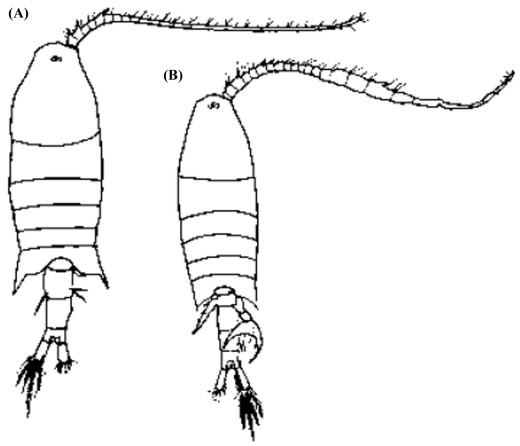

Figure 1.1: *Centropages typicus*: female dorsal view (A); male dorsal view (B). Modified from Avancini *et al.* (2006).

Acartia clausi (Giesbrecht, 1889)

Acartia clausi is consider as an opportunist that is able to switch from ambrush-feeder (Takahashi and Tiselius, 2005) in low food concentration to montionless sinker Tiselius and Jonsson (1997). Total female length $\sim$ 1.1 mm.

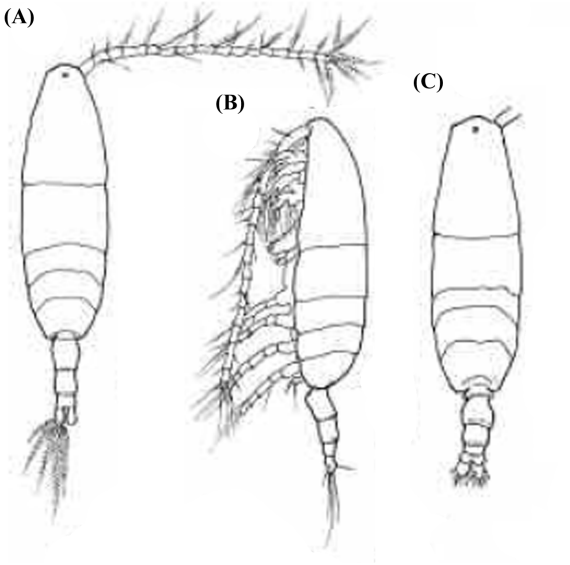

Figure 1.2: *Acrtia clausi*: female dorsal view (A) and lateral view (B); male dorsal view (C). Modified from Avancini *et al.* (2006).

***Temora stylifera* (Dana, 1848)**

Omnivorous, slow swimmer, species. Total female length $\sim$ 1.5 mm.

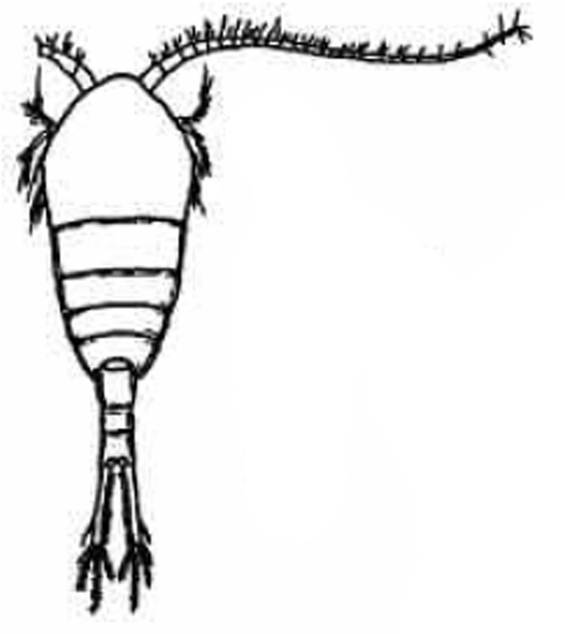

Figure 1.3: *Temora stylifera* female dorsal view. Modified from Avancini *et al.* (2006).

***Paracalanus parvus*(Claus, 1863)**

Paracalanus parvus is a slow swimmer. Total female length ~ 0.9 mm.

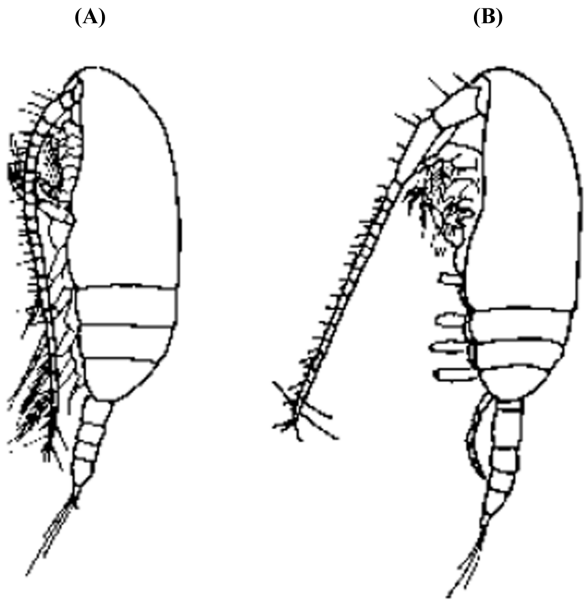

Figure 1.4: *Paracalanus parvus*: female lateral view (A); male lateral view (B). Modified from Avancini *et al.* (2006).

***Clausocalanus furcatus* (Brady, 1883)**

Clausocalanus furcatus is considered as an herbivorous which moves continuously along convoluted small loops with a preference feeding on motile dinoflagellate (Mazzocchi and Paffenhöfer, 1999; Uttieri *et al.*, 2008). *Clausocalanus furcatus* occurs in tropical and subtropical areas of both hemispheres (Frost and Fleminger, 1968) and is one of the most abundant calanoids in epipelagic waters of both oligotrophic (Peralba and Mazzocchi, 2004). Total female length $\sim$ 1.0 mm.

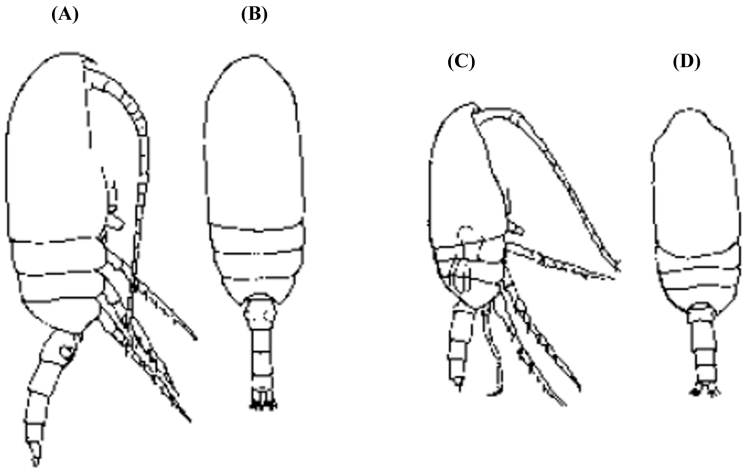

Figure 1.5: *Clausocalanus furcatus*: female dorsal and lateral view (A, B); male dorsal and lateral view (C, D). Modified from Avancini *et al.* (2006).

1.5 The LTER-MC time series

The five calanoids selected as target species for the present study are monitored since 1984 at the Long Term Ecological Research Station MareChiara (LTER-MC), a fixed station in the Gulf of Naples (Italy) (Mazzocchi and Ribera d'Alcalà, 1995; Ribera d'Alcalá *et al.*, 2004), *i.e.*, two nautical miles from the shore and by 40° 48.5' North and 14° 15' East (Ribera d'Alcalá *et al.*, 2004) (Fig. 1.6). This investigation has provided information on the seasonal patterns and inter-annual variability of calanoid monitored populations, as well on their population structure via typical coastal Mediterranean site.

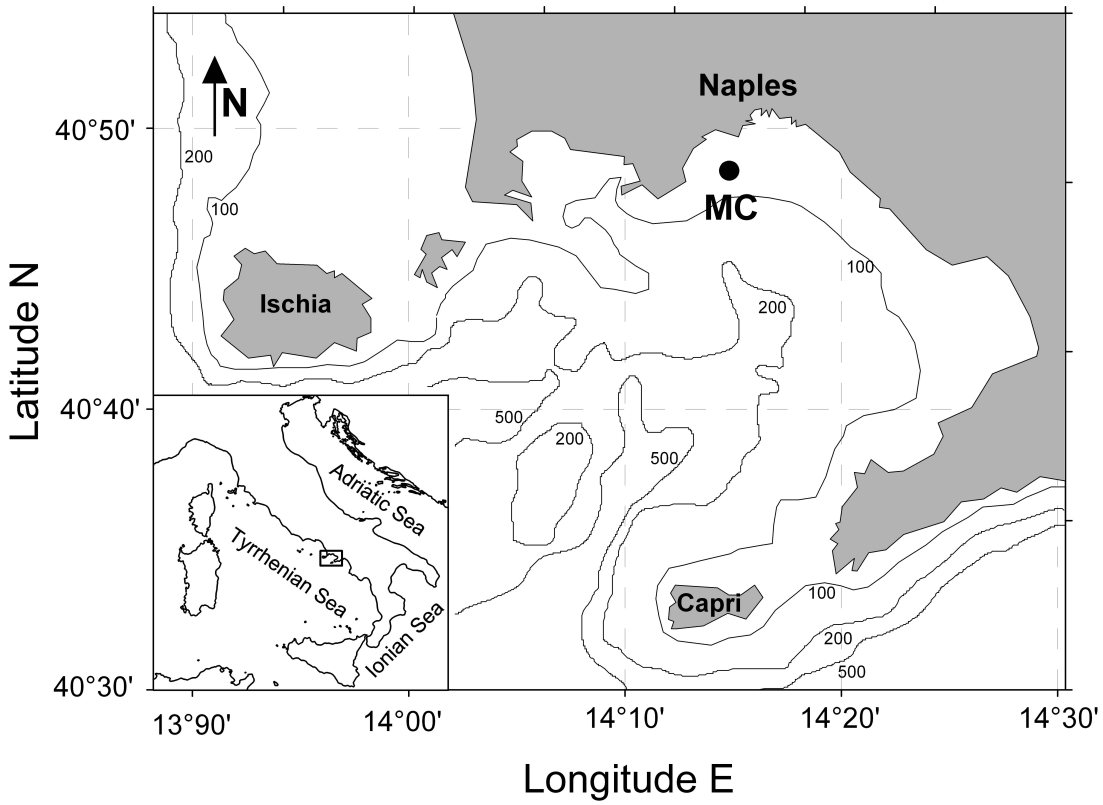

Figure 1.6: Map of the Gulf of Naples (Tyrrhenian Sea, Western Mediterranean) with the sampling site (MC) of the LTER-MC time series.

The lowest surface temperatures, integrated 0–10 m, are generally recorded in February–March (14°C) and the highest in August (26°C) while the irradiances

are low in December ($\sim$ 9.5 hours of light) and high in June ($\sim$ 14.5) (Management and Ecology of Coastal Areas database, 1984–2009, SZN). Plankton communities (phyto-, micro- and meso-zooplankton) were investigated biweekly from 1984 to 1990 and weekly since 1995 onwards (Ribera d'Alcalá *et al.*, 2004). At LTER-MC, the mesozooplankton is dominated by copepods, then cladocerans, appendiculars and mero-plankton (Ribera d'Alcalá *et al.*, 2004). Copepods, which are represented by numerous specied (up to 120) and constitute a very diversified assemblage, show a major peak of abundance in spring (Fig. 1.7) and high abundances in July–August and October (Ribera d'Alcalá *et al.*, 2004). Over the year, the copepod assemblage is characterized by peaks of succession of a few abundant species: *Acartia clausi*, *Centropages typicus*, *Paracalanus parvus* and *Temora stylifera*. On mean annual basis these species (adult and juveniles) comprises $\sim$ 47% of total copepod abundance.

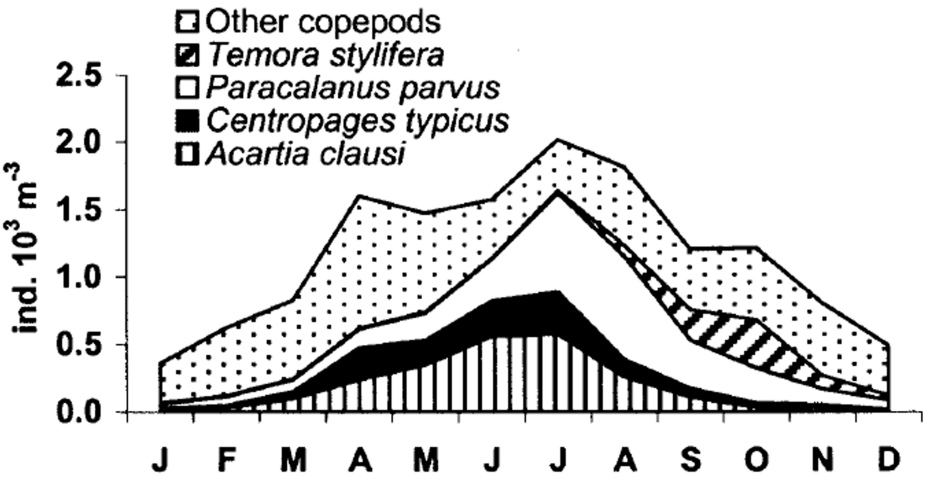

Figure 1.7: Contribution of the four most abbundant calanoid species to the mean seasonal cycle of total copepod abbundance at LTER-MC. Montly averages for the period 1984–1998 (Ribera d'Alcalá *et al.*, 2004).

Acartia clausi and *C. typicus* use to be monitored in June–July, *P. parvus* in July–August, the small calanoids (*e.g., C. furcatus*) and oithonoids in late autumn–winter together with *T. stylifera* in September–October (Ribera d'Alcalá *et al.*, 2004). Seasonal occurrence of the five species is reported in Fig. 1.8.

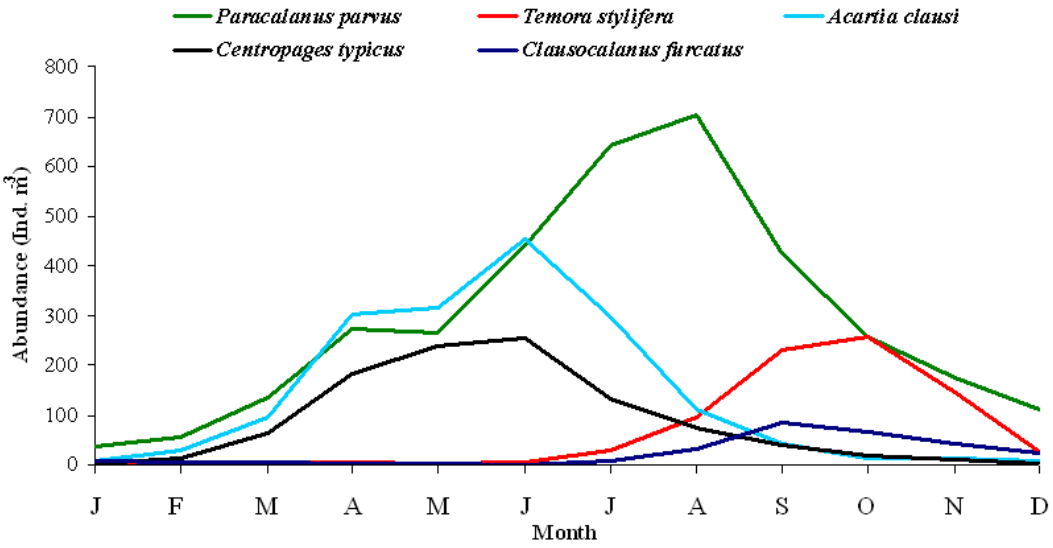

Figure 1.8: Abundance annual cycle of the five target species at LTER-MC. Monthly averages for the period 1984–2009.

Both *A. clausi* and *C. typicus* showed egg production in February (Ianora and Buttino, 1990), the presence of juveniles together with the adults is monitored from March–April onwards. Thanks to their opportunistic feeding habits the species can survive over the spring and summer periods. They survive wide range of temperature from 14°C in winter to 26°C in summer.

Paracalanus parvus major abundance is recorded in June–August (Fig. 1.8). The species is monitored over the year and is therefore adapted to survive over a wide range of temperature from 14°C in winter to 26°C in summer. However, the main occurrence of this species is detected when the seawater surface reaches the highest temperature.

Temora stylifera and *Clausocalanus furcatus* occur in autumn. The first exhibit a maximum abundance in September–October while the second occur in a restricted period localized during the autumn–winter seasons. *Temora* species is recorded when seawater temperature (0–10 m) is comprised from 19 to 24°C in autumn. However, its main occurrence corresponds to the highest seawater surface temperature and the moment when the thermocline is not totally disrupted

and the phytoplankton blooming.

1.6 Aims

This thesis was aimed to analyse the 3D swimming motion of five calanoid species that are very common and abundant in Mediterraneans waters in order to evaluate if differences or analogues could be highlighted to better understand the traits that allow their co-occurrence or succession in the coastal waters in the Gulf of Naples. Video observations and recording were conducted on wild populations sorted from the field and under two conditions: absence and presence of food (field-concentration dependent). The species were also monitored at different population density.

A software was implemented to recording and the reconstructing copepod swimming trajectories and analyse the motion parameters. Four of them were recorded: the swimming mode, the speed, the net to gross displacement ratio (NGDR) and the explored volume for each of the five species of copepod target (*Centropages typicus*, *Acartia clausi*, *Temora stylifera*, *Paracalanus parvus* and *Clausocalanus furcatus*).

The five copepod species have been chosen for three main reasons: (1) the occurrence at the LTER-MC; (2) their periodical bloom over season, and (3) their ecological relevance. *Centropages typicus*, *A. clausi*, *T. stylifera* and *P. parvus* are the most abundant species at LTER-MC. *Clausocalanus furcatus* occurs in a very restricted period and is adapted to oligotrophic area.

Therefore through the present PhD-thesis, the species-specific behaviour at small scales of the females, the males, and a comparison of the two genders are proposed. Then, ecological implication and environmental adaptation through the 3D detected swimming behaviour of each species will be assessing the following aims:

I) Is there a species-specific swimming behaviour among copepod species?

II) Are the strategies of swimming behaviour of two species co-occuring at the same seasonal period different?

III) Are the strategies of swimming behaviour of two species co-occuring at different seasonal period similar?

IV) Is the swimming behaviour impacted along copepod occurrence?

Chapter 2

Materials and Methods

2.1 Experimental set-up

2.1.1 Overall description

The experimental video set-up used for behavioural observation and recording was designed and assembled at Stazione Zoologica Anton Dohrn of Naples (SZN) (Bianco, 2007) and is based on two identical optical-systems, each of them composed by: (1) a digital camera, (2) a specific designed lens, and (3) an infra-red (IR) light source. The two optical-systems are disposed orthogonally, on an anti-vibrating table, and are connected to a personal computer (PC) (Fig. 2.1 and 2.2).

In a central position between the two optical systems, is positioned a 1 L cubic couvette, in which where copepods are placed for video recording. The couvette is between the IR light sources and the lenses. The IR light beams that cross the couvette arrive to the camera through the lenses. When a free swimming copepod crosses the light-beams, the two cameras record its silhouette like a dark array of pixels against a light background. The cameras operate simultaneously from two orthogonally perspectives allowing recording three-dimensional (3D) views of the copepod swimming activity.

For further protection from possible external perturbations, starting from experiment #15 (see Table 2.1), the 1 L couvette was placed in a larger (8 L) empty

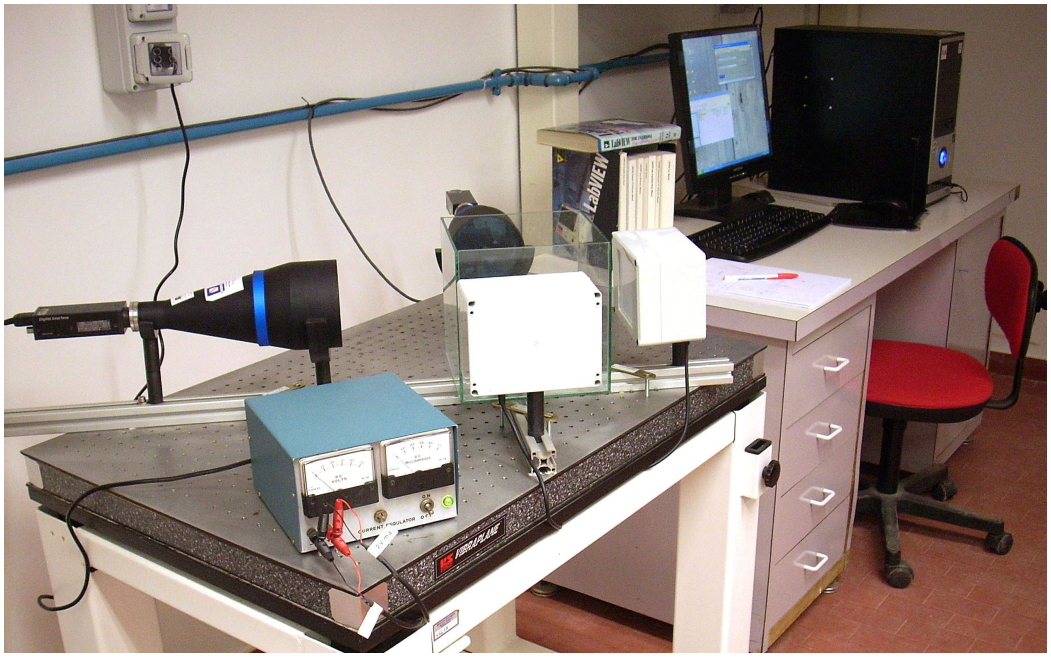

Figure 2.1: Experimental set-up for recording zooplankton swimming activity in a three-dimensional space (3D).

couvette (Fig. 2.2). Both couvettes are closed by glass tops.

The whole equipment is placed in a temperature-controlled room to simulate the *in situ* conditions.

2.1.2 Hardware

The two digital cameras, Sony XCD-X700, are equipped with a 1/2 inch type progressive scan charge-coupled device (CCD) sensor with 6.25 μm square pixels. The CCD delivers 8 bit monochromatic images at 1024×768 (8×10^5) pixel resolution and 15 frames per second (fps). Each camera is connected to the lens with a standard C-type mount system and linked to the PC through FireWire IEEE-1394 interface that allows transferring 15 fps full resolution uncompressed images.

The lenses and IR light sources were designed and realized by engineer Paolo Trampus (Centre for Advanced Research in Space Optics, Trieste, Italy). The lenses, coupled with the 1/2 inch CCD, realize a field of view of 80×60 mm and

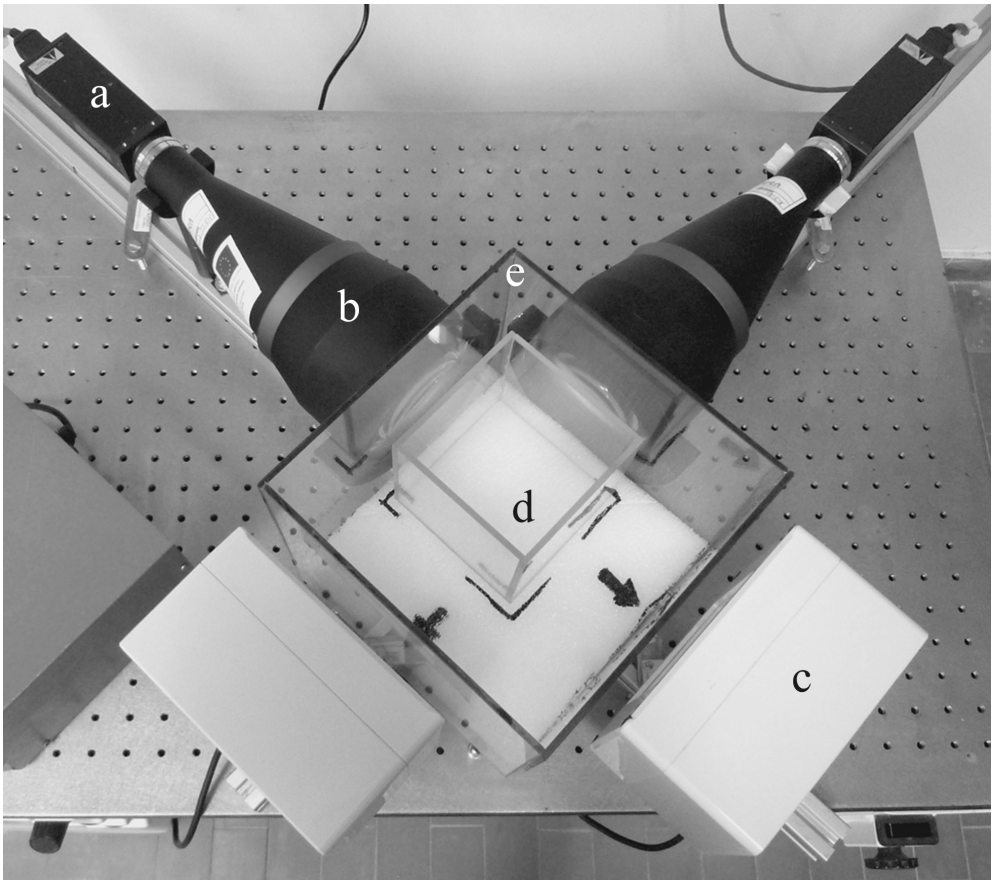

Figure 2.2: Video-equipment from the top view. Each optical-system is composed by: (a) a digital camera, (b) a lens and (c) an infra-red light source. The experimental 1 L glass couvette (d) is positioned into a larger couvette (e).

a spatial resolution of 78 μm/pixel with no measurable distortion and very low vignetting effect (i.e., brightness reduction at images' periphery). Because the two optical-systems are disposed orthogonally, the 3D volume of observation is a parallelogram of $80 \times 80 \times 60$ mm, that is 38.4% of the 1 L experimental couvette.

The light source correspond to an array of four 18 mW infra-red (780 ηm) Light-Emitting Diodes (LED) and is connected to a 12 volt DC power supply.

The entire equipment is mounted on a 60×90 cm Kinetic System inc. Vibro-Plane 9100 table to avoid mechanical vibrations (Fig. 2.1). Two 1 m aluminium ranks are disposed orthogonally and screwed on the table surface and the lenses and the light sources are positioned on plastic supports that can be moved longi-

tudinally along the ranks for fine tuning the set-up geometry. The couvettes are positioned on four M6 screws with a rubber piece on the top and fixed on the table.

The PC is assembled on an ASUS mother-board M2NPV-VM and has an AMD Athlon 64 X2 Dual Core 3500+ CPU, 4 gigabytes (GB) of RAM and a total mass storage of 750 GB on three SATA-2 hard disks (HD). The PC has a dedicated FireWire port for each camera and runs Windows XP operation system.

2.1.3 Software

The software utilized at the SZN to obtain the copepod 3D swimming trajectories is composed by three main parts, which allows: (1) controlling directly the digital cameras and recording simultaneously the videos of both cameras on the PC HDs, (2) compressing the videos for saving space and maintaining a back-up copy of each experiment, (3) analysing images and reconstructing the 3D copepod trajectories.

2.1.3.1 Video recording

The video recording software has been developed by Francesco M. Sacerdoti (e-voluzione s.r.l., Naples, Italy) in National Instrument LabView software (Bianco, 2007). The two digital cameras are controlled and synchronized by this software and the videos are stored in real time on PC HDs. This software merges the two monochromatic videos of both cameras and records a single 32 bit RGBA (red, green, blue and alpha channels) uncompressed AVI video-file. The output file contains information for the first camera recorded as red channel (R), and the for the second camera, as the green channel (G).

The software allows controlling the shutter and the gain of the cameras and the numbers of frames of the output video-files (Fig. 2.3). During the experiments of this thesis, the output file was set at 300 frames, equivalent, at 15 fps, to 20 seconds of film per file.

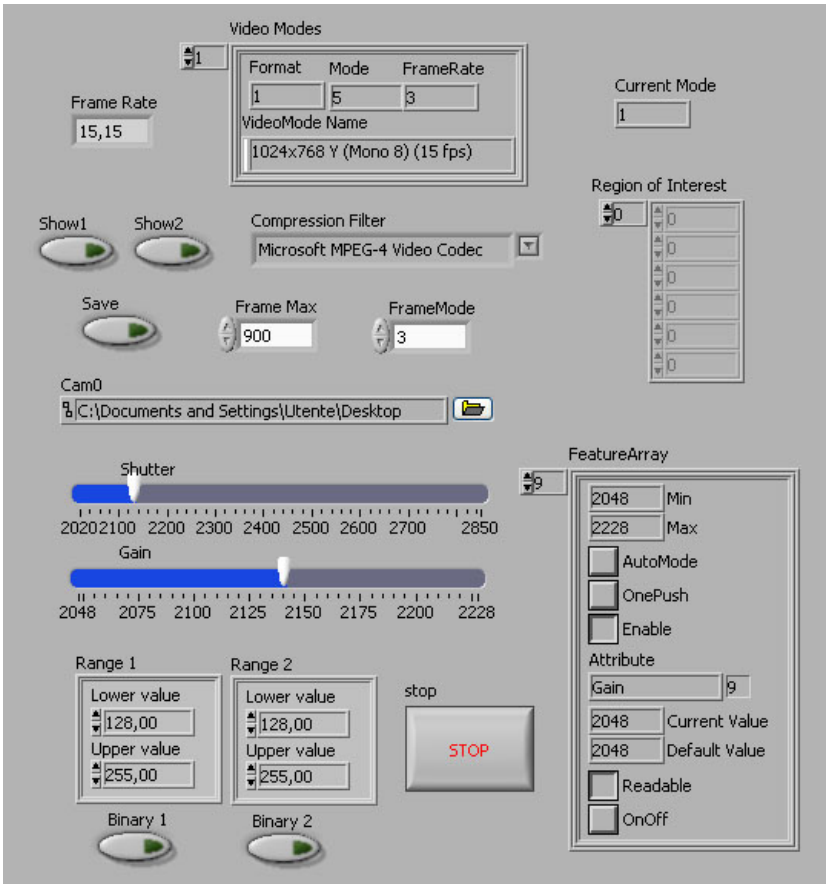

Figure 2.3: Video-recording software implemented at SZN for synchronizing and recording videos from two digital cameras simultaneously. The software controls the shutter and the gain of the cameras, the numbers of frames of the output video-files, and the compression filter (not used for this thesis).

2.1.3.2 Video compression

Each 20 s video was recorded as raw modality, *i.e.*, with no compression codec, and occupied about 1 GB. It was therefore necessary to compress the video files. The compression mode used in the experiments conducted in 2008 (#1–33) consisted in converting all videos in JPEG image sequences using VirtualDub software version 1.8.5 (www.virtualdub.org). The compression ratio techniques was of $\sim 1000 : 1$. For the experiments conducted in 2009 (#34–43), the compression

mode consisted in extracting from the raw RGBA files the R and G channels, containing the videos from the two cameras, and saving each of them in a PNG image sequences of 8 bit monochromatic AVI file. The compression ratio was $\sim 7.7 : 1$ and depended on two factors: (1) the reduction from a 32 bits RGBA file to two 8 bits monochromatic files, (2) the lossless compression of each frame in PNG image. This modality was performed by writing an *ad hoc* macro using ImageJ software (Abramoff *et al.*, 2004). The first method allowed an higher compression of the data. Moreover, the second permitted to also preserve the raw data information of the video, even at the cost of higher HDs space.

In spite the first method performs a higher compression ratio, the second one preserves the raw information available in the videos. The second compression method represented therefore a better choice for the image processing analysis (see next section), at cost of higher storage space on HDs.

2.1.3.3 Image analysis

The reconstruction of 3D swimming trajectories was performed following four steps: (1) importing a video-file, (2) segmenting the image into objects of interest (*i.e.*, copepods) and background, (3) tracking the 2D trajectories from each video, (4) merging of the swimming tracks from the two cameras into 3D trajectories.

The first three steps of image analysis were carried out using a macro script for ImageJ software. Once a video file was loaded on the software as an image stack, the macro applied to this stack a binary contrast enhancement utilising the default ImageJ threshold method. Successively, the macro run the Mtrack2 plug-in (Klopfenstein and Vale, 2004) to perform the 2D tracking. The output of the macro was an ASCII file containing the 2D tracks of copepod motion for each camera. The fourth step was performed in custom C++ software. The input of this software are the ASCII files that contain the 2D tracks of both cameras. The 2D trajectories obtained from the two cameras are merged in 3D trajectories by comparing the common z values. The results are stored in an ASCII file containing the the 3D trajectories x, y and z coordinates converted from pixels to millimetres.

A *trajectory* is drawn by the connection of successive *points*, which are defined by all discrete x, y, z coordinates of copepod's positions (Fig. 2.4). Two consecutive points are temporally separated by 1/15 s (*i.e.*, 1/fps), consequently the duration of the trajectory betwen the start (S) and end (E) points of the trajectory was computed as $(\mathrm{E} - \mathrm{S}) \cdot 1/15$ s.

Different kinds of behaviour were considered: (1) *Swimming*, when the copepod actively propels its body forward moving the appendages; (2) *Sinking*, when the copepod stops moving appendages, and sinks; (3) *Jumping*, when the copepod moves between the two successive points at highly speed, generally with flinging its first antennae and abdomen; (4) *Hovering*, when the copepod avoids sinking and keeps suspended moving the appendages. Along the trajectory track here reported in Fig. 2.4; each behaviour is represented by a different color.

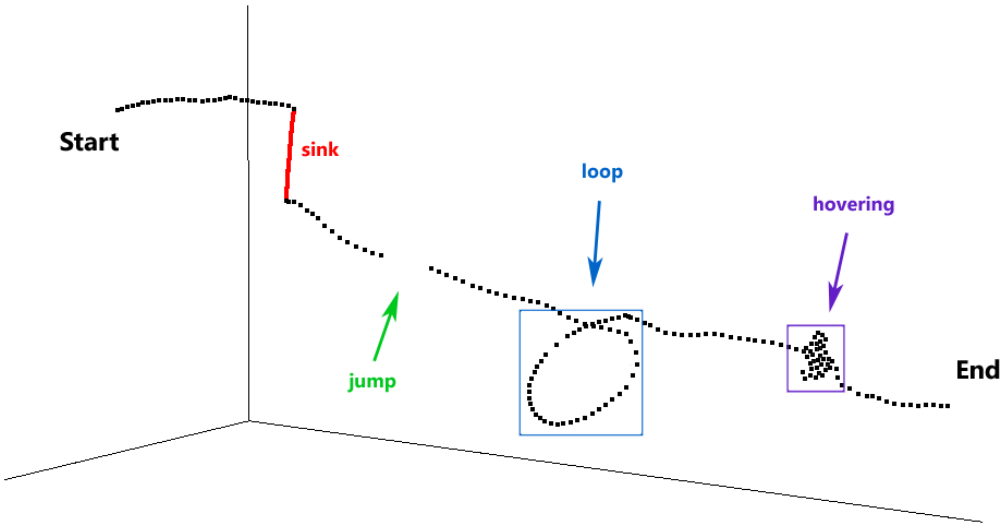

Figure 2.4: Example of three-dimensional trajectory representation. Dots indicate in constant time interval (1/15 s) the copepod position along x, y, z coordinates. Black independent dots represent active swimming; red dots indicate sinking phases; green arrow indicates a jump event; blue arrow indicates a looping track of copepod's motion; black gathered dots (purple arrow) indicates an hovering-like behaviour.

2.2 Experiments

2.2.1 Sample collection and copepod treatment

Zooplankton samples were collected in the inner Gulf of Naples (Tyrrhenian Sea) at long-term ecological research station Mare Chiara (LTER-MC), from which plankton time-series are recorded (Ribera d'Alcalá *et al.*, 2004). Vertical tows were performed in the upper 50 m of the water column with a Nansen WP2 200 μm mesh net equipped with a 5 L non-filtering cod-end. Within 1 hour after collection, the samples were transported in a isotherm container to a cold room in the laboratory. The samples were immediately cleaned from settled matter and gently diluted into large glass jars (3–5 L) by adding sea water, collected the same day at the sampling site, in order to reduce the overcrowding stress and provide copepods with fresh food. The jars were kept at *in situ* temperature and light conditions.

After $\sim$ 1 h acclimatisation, individuals of the target species were sorted from the jars with a large-bore glass pipette using a fluorescent back-light. The identify the target species was based on the body shape and swimming activity. Single individuals were gently transferred to small (100 ml) glass cups and observed at an Olympus SZH10 dissecting microscope to be checked for their stage and sex. Only undamaged and healthy adult females and males were selected, transferred into the 1 L glass couvette filled with sea water (with or without food depending on the experiment) and brought to the video-equipment in another room kept at the same temperature. Before recording, copepods were left to acclimatize in the glass couvette for 15–30 minutes.

2.2.2 Video recording

The experiments consisted in video-recording the swimming activities of females and males, separately, in different food conditions and at different copepod abundance (ind. L^{-1}). All experiments were conducted in the dark, in precence of the IR light provided by the system.

For the experiments in presence of food, natural particle assemblages collected in surface water at LTER-MC with a Niskin bottle, were gently transferred to a

10 L plastic tank with a silicon tube. In the laboratory, the experimental water was gently filtered through 200 μm mesh Nitex to remove meso-zooplankters. Information on phytoplankton composition and abundance was obtained from the LTER-MC and kindly provided by Dr Diana Sarno (Taxonomy and Identification of Marine Phytoplankton, SZN). Ciliates abundance were obtained from the Management and Ecology of Coastal Areas database at SZN. When the experiment could not be performed in the same day of the LTER-MC serial sampling, but 1–2 days apart, sea water was collected from the same time and site (LTER-MC) of copepod collection was used and the closest sample of LTER-MC time-series was utilized for information on phytoplankton composition and abundance. When possible, the same group of copepods were filmed in different food conditions within 24 h, and different groups of individuals were used in the same conditions as replicates. In the experiments without food, copepods were recorded in sea water filtered on GF/F (micropore, 0.22 μm) filter.

Copepod swimming behaviour was also recorded at different population density, *i.e.*, number of individuals present in the couvette. After a group of copepods was filmed, a new acclimated group, was added to increase the number of individuals in the couvette. During the experiments the population density was much higher than the total copepod abundance recorded at LTER-MC from the same day. The experimental density was from $\sim$ 6 to 60 times higher than at sea for *Centropages typicus*, $\sim$ 50–100 times for *Acartia clausi*, $\sim$ 25–50 times for *Temora stylifera*, $\sim$ 10–40 times *Paracalanus parvus* and $\sim$ 20–60 times *Clausocalanus furcatus*. Such high numbers of individuals were necessary to simulate different crowding conditions and to ensure that many individuals could be recorded simultaneously in the volume of observation.

A total number of 43 video-recording experiments was performed with the above mentioned five calanoid copepod species (Table 2.1) for more than 21 hours of recording time.

Table 2.1: Summary of experiments performed per copepod species. The five copepod species. The experiment number and date. The temperature condition and the time of record.

Species	Exp.	Date	Temp. (°C)	Tot. recording time (min)
Centropages	1–4	29, 30 Apr 2008	16	80
typicus	5–10	11 Jun 2008	17	122
Acartia	11–14	10, 11 Jul 2008	20	80
clausi	34–35	15, 19 May 2009	21	68
	15–18	30 Sep 2008	20	80
Temora	19–22	7 Oct 2008	20	80
stylifera	23–28	14, 15 Oct 2008	20	120
	29–31	21 Oct 2008	20	60
Paracalanus	36–38	15, 16, 17 Jul 2009	21	222
parvus	39–41	28 Jul 2009	21	83
Clausocalanus	32–33	27, 28 Nov 2008	18	134
furcatus	42–43	30 Sep, 1 Oct 2009	21	162

2.3 Data analysis

For the numerical analysis of copepod 3D swimming trajectories, a Java software has been developed for the construction of a data base containing, for each experiment, the metadata (experiment date and time, temperature, food conditions, copepod species, sex and abundance) and the basic metrics for quantifying copepod swimming behaviour: time steps, move steps, velocity and sinking events.

The *time steps*, *i.e.*, the time lag between 2 following points, are setted by the cameras fps performance (at 1/15 s and are reported in the database as absolute number of frames (of video recorded experiment), absolute time step (0 at experiment frame #1) and relative time (0 at trajectory frame #1). Time steps are useful for further measurements (e.g., velocity, co-occurrence events, pattern duration, etc.)

The *move steps*, *i.e.*, distance moved per unit time, are computed for each point of all trajectories in the database as net displacement (ND), i.e., the linear distance between the starting point and end the point of a path, and gross displacement (GD), *i.e.*, the total distance travelled. Using three-dimensional euclidean distance for the *i-th* trajectory point:

$$\mathrm{ND}_i = \sqrt{(x_i - x_0)^2 + (y_i - y_0)^2 + (z_i - z_0)^2} \quad (\mathrm{mm}) \tag{2.1}$$

and

$$\mathrm{GD}_i = \sqrt{\sum_{k=1}^{i} (x_k - x_{k-1})^2 + (y_k - y_{k-1})^2 + (z_k - z_{k-1})^2} \quad (\mathrm{mm}) \tag{2.2}$$

with x_0, y_0, z_0 being the coordinates of the trajectory starting point.

In each point of the trajectories, the *instantaneous velocity* was calculates using the central difference method. Along each of the three axes the velocity was computed as:

$$\mathbf{u}(x_i) = \frac{x_{i+1} - x_{i-1}}{2\Delta t} \quad (\mathrm{mm\ s^{-1}}) \tag{2.3}$$

$$\mathbf{v}(y_i) = \frac{y_{i+1} - y_{i-1}}{2\Delta t} \quad (\text{mm s}^{-1}) \tag{2.4}$$

$$\mathbf{w}(z_i) = \frac{z_{i+1} - z_{i-1}}{2\Delta t} \quad (\text{mm s}^{-1}) \tag{2.5}$$

where Δt is the time lag between 2 consecutive frames, i.e., 1/15 s.

The magnitude of the 3D velocity (*instantaneous speed*) was calculated as:

$$V = \frac{\sqrt{(x_{i+1} - x_{i-1})^2 + (y_{i+1} - y_{i-1})^2 + (z_{i+1} - z_{i-1})^2}}{2\Delta t} \quad (\text{mm s}^{-1}) \tag{2.6}$$

For the first and last point of each trajectory, the velocity was computed as the forward and backward difference. The examples along the x axis were, respectively:

$$\mathbf{u}(x_i) = \frac{x_{i+1} - x_i}{\Delta t} \quad \text{and} \quad \mathbf{u}(x_i) = \frac{x_i - x_{i-1}}{\Delta t} \quad (\text{mm s}^{-1}) \tag{2.7}$$

Instantaneous speed was converted in Body Length (BL) per seconds to allow the speed comparison between species. This measure was obtained by dividing the speed by average measurements of adult individuals length, measured thanks to a Leica MZ 12.5 stereoscope, from the tip of prosome to the distal end of caudal ramus.

Sinking events were determined using an algorithm that includes 4 parameters: (1) downward movement (negative vertical velocity, $w(z_i) < 0$), (2) 3D speed under a determined threshold (depending on the species), (3) duration (1–10 s depending on the species and food condition), (4) direction (*i.e.*, vertical or oblique). Spikes due to measurement errors in image processing were eliminated.

The trajectories were checked manually one by one using R software (R Development Core Team, 2010) to: (1) eliminate wrong trajectories due to presence of noise or ghost images generated by the image processing, (2) separate trajectories that were linked in non correct way by the C++ software, (3) check if the sinking

events were correctly computed. After corrections, the Java code was ran again. R was then used for further analysis of trajectories and statistical tests.

Successively, jumps were determined in R by using 2 parameters: (1) the duration in 1–5 frames range and (2) the 3D instantaneous speed ($V(x_i, y_i, z_i)$) over a determined threshold (8–12 mm s^{-1}). The lowest fps and velocity thresholds were determined for each experiment by manual check.

According to Buskey (1984), the Net to Gross Displacement Ratio (NGDR) provides a measure of the relative linearity of trajectory paths. For each trajectory the NGDR was computed as the average of the net (ND) to gross (GD) displacement ratios calculated at the smallest move step that corresponds to 1/15 s frame acquisition:

$$\mathrm{NGDR} = \sum_{i=1}^{n} \frac{\mathrm{ND}_i}{\mathrm{GD}_i} \cdot \frac{1}{n} \tag{2.8}$$

with ND_i and GD_i computed as in equation 2.1 and 2.2, respectively, and n number of trajectory's points. NGDR assumes values between 0 and 1 with smaller values representing more convoluted trajectories.

The horizontal component of displacement (HC) was computed for each trajectory as the average ratio of the horizontal displacement to the 3D displacement, at 1/15 s:

$$\mathrm{HC} = \sum_{i=1}^{n} \frac{\sqrt{(x_i - x_{i-1})^2 + (y_i - y_{i-1})^2}}{\sqrt{(x_i - x_{i-1})^2 + (y_i - y_{i-1})^2 + (z_i - z_{i-1})^2}} \cdot \frac{1}{n} \tag{2.9}$$

with n number of trajectory's points. HC assumes values from 0 to 1, limits that correspond to vertical and horizontal trajectories, respectively.

Since it was not possible to map the three-dimensional location of food particle captured by copepods, it was evaluated the minimum volume perceived by the copepod based on span of first antennae (A1) and the extend of its setae. The 2D area of perception (A_p) (Fig. 2.5) was based on average measurements of adult individuals of each species with a Leica MZ 12.5 stereoscope. The minimum explored volume (EV) is computed for each trajectory integrating A_p along the

gross distance travelled by copepod while swimming actively (i.e., not considering sinking and jumping) as:

$$\mathrm{EV} = \mathrm{A}_p \cdot \sum_{i=1}^{n} \mathrm{GD}_i \quad (\mathrm{L\ d^{-1}}) \tag{2.10}$$

with GD_i computed as in equation 2.2 and n number of trajectory's points.

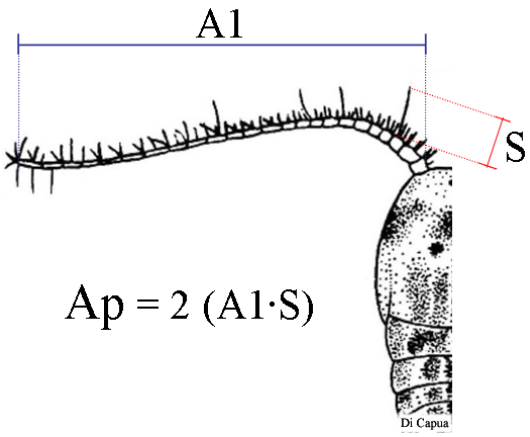

Figure 2.5: Example of measurement of the copepod minimum area of perception A_p. A1 = extend of first antennae. S = setae longest extend.

2.3.1 Statistical analysis

For each experiment, the relative frequency state of swimming behaviour was represented as the percentage of time allocated for swimming, sinking, jumping or hovering. The average duration of each activity was computed on the entire set of trajectories.

For each experiment, the distribution of instantaneous speeds was represented by histograms using 1 mm $\mathrm{s^{-1}}$ bin interval. The comparison between distributions of different experiments was done by using polygon frequency distribution. The averages values of swimming speed, NGDR, horizontal component and explored volume, were computed averaging the mean values of each trajectory.

To compare the metrics from different experiments, Wilcoxon-Mann-Whitney non-parametric test (U-test) was applied for assessing whether the swimming

parameters were or not significantly different in function of the gender and the food condition. The non-parametric test was chosen because the activity duration, swimming speed, NGDR, HC and EV did not have a normal distribution (Kolmogorov-Smirnov test).

Chapter 3

Results

The swimming behaviour of *Centropages typicus*, *Acartia clausi*, *Temora stylifera*, *Paracalanus parvus* and *Clausocalanus furcatus* were analysed through 43 experiments, *i.e.*, 9,369 3D trajectories equivalent to $\sim$ 60 h (Table 3.1).

Table 3.1: General information on 3D swimming trajectories recorded during 43 experiments.

Species	N. Exp.	Recording time	N. trajectories	N. points	Cumulative trajectories duration
Centropages typicus	10	3h 24' 20"	1,451	359,823	6h 39' 48"
Acartia clausi	6	2h 28' 40"	2,151	660,368	11h 13' 44"
Temora stylifera	17	5h 45' 40"	1,857	590,159	10h 55' 45"
Paracalanus parvus	6	5h 06' 00"	2,248	967,188	17h 54' 38"
Clausocalanus furcatus	4	4h 56' 00"	1,689	711,222	13h 10' 15"
Total	43	21h 40' 40"	9,396	3,288,760	59h 54' 10"

3.1 *Centropages typicus*

The swimming behaviour of *Centropages typicus* was analysed in the course of 10 experiments that allowed to acquire 1,451 three-dimensional (3D) trajectories lasting more than 6 hours complexively (Table 3.2). For each experiment, a large number of trajectories was long enough (up to 4 min and 46 s) to provide an extensive dataset suitable for statistical treatment.

Three states characterized *C. typicus* motion behaviour: (1) swimming, (2) sinking, and (3) jumping. Swimming is due to the rhythmic high frequency motion of cephalic appendages (second antennae, maxillae and maxillipeds), which propel the copepod forward while creating a feeding current. During fast swimming, also the thoracic appendages (legs) move rhythmically. The urosome is used as rudder for changing direction. The usual swimming posture of *C. typicus* females and males is slightly obliquely orientetion of the body along the swimming direction, the dorsal side up and the first antennae (A1) open. The most frequent observed swimming path is helicoidal, as reported in Fig. 3.1. The path appears made of consecutive loops of similar diameter, with a few changes of travelling direction. In the same path, the looping may develop in both horizontal and vertical planes (Fig. 3.1 A, C) or show a preference for the vertical one (Fig. 3.1 B, D). Rarely *C. typicus* looping was monitored more than few seconds on a horizontal plane.

At variable frequency, *C. typicus* stops moving both the legs and the cephalic appendages and starts sinking. Sinking events may interrupt looping (Fig. 3.2 A) or more rectilinear swimming mode (Fig. 3.2 B). The duration of sinking is very short during fast looping (Fig. 3.3 A, C) and is much longer during rectilinear upward swimming (Fig. 3.3 B, D). The usual posture of females and males during sinking depends on the previous swimming mode, *e.g.*, more horizontal after looping, and more vertical after rectilinear swimming upward.

Jumping correspond to a quick ($\sim 1/10$ s) and short ($\geqslant 10$ mm) displacement that *C. typicus* performs by fast flapping of A1 and by folding the abdomen. Jump events (Fig. 3.5 and 3.6) were observed quite rarely in *C. typicus* under undisturbed hydrodynamic conditions compared to swimming and sinking phases (Table 3.3).

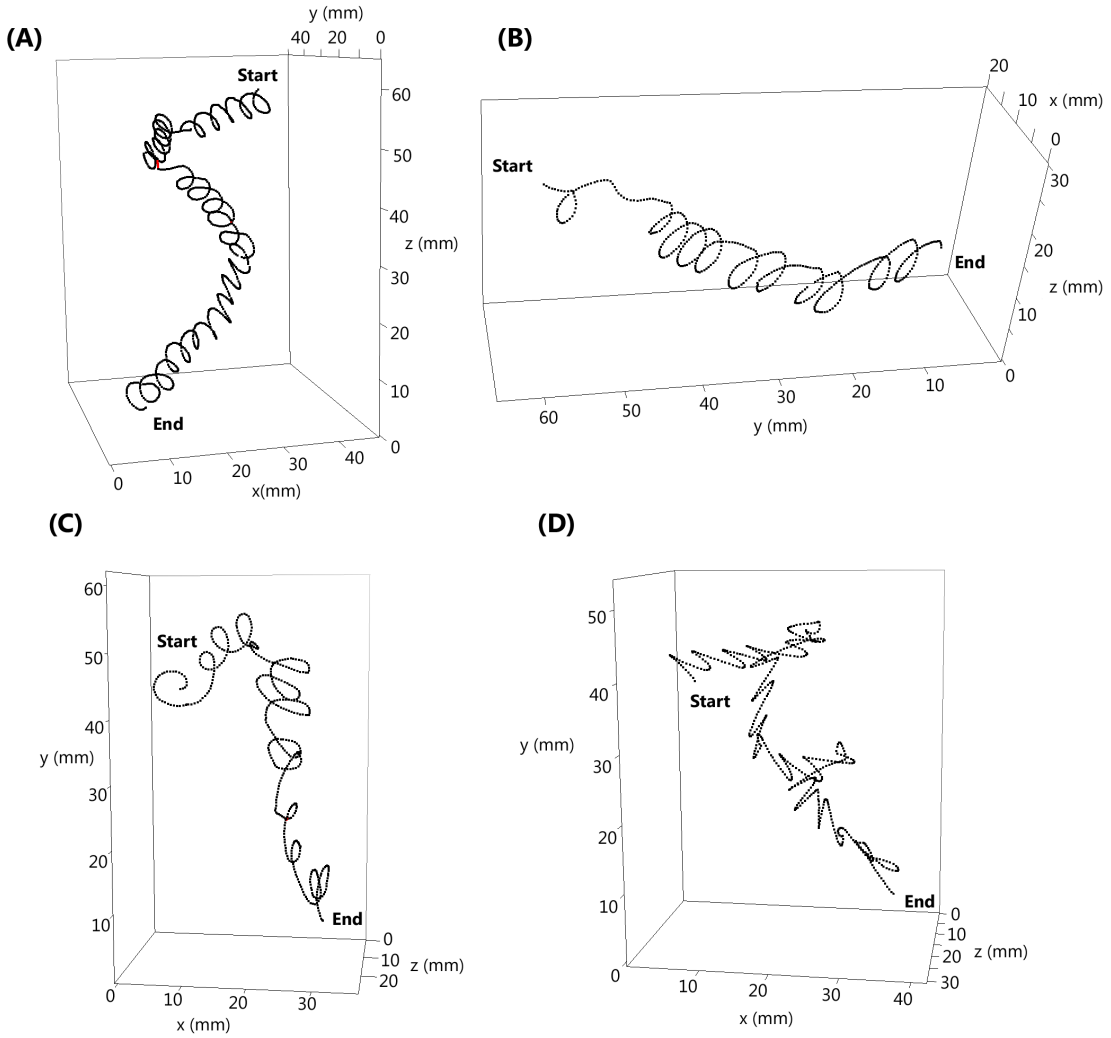

Figure 3.1: Examples of *Centropages typicus* swimming trajectories in presence of food. Dots represent the copepod positions at 1/15 s intervals. (A) Lateral view, Exp. #7, female, 73 s; (B) Lateral view, Exp. #10, male, 33 s; (C) Top view, Exp. #9, female, 37 s; (D) Top view, Exp. #8, female, 39 s.

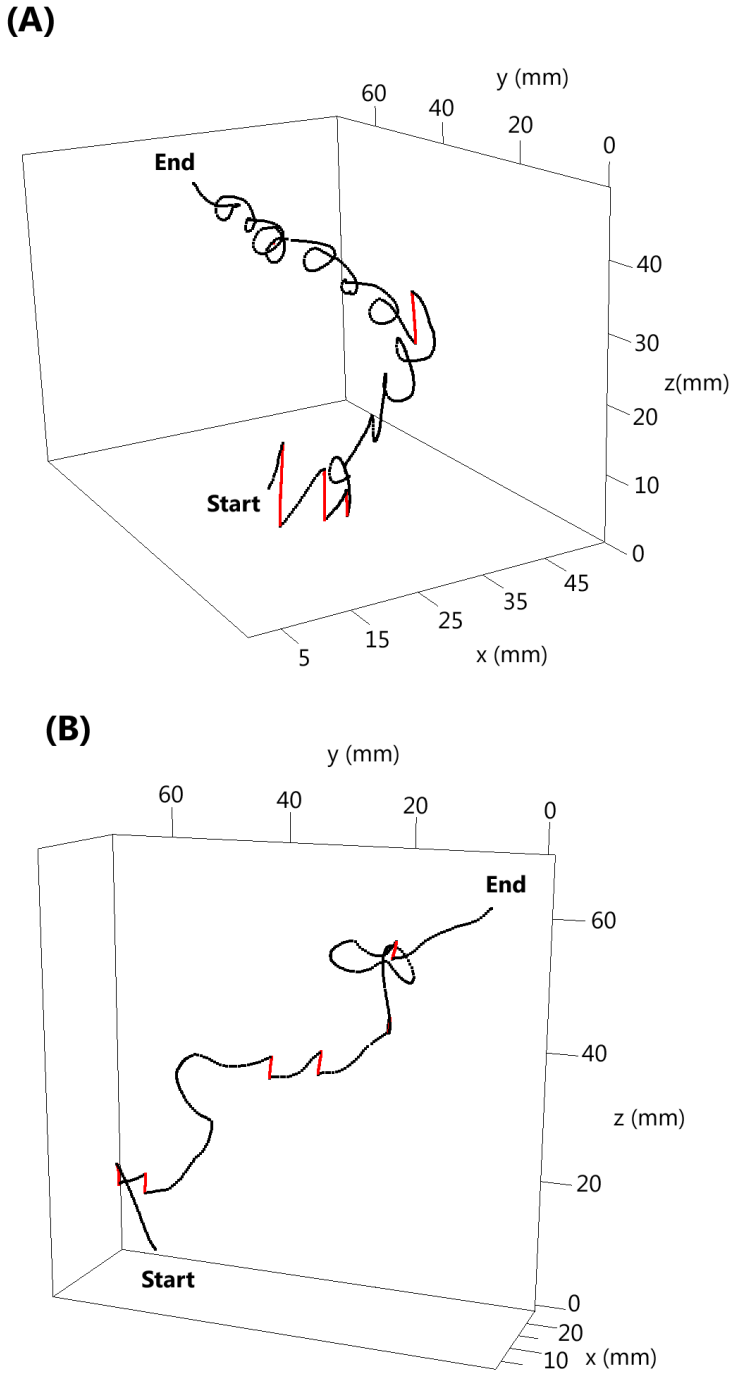

Figure 3.2: Examples of *Centropages typicus* female trajectories in presence of food. Swimming state in black and sinking state in red. (A) Exp. #7, 50 s; (B) Exp. #9, 36 s. Both panels in lateral view.

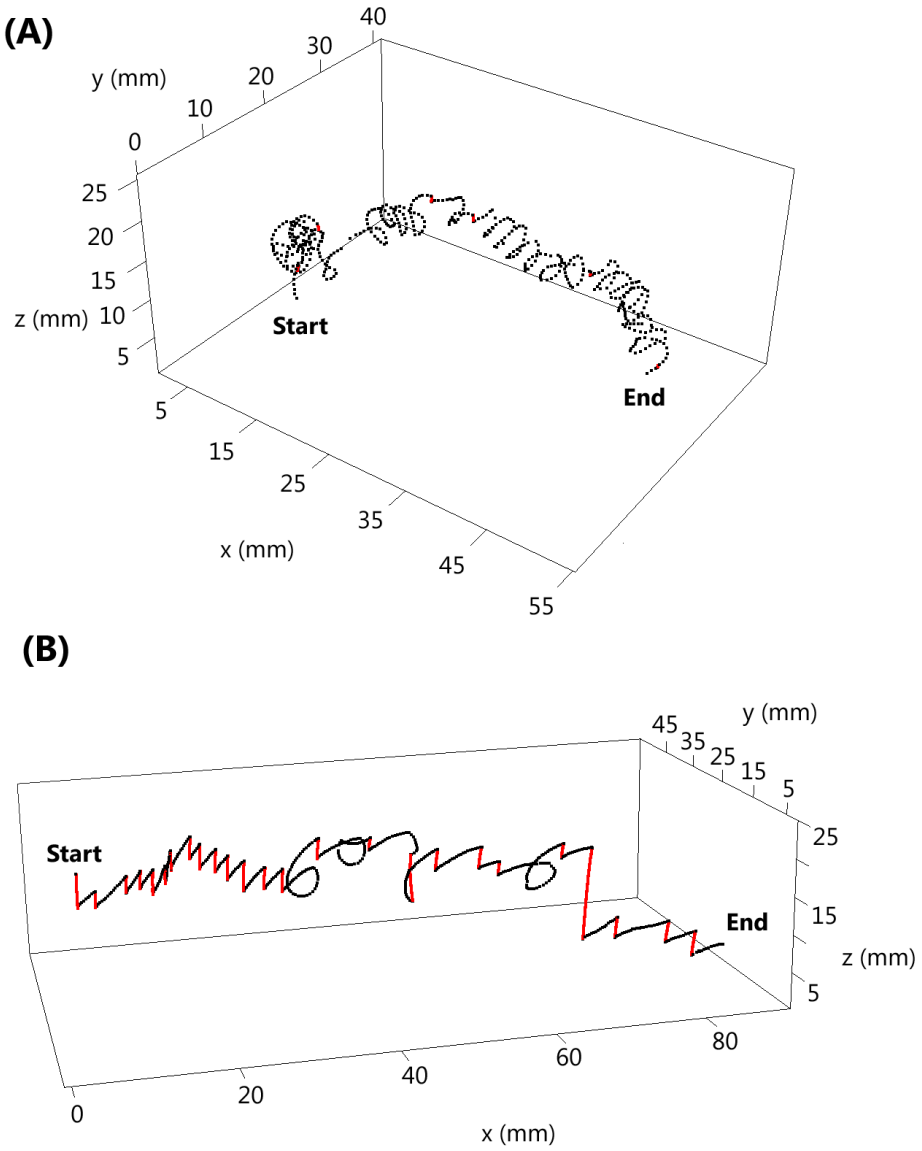

Figure 3.3: Examples of *Centropages typicus* swimming trajectories in presence of food. Dots represent the copepod positions at 1/15 s intervals. Swimming state in black and sinking state in red. (A) Exp. #5, female, 34 s; (B) Exp. #3, male, 83 s. Both panels in lateral view.

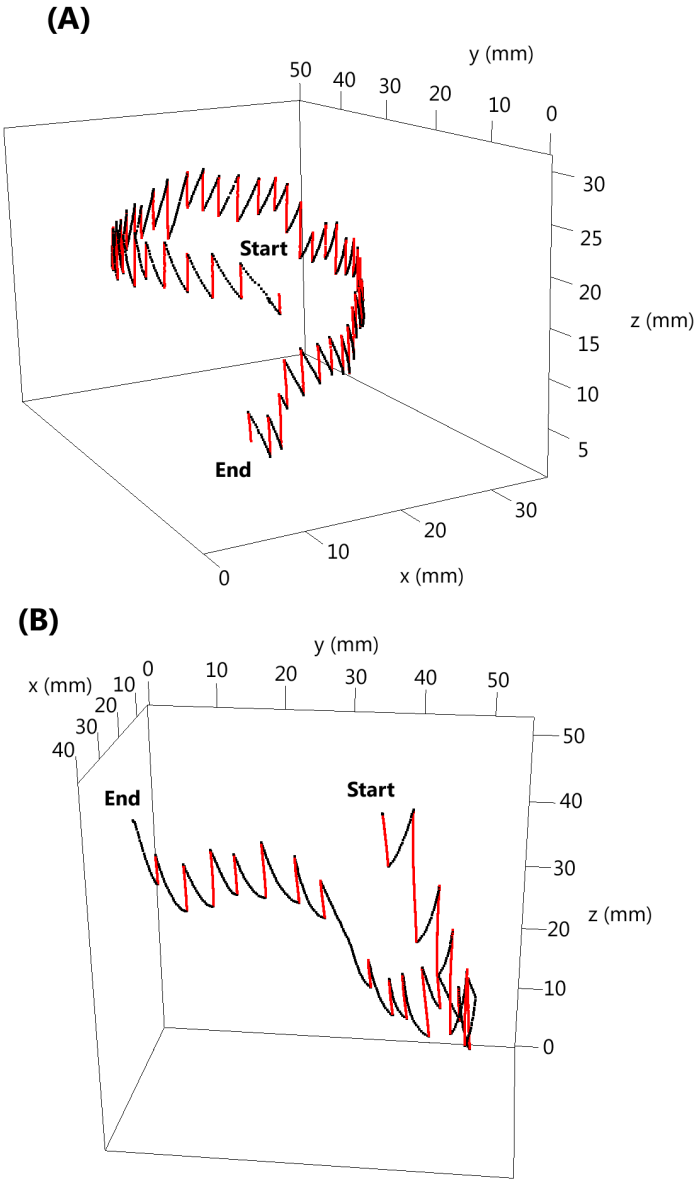

Figure 3.4: Examples of *Centropages typicus* swimming trajectories in filtered sea water. Dots represent the copepod positions at 1/15 s intervals. Swimming state in black and sinking state in red. (A) Exp. #1, male, 146 s; (B) Exp. #2, female, 118 s. Both panels in lateral view.

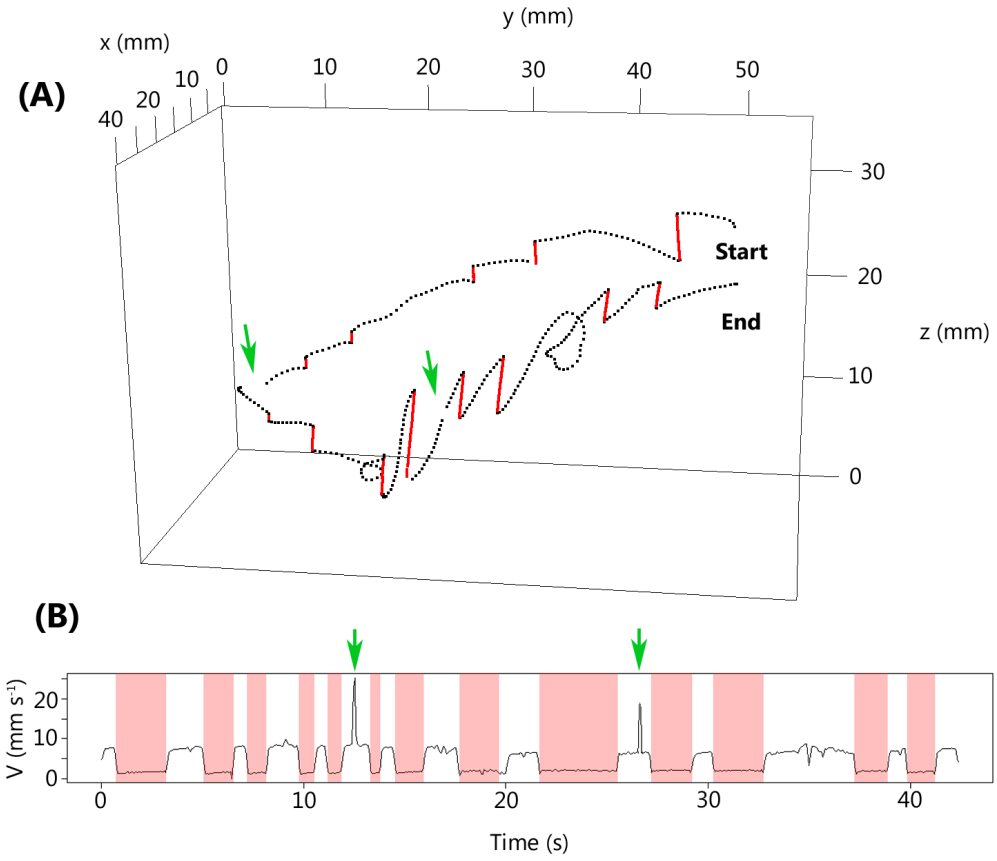

Figure 3.5: Example of *Centropages typicus* female trajectory in presence of food (A) and relative 3D speed diagram (B). Dots represent the copepod positions at 1/15 s intervals. Swimming state in black; sinking state in red; green arrows indicate jumps. Lateral view, Exp. #5, 42 s.

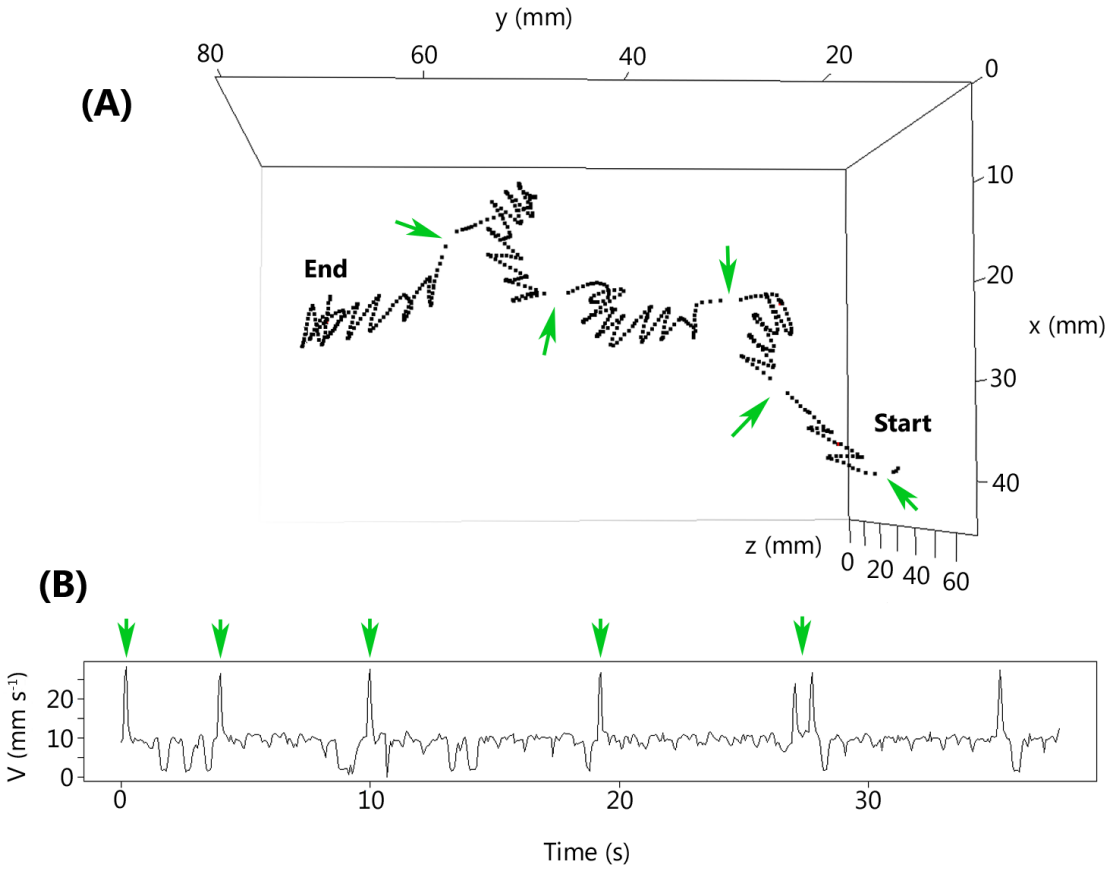

Figure 3.6: Example of *Centropages typicus* female trajectory in presence of food (A) and relative 3D speed diagram (B). Dots represent the copepod positions at 1/15 s intervals; green arrows indicate jumps. Top view, Exp. #5, 38 s.

Table 3.2: General information on *Centropages typicus* swimming trajectories recorded during 10 experiments.

Exp	Date	Gender	ind. L^{-1}	Food	Recording time	N. trajectories	N. points	Cumulative trajectory duration	Max trajectory duration	Max N. simultaneous trajectories
1	29 Apr '08	M	20	No	20' 20"	57	24,567	27' 18"	4' 46"	5
2	29 Apr '08	F	20	No	20' 20"	85	23,295	25' 53"	1' 58"	6
3	30 Apr '08	M	20	Yes	19' 40"	68	23,633	26' 16"	2' 09"	6
4	30 Apr '08	F	20	Yes	20' 20"	129	32,496	36' 06"	1' 19"	5
5	11 Jun '08	F	10	Yes	20' 20"	59	16,911	18' 47"	1' 02"	3
6	11 Jun '08	M	10	Yes	20' 20"	50	16,183	17' 59"	1' 42"	3
7	11 Jun '08	F	50	Yes	20' 20"	242	71,643	1h 19' 36"	3' 33"	9
8	11 Jun '08	M	50	Yes	20' 20"	123	26,512	29' 27"	54"	5
9	11 Jun '08	F	100	Yes	21' 40"	262	55,222	1h 01' 21"	1' 56"	12
10	11 Jun '08	M	100	Yes	21' 40"	376	69,361	1h 17' 04"	1' 05"	15
				Total	3h 24' 20"	1,451	359,823	6h 39' 48"		

F = female, M = male.

Table 3.3: *Centropages typicus* experimental food conditions and swimming activity. Food is reported as cell concentration (cells L^{-1}) and quality (FSW = filtered sea water without particles). Swimming behaviour is reported as occurrence (percentage of time allocation) and duration (s) of the three states: swimming (Sw), sinking (Sk), and jumping (Jp).

					Activity					
			Food condition		**Occurrence (%)**			**Average duration ± SD (s)**		
	Exp.	**ind. L^{-1}**	**cells L^{-1}**	**Quality**	**Sw**	**Sk**	**Jp**	**Sw**	**Sk**	**Jp**
Females	2	20	—	FSW	38.5	61.0	0.5	1.5 ± 1.2	2.8 ± 2.1	0.10 ± 0.05
	4	20	2.8×10^7	∼ 39% *Skeletonema pseudocostatum** ∼ 1.5% cells > 10 µm	75.3	22.5	2.2	2.9 ± 3.6	1.5 ± 1.1	0.08 ± 0.04
	5	10	1.5×10^7	∼ 63% phyto-flagellates < 5 µm	45.4	45.9	8.7	2.6 ± 2.7	2.0 ± 2.7	0.13 ± 0.08
	7	50			69.7	29.0	1.3	3.9 ± 4.5	1.8 ± 1.8	0.11 ± 0.06
	9	100		∼ 24% cells > 10 µm	58.1	40.7	1.2	2.5 ± 2.8	2.4 ± 1.9	0.08 ± 0.04
Males	1	20	—	FSW	36.7	63.1	0.2	1.4 ± 0.7	2.5 ± 1.0	0.09 ± 0.04
	3	20	2.8×10^7	∼ 39% *Skeletonema pseudocostatum** ∼ 1.5% cells > 10 µm	43.8	55.6	0.6	1.2 ± 1.0	1.9 ± 1.2	0.08 ± 0.03
	6	10	1.5×10^7	∼ 63% phyto-flagellates < 5 µm	46.7	51.8	1.5	2.3 ± 1.7	2.3 ± 2.6	0.11 ± 0.05
	8	50			68.2	31.0	0.8	1.9 ± 1.7	1.8 ± 1.2	0.09 ± 0.04
	10	100		∼ 24% cells > 10 µm	58.9	39.9	1.2	1.9 ± 2.1	2.2 ± 1.6	0.09 ± 0.04

* Not colonial (∼ 5 × 10 µm).

3.1.1 Females

In presence of food particles at 2.8×10^7 cells L^{-1} represented mainly by small species ($\sim 10\ \mu$m) and a very few larger cells (Table 3.3), the predominant motion behaviour of *Centropages typicus* females was represented by swimming (75.5%). The average swimming duration was significantly longer in presence of food (2.8 ± 2.1 s) than in filtered sea water (1.5 ± 1.1 s), while sinking was shorter in presence of food (1.5 ± 1.2 s) than without food (2.9 ± 3.6 s) (Table 3.4). In absence of food, 61.0% of the time was allocated to sinking. Jumping represented only a little fraction of the overall activity ($\leqslant 2.2\%$) both in presence and absence of food and had a similar duration of $\sim 1/10$ s in both conditions (Table 3.4).

Table 3.4: Results of the U-test for the statistical comparison of activity duration (swimming, sinking, jumping) of *Centropages typicus* females in presence of food (Exp. #4) and in filtered seawater (FSW) (Exp. #2). $\star$, significant values at $p < 0.05$; $\star\star$ $p < 0.01$; $\star\star\star$ $p < 0.001$; ns, not significant.

	Food		
	Swimming	**Sinking**	**Jumping**
FSW	$\star\star\star$	$\star\star\star$	ns

The frequency distribution of instantaneous speed of *C. typicus* females was three-modal, both in presence and absence of food particles (Fig. 3.7). In presence of food the first peak was observed at 1–3 mm s^{-1}, mainly represented by sinking speed. In absence of food this peak was highest. In presence of food the second peak was higher than in absence of food and were recorded at 7–8 mm s^{-1} and 5–6 mm s^{-1}, respectively. A third peak was rarely observed and was located at 14–18 mm s^{-1} in both conditions.

The mean speed of *C. typicus* females in presence of food (5.6 ± 3.0 mm s^{-1}) was significantly higher ($p < 0.001$) than without food (4.8 ± 4.0 mm s^{-1}). However, excluding sinking states and considering only active swimming in the computation, its mean speed was similar in both conditions (Table 3.7).

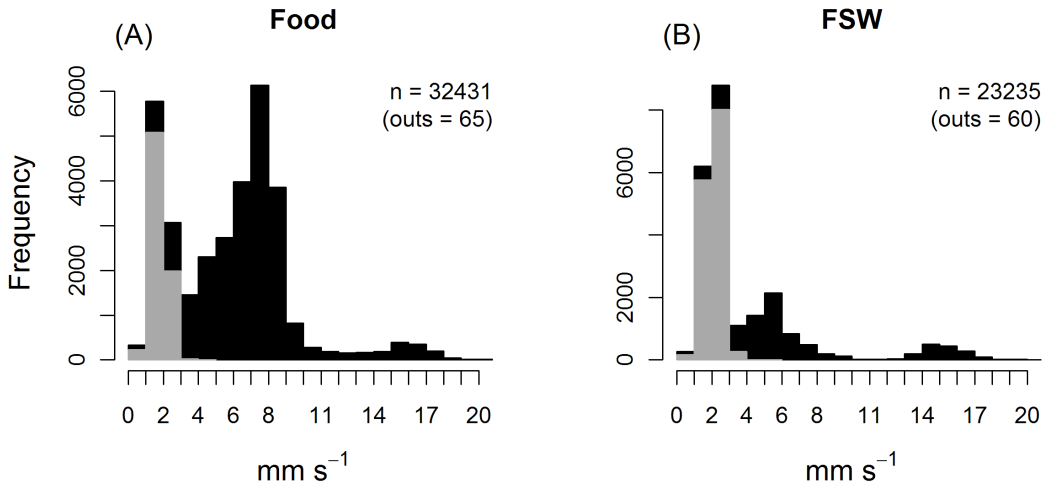

Figure 3.7: Distribution of instantaneous speed (mm s^{-1}) of *Centropages typicus* females during swimming (black) and sinking (grey) states in presence of food (A, Exp. #4) and in filtered sea water (FSW) (B, Exp. #2). Number of points (n) and corresponding values > 20 mm s^{-1} not reported (outs).

Mean values of NGDR estimated at the smallest available resolution (1/15 s) was similar in presence (0.49 ± 0.24) or absence of food (0.54 ± 0.27) (Table 3.5). The horizontal component (HC) of *C. typicus* females trajectories was significant higher with (0.60 ± 0.20) than without (0.37 ± 0.21) food (Table 3.5). The explored volume was significantly larger in presence of food (1.4 ± 0.9 L d^{-1}) than in filtered sea water (1.1 ± 1.2 L d^{-1}) (Table 3.5).

The experiments at different population density (10, 50, 100 ind. L^{-1}) of *C. typicus* females were performed in presence of food particles at 1.5×10^7 cells L^{-1} represented mainly by phytoflagellates < 5 μm (Exp. #5, 7, 9) (Table 3.3). At 10 ind. L^{-1}, the motion activity was equally shared in swimming (45.4%) and sinking (45.9%), with short time allocated to jumping (8.7%). At 50 and 100 ind. L^{-1}, the motion behaviour was mainly dominated by swimming (69.7% and 58.1%, respectively) with less time spent in sinking (29.0%, 40.7%) and very short time in jumping (1.3%, 1.2%). The swimming duration was similar at lowest and highest densities (2.6 ± 2.7 s, 2.5 ± 2.5 s, respectively), while at 50 ind. L^{-1} it was

Table 3.5: Results of the U-test for the statistical comparison of NGDR, horizontal component (HC)and explored volume (EV) of *Centropages typicus* females in presence of food (Exp. #4) and in filtered seawater (FSW) (Exp. #2). ⋆, significant values at $p < 0.05$; ⋆⋆ $p < 0.01$; ⋆⋆⋆ $p < 0.001$; ns, not significant.

	Food		
	NGDR	**HC**	**EV**
FSW	ns	⋆⋆⋆	⋆⋆⋆

significantly higher (3.9 ± 4.5 s) (Table 3.6). The sinking duration at 10 ind. L^{-1} (2.0 ± 2.7 s) was significantly higher than at 50 ind. L^{-1} (1.8 ± 1.8 s) and at 100 ind. L^{-1} (2.4 ± 1.9 s). At different population density, *C. typicus* females jumps had slight but regular decrease (Table 3.3).

Table 3.6: Results of the U-test for the statistical comparison of activity duration (swimming, sinking, jumping) of *Centropages typicus* females at different population density (Exp. #5, 7, 9). ⋆, significant values at $p < 0.05$; ⋆⋆ $p < 0.01$; ⋆⋆⋆ $p < 0.001$; ns, not significant.

	10 ind. L^{-1}			**50 ind. L^{-1}**		
	Swimming	**Sinking**	**Jumping**	**Swimming**	**Sinking**	**Jumping**
100 ind. L^{-1}	ns	⋆⋆⋆	ns	⋆⋆⋆	⋆⋆⋆	ns
50 ind. L^{-1}	⋆⋆	⋆⋆	ns			

The distribution of instantaneous speed of *C. typicus* females at different population density showed two main peaks (Fig. 3.8). The most frequent peak was at 1–3 mm s^{-1} and was mainly dominated by sinking speeds in all three density conditions. The second peak was recorded at 7–8 mm s^{-1} at 10 ind. L^{-1}, 6–8 mm s^{-1} at 50 ind. L^{-1}, and 6–7 mm s^{-1} at 100 ind. L^{-1}. The frequency

polygon plot (Fig. 3.8, D) shows that speeds of 3–6 mm s^{-1} were less frequent at the lowest population density.

The mean speed of *C. typicus* females showed lower values at increasing population density (Fig. 3.9). The same trend is followed by the mean active swimming.

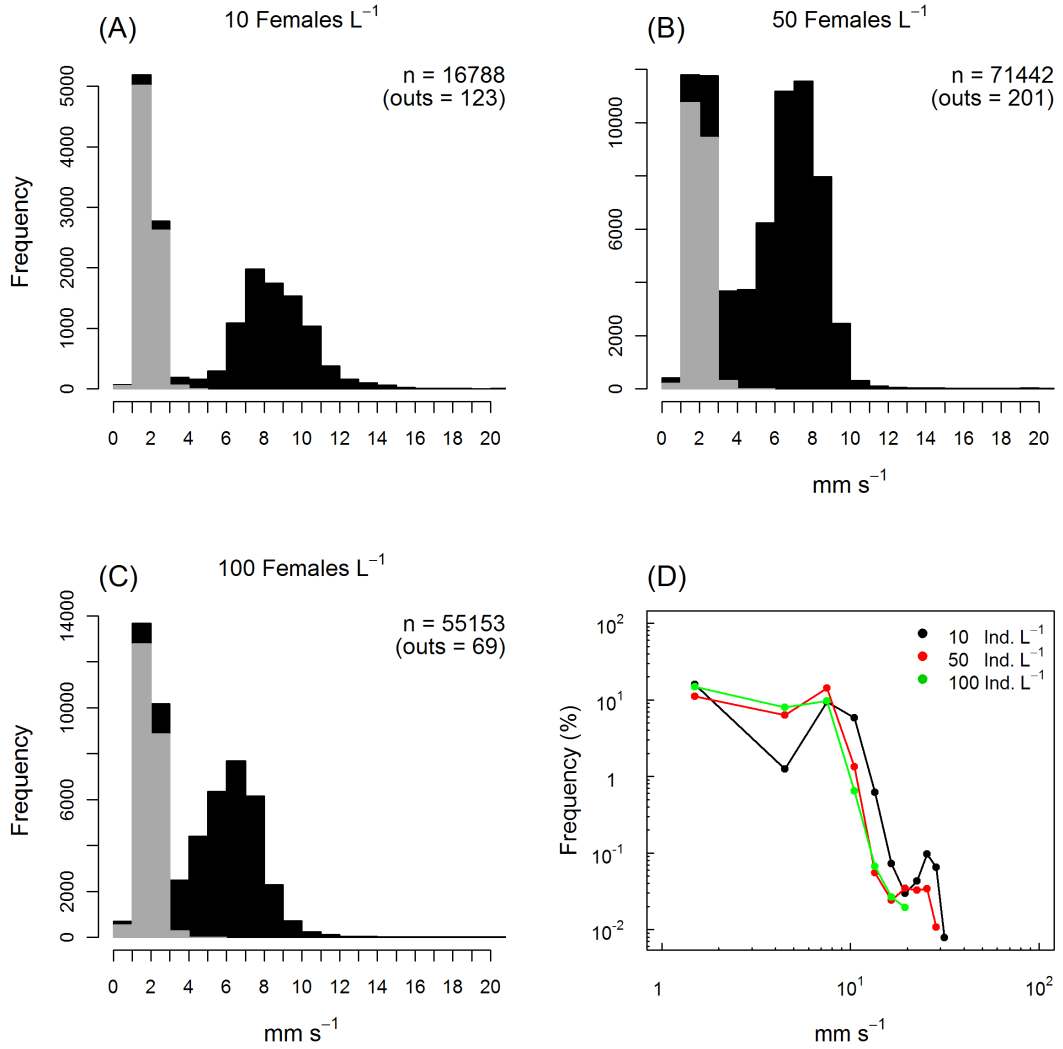

Figure 3.8: Distribution of instantaneous speed (mm s^{-1}) of *Centropages typicus* females during swimming (black) and sinking (grey) states at different population density (ind. L^{-1}) (Exp. #5, 7, 9) (A–C). Number of points (n) and corresponding values > 20 mm s^{-1} not reported (outs). Polygon frequency distribution of instantaneous speed (mm s^{-1}) in Exp. #5 (black), Exp. #7 (red) and Exp. #9 (green) (D).

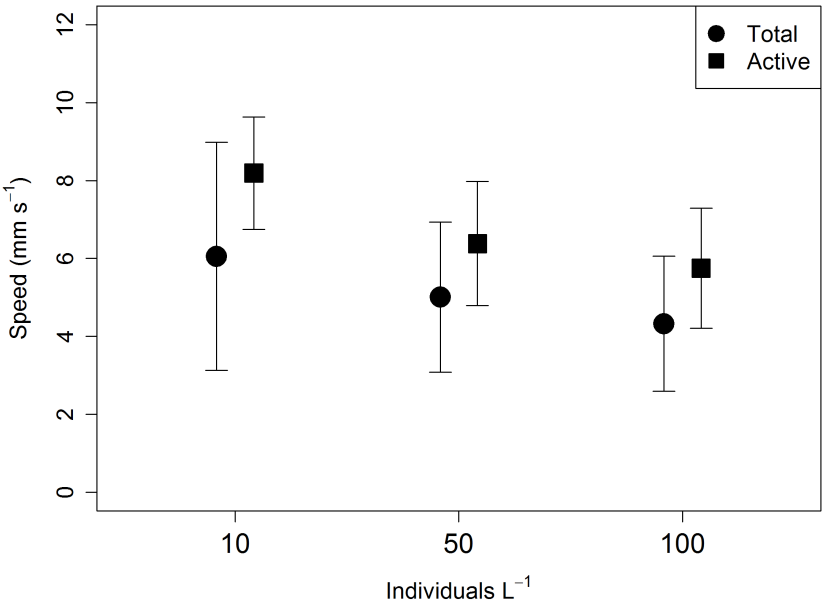

Figure 3.9: Total and active mean speed of *Centropages typicus* females at different population density (Exp. #5, 7, 9) (average ± SD).

The NGDR and horizontal component of *C. typicus* female swimming trajectories did not show significant changes at different population density, with a single exception: NGDR was significantly higher ($p < 0.001$) at 100 ind. L^{-1} than at 50 ind. L^{-1}. The explored volume showed significantly lower values with increasing population density (Table 3.7).

Table 3.7: *Centropages typicus* swimming speed (mean ± SD) computed averaging all instantaneous speed values in all trajectories (Total) or excluding sinking events (Active). Net to Gross Displacement Ratio (NGDR ± SD) was estimated as mean value for each individual track at the smallest resolution (1/15 s). Horizontal Component (HC ± SD) was computed as mean value for each individual track. Explored Volume (EV ± SD).

			Food	**Speed ± SD (mm s^{-1})**		**NGDR**	**HC**	**EV**
	Exp.	**ind. L^{-1}**	**(cells L^{-1})**	**Total**	**Active**	**(adim.)**	**(adim.)**	**(ml h^{-1})**
Females	2	20	—	4.8 ± 4.0	6.7 ± 3.9	0.54 ± 0.27	0.37 ± 0.21	4.8 ± 5.4
	4	20	2.8×10^7	5.6 ± 3.0	6.6 ± 3.1	0.49 ± 0.24	0.60 ± 0.20	6.4 ± 4.0
	5	10	1.5×10^7	6.1 ± 2.9	8.2 ± 1.4	0.52 ± 0.25	0.49 ± 0.25	7.0 ± 4.0
	7	50	1.5×10^7	5.0 ± 1.9	6.4 ± 1.6	0.49 ± 0.25	0.53 ± 0.21	5.6 ± 2.7
	9	100	1.5×10^7	4.3 ± 1.7	5.8 ± 1.5	0.58 ± 0.24	0.51 ± 0.23	4.7 ± 2.4
Males	1	20	—	3.2 ± 1.6	5.3 ± 2.0	0.51 ± 0.23	0.32 ± 0.13	2.9 ± 2.0
	3	20	2.8×10^7	3.4 ± 1.1	5.1 ± 1.1	0.54 ± 0.23	0.43 ± 0.20	3.3 ± 1.6
	6	10	1.5×10^7	4.5 ± 2.3	6.6 ± 2.3	0.59 ± 0.25	0.42 ± 0.20	4.7 ± 3.2
	8	50	1.5×10^7	5.1 ± 2.3	6.6 ± 2.4	0.58 ± 0.24	0.57 ± 0.18	5.6 ± 3.2
	10	100	1.5×10^7	4.5 ± 2.1	6.1 ± 2.0	0.63 ± 0.21	0.53 ± 0.21	5.0 ± 2.9

3.1.2 Males

The prevalent motion behaviour of *Centropages typicus* males was the swimming mode both in presence of food particles, 2.8×10^7 cells L^{-1} concentration, and in absence of food (55.6% and 63.1% allocated time, respectively) (Table 3.3). Sinking occurred more frequently in presence of food (43.8%) than in filtered sea water (36.7%). Jumping represented only a little fraction of the overall activity ($\leqslant 0.6\%$). Swimming and sinking duration were significantly ($p < 0.001$) shorter in presence of food than in filtered sea water while jumps had similar duration of $\sim 1/10$ s in both conditions (Table 3.3).

The distribution of instantaneous speed of *C. typicus* males showed a major peak at 1–2 mm s^{-1} mainly dominated by sinking speeds, independently of food conditions (Fig. 3.10). A second and minor peak was recorded at 5–6 mm s^{-1} only in presence of food. The mean speed of *C. typicus* males was higher ($p < 0.05$) with (3.4 ± 1.1 mm s^{-1}) than without (3.2 ± 1.6 mm s^{-1}) food (Table 3.7). Considering only active swimming states, the mean speed was similar in both conditions (Table 3.7).

The NGDR values computed on *C. typicus* males swimming trajectories were very similar both with and without food (Table 3.7). The horizontal component of trajectories was higher ($p < 0.05$) in presence of food while the explored volume did not differ significantly (Table 3.7).

The experiments at different population density of *C. typicus* males showed that swimming prevailed over sinking at intermediate and highest individual abundance (Table 3.3). The average swimming duration was significantly higher ($p < 0.001$) at the lowest concentration, while the sinking duration was significantly shorter ($p < 0.01$) at intermediate density (Table 3.7). Jumps had similar duration ($\sim 1/10$ s) at all density conditions (Table 3.8).

The distribution of instantaneous speed of *C. typicus* males showed the most frequent peak at 1–2 mm s^{-1}, mainly dominated by sinking speeds, for all three population densities (Fig. 3.11). Frequency peaks at 5–6 mm s^{-1} and 7–8 mm s^{-1} were recorded at 10 ind. L^{-1} and 50 ind. L^{-1}, respectively. For the highest population density (100 ind. L^{-1}), the instantaneous speed had the highest frequency at 5–7 mm s^{-1}. No major differences were observed among different population

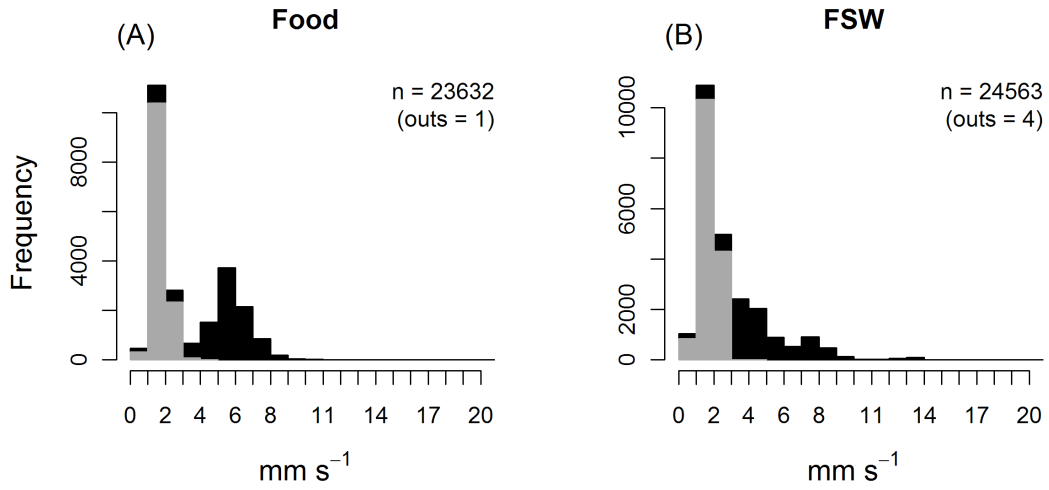

Figure 3.10: (A–C) Distribution of instantaneous speed (mm s^{-1}) of *Centropages typicus* males during swimming (black) and sinking (grey) states at different population density (ind. L^{-1}) (Exp. #6, 8, 10). Number of points (n) and corresponding values $>$ 20 mm s^{-1} not reported (outs). (D) Polygon frequency distribution of instantaneous speed (mm s^{-1}) in Exp. #6 (black dots), Exp. #8 (red dots) and Exp. #10 (green dots).

densities in terms of instantaneous speed distribution along the entire speed range (Fig. 3.11, D).

The mean speed of *C. typicus* males showed similar values at the lowest (4.5 ± 2.3 mm s^{-1}) and highest(4.5 ± 2.1 mm s^{-1}) population density (Table 3.7). At intermediate density of 50 ind. L^{-1}, the mean speed was significantly higher than at the highest population density both considering the total ($p < 0.05$) or the active ($p < 0.01$) phase.

The NGDR values were similar whatever the population densities (Table 3.9). However, the horizontal component of trajectories was significantly higher at intermediate population density (Table 3.7). The explored volume was similar at 10 and 100 ind. L^{-1} (1.1 ± 0.7, 1.1 ± 0.7 L d^{-1}) but statistically higher at intermediate density (1.3 ± 0.7 L d^{-1}) (Table 3.9).

Table 3.8: Results of the U-test for the statistical comparison of activity duration (swimming, sinking, jumping) of *Centropages typicus* males at different population density (Exp. #6, 8, 10). $\star$, significant values at $p < 0.05$; $\star\star$ $p < 0.01$; $\star\star\star$ $p < 0.001$; ns, not significant.

	10 ind. L^{-1}			**50 ind. L^{-1}**		
	Swimming	**Sinking**	**Jumping**	**Swimming**	**Sinking**	**Jumping**
100 ind. L^{-1}	$\star\star\star$	ns	ns	ns	$\star\star$	ns
50 ind. L^{-1}	$\star\star\star$	ns	ns			

Table 3.9: *Centropages typicus* males NGDR, HC, EV test U di Wilcoxon-Mann-Whitney at different population density (Exp. #6, 8, 10). $\star$, significant values at $p < 0.05$; $\star\star$ $p < 0.01$; $\star\star\star$ $p < 0.001$; ns, not significant.

	10 ind. L^{-1}			**50 ind. L^{-1}**		
	NGDR	**HC**	**EV**	**NGDR**	**HC**	**EV**
100 ind. L^{-1}	ns	$\star\star\star$	ns	ns	$\star$	$\star$
50 ind. L^{-1}	ns	$\star\star\star$	$\star$			

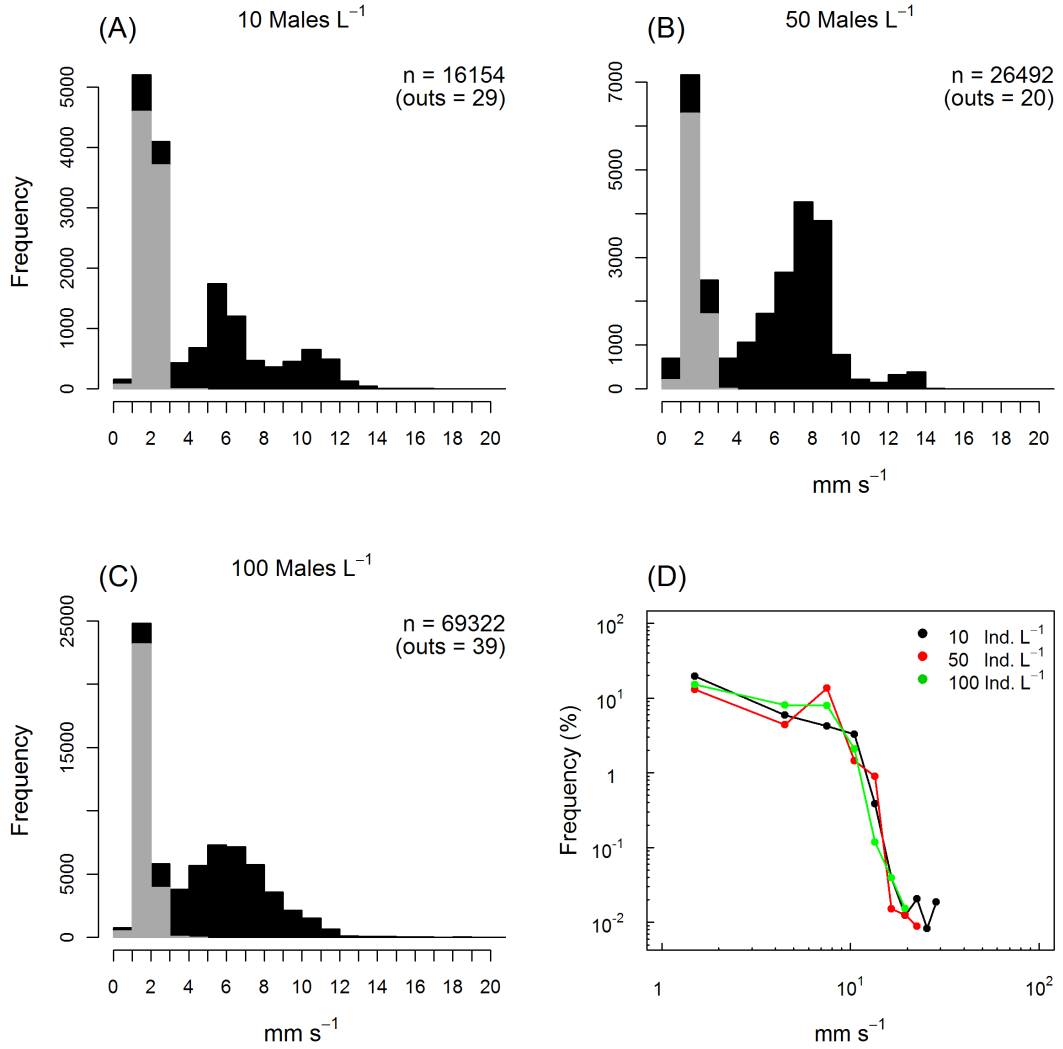

Figure 3.11: Distribution of instantaneous speed (black) (mm s^{-1}) of *Centropages typicus* males at different population density (ind. L^{-1}) (Exp. #6, 8, 10) (A–C). Superimposed sinking instantaneous speed (grey). Number of points (n) and number of values > 20 mm s^{-1} not presented in figure (outs). Frequency distribution of instantaneous speed (mm s^{-1}) in Exp. #6 (black), Exp. #8 (red) and Exp. #10 (green) (D).

3.1.3 Gender comparison

Centropages typicus females and males behave differently, both in presence of food and in filtered sea water. Females' predominant behaviour was swimming in presence of food and sinking without food, while males spent most of the time sinking in both food conditions (Fig. 3.12, A).

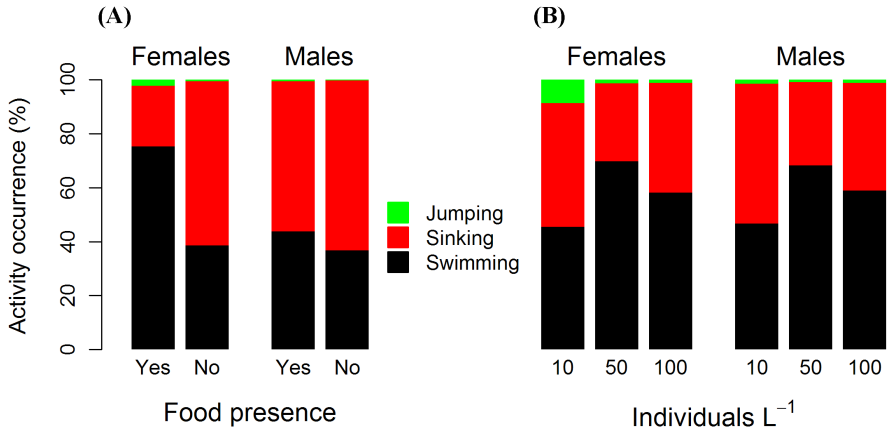

Figure 3.12: Activity occurrence (%) (swimming, sinking, jumping) in *Centropages typicus* females and male in presence or absence of food (A) and at different population density (B).

Over the different population density, females and males had very similar swimming behaviour. The only difference was represented by the females jumping at the lowest population density (Fig. 3.12, B).

Swimming duration for females was longer in presence of food than in filtered sea water, while no significant differences were recorded for males (Fig. 3.13). Females tended to sink shorter than males in presence of food, while the opposite was recorded without food. Females and males were similar in sinking and jumping.

The swimming duration of females was longer than males at all population density. However, sinking duration were similar between the gender at higher concentrations.

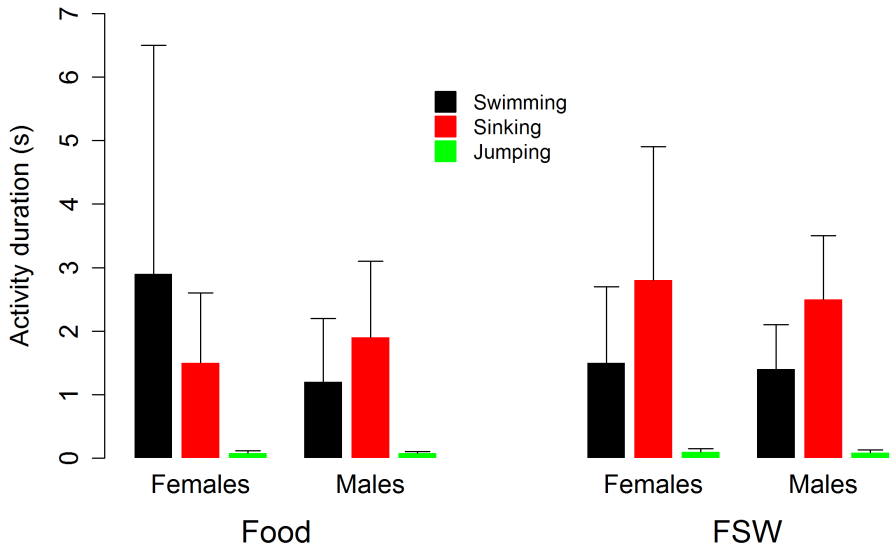

Figure 3.13: Activity duration (swimming, sinking, jumping) in *Centropages typicus* females and male in presence of food (left panel) and in filtered sea water (right panel).

Average total and active speeds, and average horizontal component were higher in females than in males in both food conditions ($p < 0.05$).

The total and active speeds of *C. typicus* females were higher than males at the lowest density and similar at higher density (Fig. 3.14). The explored volume was higher in females only at 10 ind. L^{-1}.

3.1.4 Synthesis

Centropages typicus females and males show similar swimming trajectories composed prevalently by fast looping and less frequent rectilinear paths. The NGDR values remain similar in different experimental conditions indicating that the complexity of the trajectories do not vary in spite of changes in speed or sinking activity. Active swimming is interrupted by sinking at very low speed, more frequently in males. Two major peaks were observed in speed distribution: the first peak (1–2 mm s^{-1}) is associated with the sinking phase weather the second

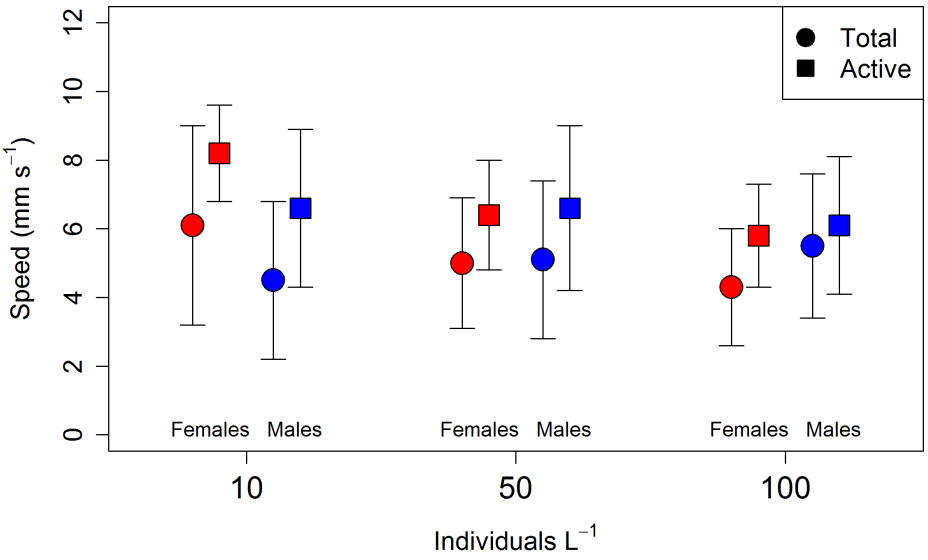

Figure 3.14: Total and active mean speed of *Centropages typicus* females (red) and males (blue) at different population density (average ± SD).

one ($> 5mm$ s^{-1} and depending of experimental condition) is associated with swimming state.

The presence of food affects the swimming behaviour by reducing the sinking and increasing the swimming phase, and thus more clearly in females than in males. When food is present, females spend more time swimming and less time sinking and they increase the swimming speed. Jumping occurs arely in both genders and in any conditions (with or without food supply).

Copepod density affects female and male behaviour by lengthening the swimming phase to decreasing of sinking and jumping, but with a significant reduction of the speed.

3.2 *Acartia clausi*

The swimming behaviour of *Acartia clausi* females and males was analysed over 6 experiments, *i.e.*, 2,151 three-dimensional (3D) trajectories. They lasted complexively more than 11 hours and provided an extensive dataset for statistical treatment (Table 3.10). Up to 16 copepods could be followed simultaneously, making possible to explore individual variability.

Both females and males moved at very slow speed and made frequent fast jumps. The slow swimming, which was associated to the creation of feeding currents, included (1) hovering, when the copepod keeps its position without sinking; and (2) sinking. Jumps were made by flapping the posterior swimming legs and then folding the first antennae (A1) backwards. The *A. clausi* usual posture was with the A1 open and the body not orientated along a preferential direction. Any jump determined the successive body orientation.

The 3D swimming trajectories of females and males developed in vertical or horizontal directions and were all characterized by frequent jumps even in different food conditions (Fig. 3.15) or population density (Fig. 3.16). Jumps were mostly oriented upward regardless the swimming path direction (Fig. 3.17).

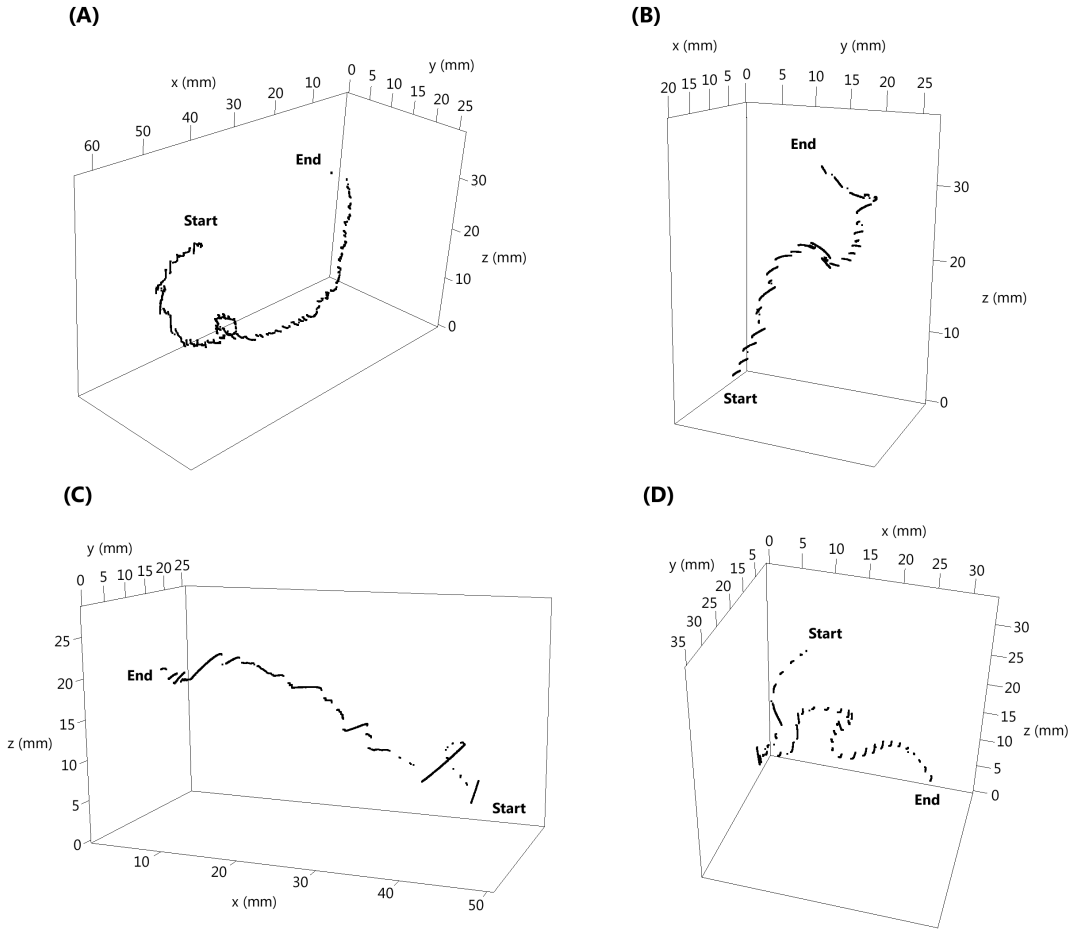

Figure 3.15: Examples of *Acartia clausi* swimming trajectories at 50 ind. L^{-1} concentration. Dots represent the copepod positions at 1/15 s intervals. (A) Exp. #12, female with food, 123 s; (B) Exp. #13, female in filtered sea water, 80 s; (C) Exp. #11, male with food, 64 s; (D) Exp. #14, male in filtered sea water, 70 s.

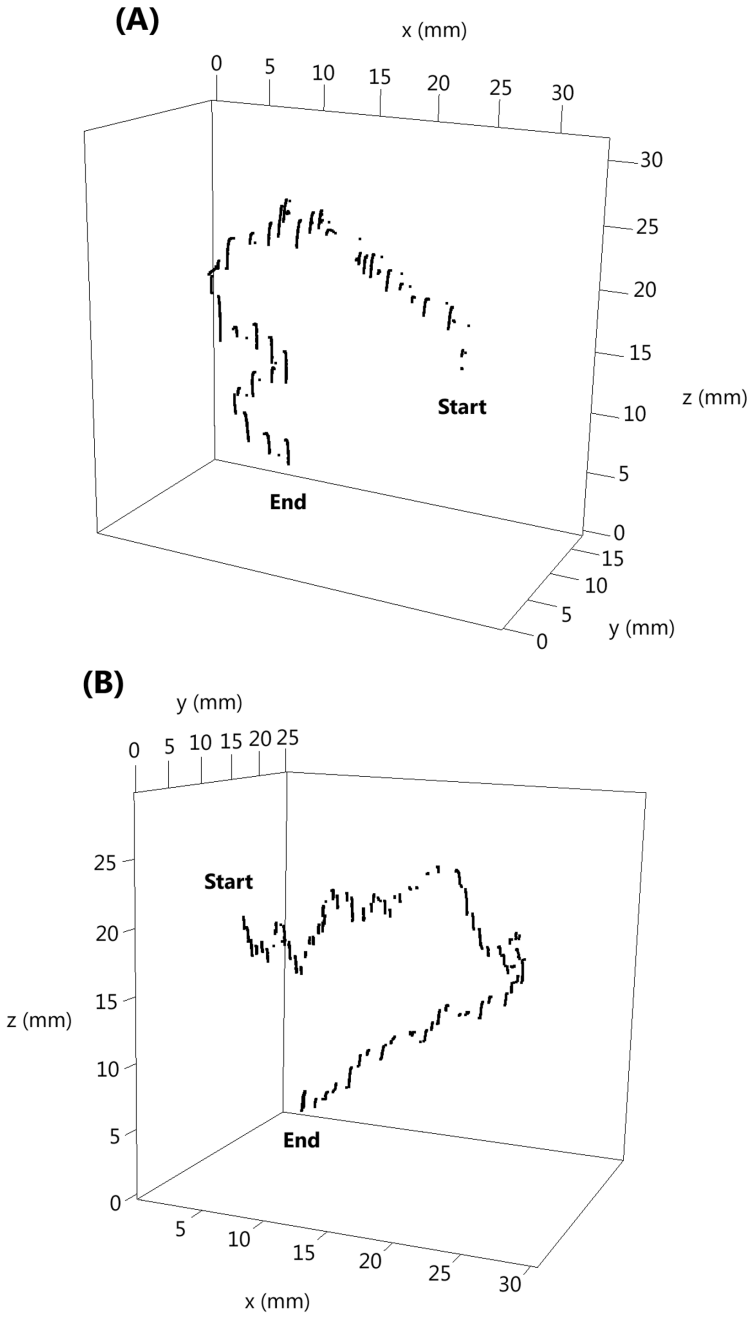

Figure 3.16: Examples of *Acartia clausi* swimming trajectories in presence of food at 25 ind. L^{-1} concentration. Dots represent the copepod positions at 1/15 s intervals. (A) Exp. #35, female, 76 s; (B) Exp. #34, male, 80 s.

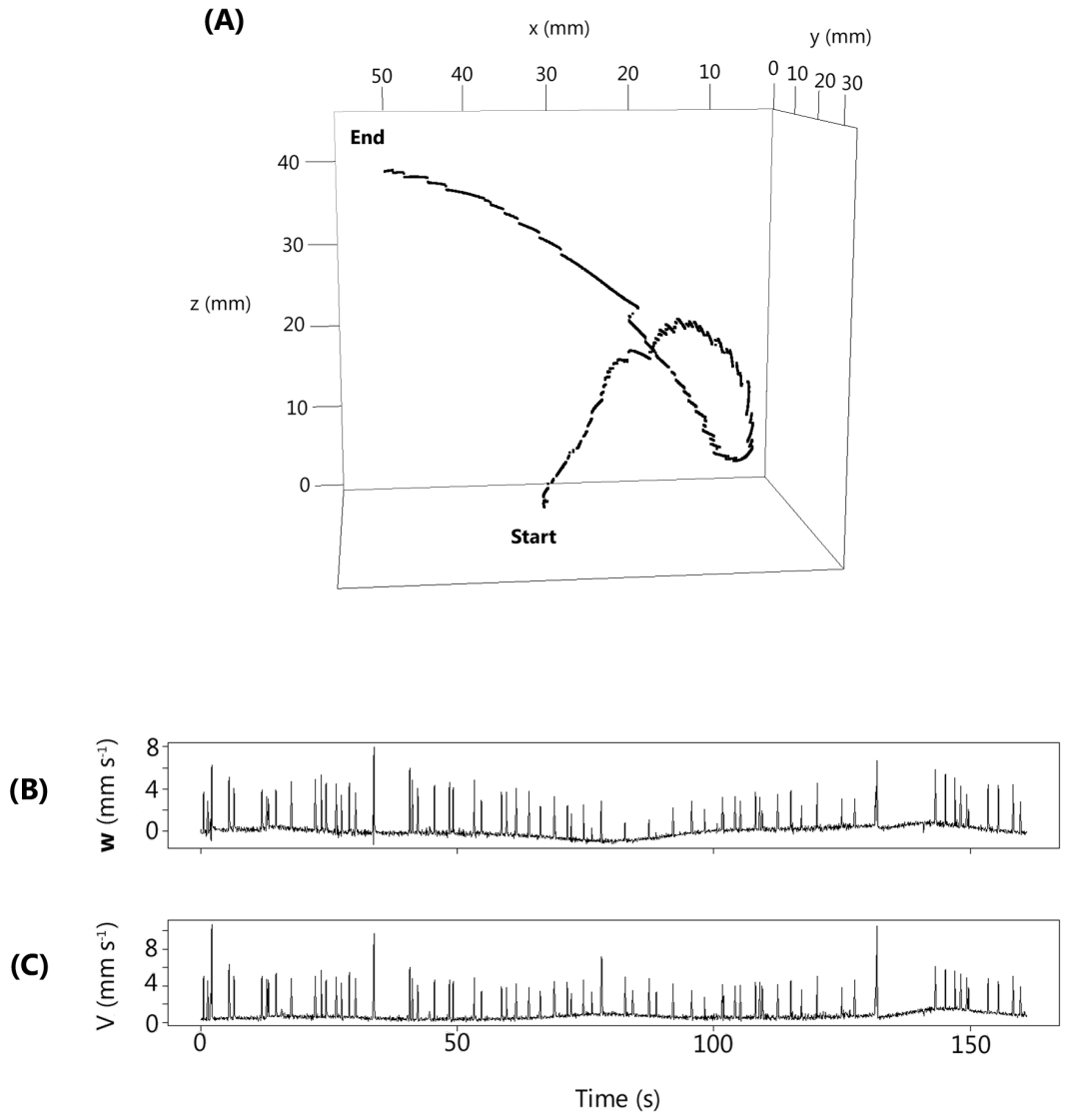

Figure 3.17: Example of *Acartia clausi* female trajectory (dots are copepod positions at 1/15 s intervals) in presence of food (A), relative vertical velocity (B), and 3D speed (C). Exp. #13, 161 s.

Table 3.10: General information on *Acartia clausi* swimming trajectories recorded during 6 experiments.

Exp	Date	Gender	ind. L^{-1}	Food	Recording time	N. trajectories	N. points	Cumulative trajectory duration	Max trajectory duration	Max N. simultaneous trajectories
11	10 July '08	M	50	Yes	20' 20"	503	145,371	2h 41' 31"	2' 01"	16
12	10 July '08	F	50	Yes	20' 20"	354	125,550	2h 19' 30"	4' 22"	13
13	14 July '08	F	50	No	20' 20"	312	107,065	1h 58' 58"	2' 41"	12
14	14 July '08	M	50	No	20' 20"	414	130,779	2h 25' 19"	2' 03"	15
34	15 May '09	M	25	No	33' 40"	229	56,407	1h 02' 40"	1' 48"	7
35	19 May '09	F	25	No	33' 40"	339	95,196	1h 45' 46"	1' 55"	7
				Total	2h 28' 40"	2,151	660,368	11h 13' 44"		

F = female, M = male.

3.2.1 Females

Acartia clausi females motion behaviour was very similar in presence of food particles at 1.0×10^7 cells L^{-1} and in filtered sea water. In both conditions, the swimming time was mainly allocated in sinking ($\sim 72\%$), then hovering ($\sim 24\%$) and jumping ($\sim 3\%$) (Table 3.11).

The average resting time, *i.e.* the time that copepod spent between two successive jumps performing hovering or sinking, was significantly smaller ($p < 0.001$) in presence of food (1.9 ± 1.7 s) than without food (2.1 ± 1.7 s). The average time spent performing jumps was the same in both food conditions of $\sim 1/10$ s.

Instantaneous speeds were most frequent in the range of 0–2 mm s^{-1} and mainly dominated by sinking (Fig. 3.18, A, C). The jumping vertical direction was mainly upward with or without food (Fig. 3.18, B, D).

In absence of food, *A. clausi* females decreased significantly the speed to 1.2 ± 0.5 mm s^{-1} ($p < 0.001$). Also jumping speed and frequency (jumps $min^{-}1$) decreased significantly ($p < 0.001$) in absence of food (Table 3.12). The NGDR and the horizontal component increased in absence of food indicating that trajectories were less convoluted and more horizontal than in presence of food. The explored volume remained similar in both conditions (Table 3.12).

In the experiment conducted in 2009, the population was reduced from 50 to 25 ind. L^{-1}. That led to the decrease time spent in hovering (from 24% to 8%) and the increase that spent in jumping (from 3.7% to 5.6%.) (Table 3.11). The duration of hovering and sinking diminished significantly ($p < 0.01$) while jumping were performed at the same $\sim 1/10$ s (Table 3.11).

At different population density, instantaneous speeds were very similar, with the major peak at 0–2 mm s^{-1} and mainly dominated by sinking. The jumping vertical direction was mainly upward in both population conditions (Fig. 3.18).

At lower population density, *A. clausi* females increased significantly the total speed ($p < 0.001$) as a consequence of the increased jumping frequency (from 31.0 ± 15.7 to 48.7 ± 21.5 min^{-1}). Also the NGDR values decreased (from 0.54 ± 0.18 to 0.39 ± 0.15) while the explored volume slightly increased (Table 3.12).

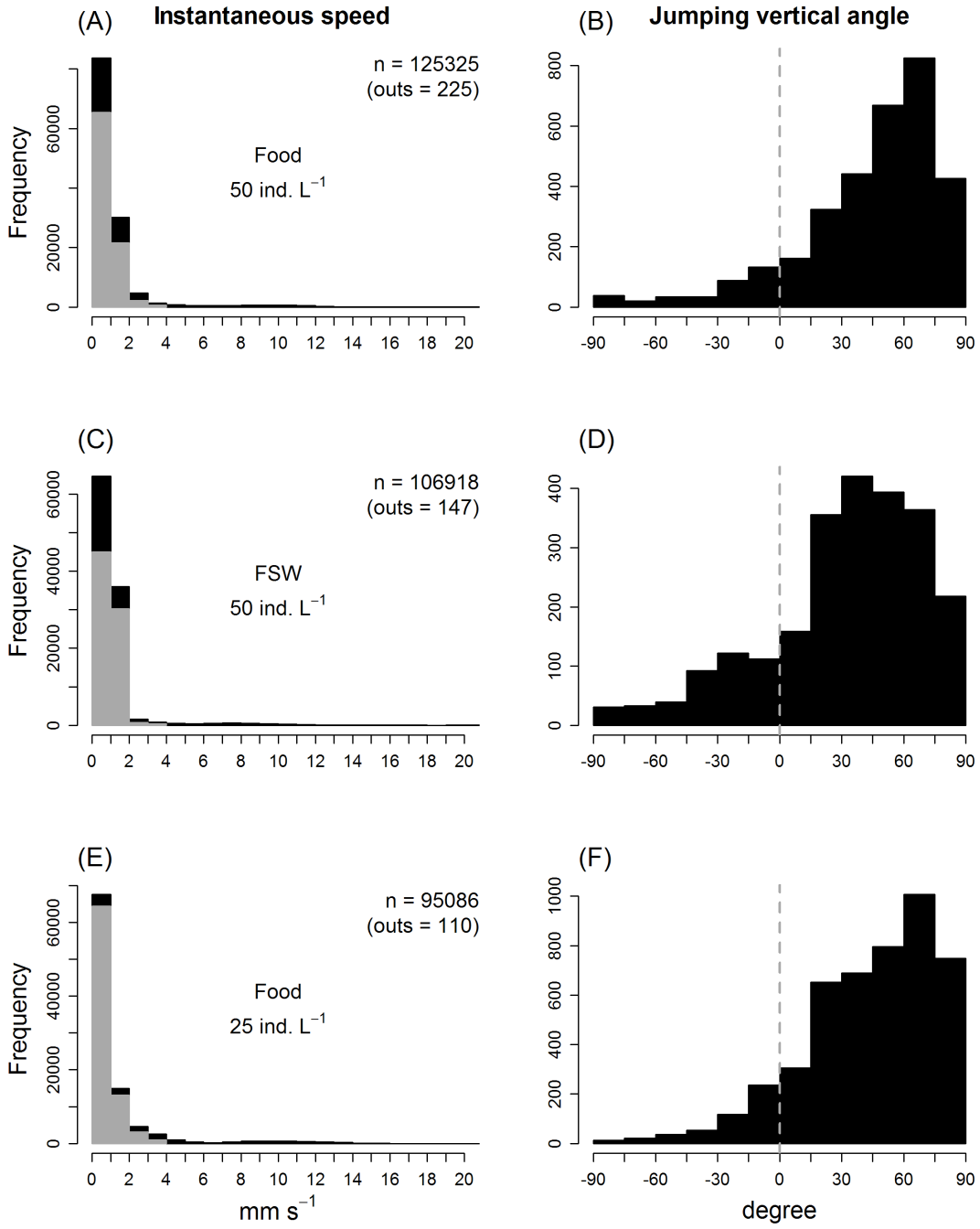

Figure 3.18: Distribution of instantaneous speed (mm s^{-1}) of *Acartia clausi* females during swimming state (black) and sinking (grey) with number of points (n) and corresponding values > 20 mm s^{-1} not reported (outs), and distribution of jumping vertical angles (deg.). Dotted line separates left side, reporting downward jumps direction (negative values), and right side, reporting upward jumps direction (positive values). A, B Exp. #12; C, D Exp. #13; E, F Exp. #35.

Table 3.11: *Acartia clausi* experimental food conditions and swimming activity. Food is reported as cells concentration (cells L^{-1}) and phytoplankton quality (FSW = filtered sea water without particles). Swimming behaviour is reported as occurrence (percentage of time allocation) and duration (s) of the hovering or jumping state.

			Food condition			**Activity**				
			Microzoo	**Phytoplankton**		**Occurrence (%)**			**Duration ± SD (s)**	
	Exp.	**ind. L^{-1}**	**(cells L^{-1})**	**(cells L^{-1})**	**Quality**	**Hv**	**Sk**	**Jp**	**Hv + Sk**	**Jp**
Females	12	50	5.6×10^3	1.0×10^7	$\sim$ 46% phyto-flagellates $< 5\,\mu$m $\sim$ 20% cells $> 10\,\mu$m	23.8	72.5	3.7	1.9 ± 1.7	0.09 ± 0.04
	13	50	—	—	FSW	24.5	72.3	3.2	2.1 ± 1.7	0.09 ± 0.04
	35	25	1.4×10^4	5.0×10^7	$\sim$ 55% *Skeletonema pseudocostatum** $\sim$ 3% cells $> 10\,\mu$m	7.6	86.8	5.6	1.2 ± 0.8	0.08 ± 0.03
Males	11	50	5.6×10^3	1.0×10^7	$\sim$ 46% phyto-flagellates $< 5\,\mu$m $\sim$ 20% cells $> 10\,\mu$m	19.9	77.5	2.6	2.0 ± 2.1	0.09 ± 0.04
	14	50	—	—	FSW	21.2	76.2	2.6	2.2 ± 1.9	0.09 ± 0.04
	34	25	1.4×10^4	5.0×10^7	$\sim$ 55% *Skeletonema pseudocostatum** $\sim$ 3% cells $> 10\,\mu$m	4.3	91.1	4.6	1.7 ± 1.4	0.10 ± 0.05

* Not colonial ($\sim 5 \times 10\ \mu$m).

Table 3.12: *Acartia clausi* swimming speed (mean ± SD) computed averaging all instantaneous speed values in all trajectories (Total) or in jumping events (Jump). Jump frequency (min^{-1}) is the average on mean values in all trajectories. Net to Gross Displacement Ratio (NGDR ± SD) was estimated as mean value for each individual track at the smallest resolution (1/15 s). Horizontal Component (HC ± SD) was computed as mean value for each individual track. Explored Volume (EV ± SD).

			Food	**Speed ± SD (mm s^{-1})**		**Jump freq.**	**NGDR**	**HC**	**EV**
	Exp.	**ind. L^{-1}**	**(cells L^{-1})**	**Total**	**Jump**	**(min^{-1})**	**(adim.)**	**(adim.)**	**(ml h^{-1})**
Females	12	50	1.0×10^7	1.3 ± 0.5	14.2 ± 5.8	31.0 ± 15.7	0.54 ± 0.18	0.58 ± 0.18	3.5 ± 1.3
	13	50	—	1.2 ± 0.5	13.0 ± 5.9	27.1 ± 14.5	0.62 ± 0.19	0.60 ± 0.17	3.2 ± 1.2
	35	25	5.0×10^7	1.4 ± 0.4	12.4 ± 3.7	48.7 ± 21.5	0.39 ± 0.15	0.50 ± 0.07	3.9 ± 0.9
Males	11	50	1.0×10^7	1.2 ± 0.5	16.3 ± 6.8	23.7 ± 16.3	0.60 ± 0.18	0.59 ± 0.18	3.2 ± 1.2
	14	50	—	1.4 ± 0.9	16.0 ± 7.8	22.7 ± 15.1	0.59 ± 0.18	0.60 ± 0.17	3.5 ± 1.2
	34	25	5.0×10^7	1.4 ± 0.4	15.8 ± 5.2	29.7 ± 13.0	0.53 ± 0.16	0.47 ± 0.08	3.7 ± 0.9

3.2.2 Males

A. clausi males had similar motion behaviour in presence of food particles and in filtered sea water. Time was mainly allocated in sinking both with (77.5%) and without (76.2%) food. In both conditions, hovering accounted for 19.9% and 21.2% of time, and jumping only 2.6% (Table 3.11).

The time spent between two successive jumps, by performing hovering or sinking, was significantly smaller in presence of food (2.0 ± 2.1 s) than without food (2.2 ± 1.9 s) ($p < 0.001$). The average time spent performing jumps was the same (0.09 ± 0.04 s) in both food conditions.

In different food conditions, instantaneous speeds were most frequent at 0–2 mm s^{-1} and mainly dominated by sinking (Fig. 3.19, A, C). The jumping vertical direction was mainly upward (Fig. 3.18, B, D). Speed increased significantly ($p < 0.001$) from food to without food conditions (1.2 ± 0.5 mm s^{-1} to 1.4 ± 0.9 mm s^{-1}, respectively) while jumping speed and frequency did not change significantly (Table 3.12). The NGDR, the horizontal component, and the explored volume remained similar.

Changing copepod abundance from 50 to 25 ind. L^{-1}, sinking time increased to 91.1%, hovering time decreased from 19.9% to 4.3%, while time spent in jumping increased from 2.6% to 4.6%. The duration of hovering and sinking diminished significantly ($p < 0.01$) from 2.0 ± 2.1 s to 1.7 ± 1.4 s while jumping duration remained the same (Table 3.11). Instantaneous speeds were very similar both population densities, with the major peak frequency in the range of 0–2 mm s^{-1} and mainly dominated by sinking (Fig. 3.19). The jumping in vertical direction was mainly upward in both conditions. Decreasing population density the total speed increased significantly ($p < 0.001$) and the jumping speed remained unchanged (Table 3.12). The jumping frequency passed from 23.7 ± 16.3 min^{-1} to 29.7 ± 13.0 min^{-1}. The NGDR values was lower as well as the horizontal component while the explored volume did not change. The frequency polygon plot shows that *A. clausi* male speed was slightly higher at lower population density (Fig. 3.20).

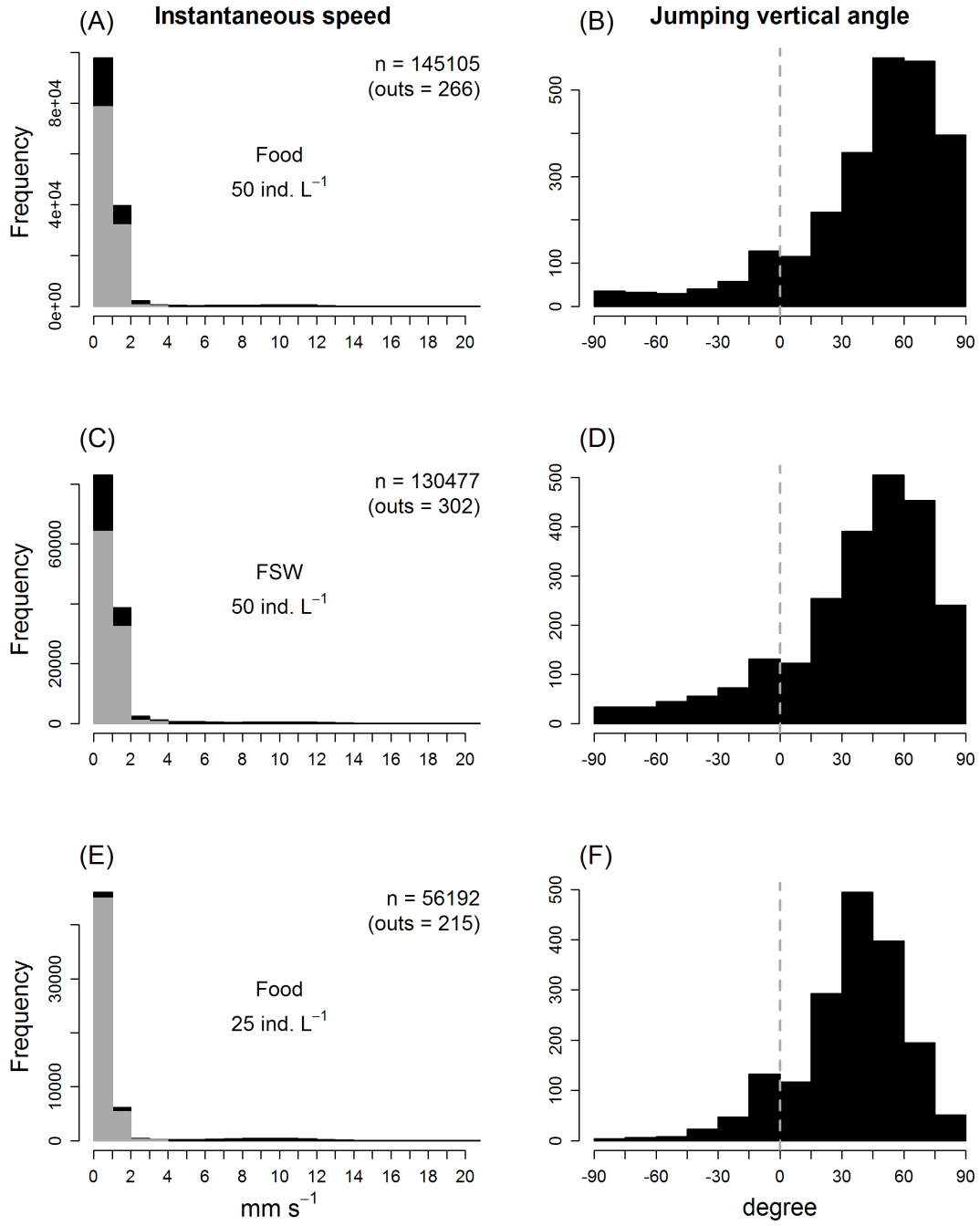

Figure 3.19: Distribution of instantaneous speed (mm s^{-1}) of *Acartia clausi* males during swimming state (black) and sinking (grey) with number of points (n) and corresponding values $>$ 20 mm s^{-1} not reported (outs), and distribution of jumping vertical angles (deg.). Dotted line separated left side, reporting downward jumps direction (negative values), and right side, reporting upward jumps direction (positive values). A, B Exp. #11; C, D Exp. #14; E, F Exp. #34.

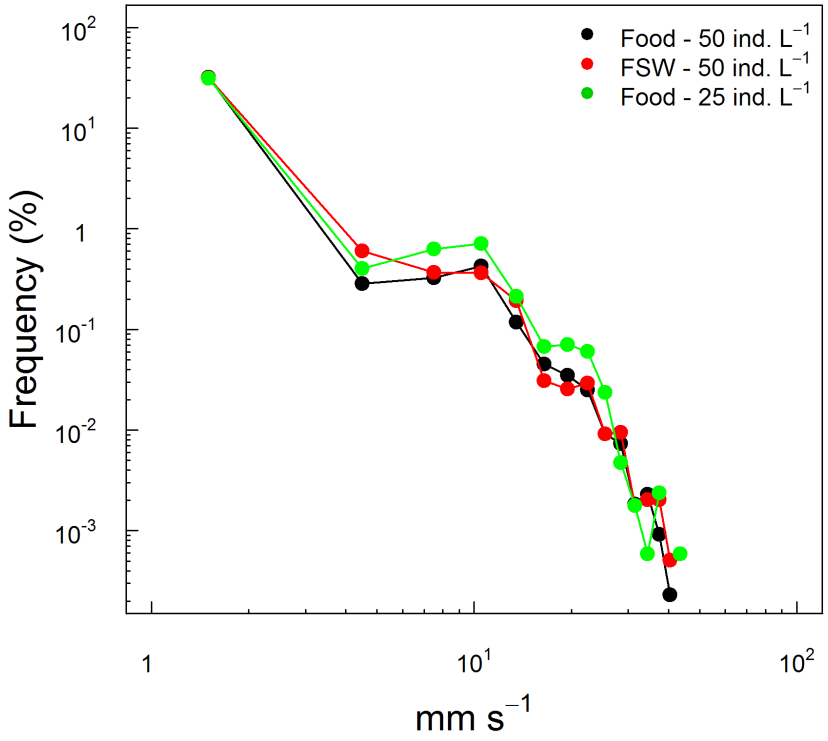

Figure 3.20: Polygon frequency distribution of *Acartia clausi* males instantaneous speed (mm s^{-1}) in Exp. #11 (black), Exp. #14 (red) and Exp. #34 (green).

3.2.3 Gender comparison

The behaviour of *Acartia clausi* females and males was similar, both in presence of food or in filtered sea water. Their predominant behaviour was sinking followed by hovering. Jumping was more frequent but slower in females than in males. Females decreased the swimming speed when the food become rare, while males slightly increased the speed.

The swimming behaviour changed in both females and males along with the population density. At lower density, sinking and jumping time increased while hovering diminished, the speed increased in both genders, while jump speed de-

creased in females and remained similar in males. Both genders increased jumping frequency while jumping speed was higher in males. NGDR and the horizontal component decreased in both genders.

3.2.4 Synthesis

Acartia clausi females and males show similar swimming behaviour, moving along quasi-linear trajectories without preferential direction or recurring patterns. Time is prevalently allocated to sinking and hovering at very low speed (< 3 mm s^{-1}) interrupted regularly by fast (> 4 mm s^{-1}) jumps. At each jump, the copepod's body assumes a different body orientation that determines the new jumping angle and relocation.

Food supply does not seem to affect significantly the swimming behaviour in both genders. More evident is the effect of copepod density. At lower population density, both genders spend more time sinking and jumping than hovering; moreover the swimming path are more convoluted and develop more in the vertical plane than at higher concentration. However in worth noting that the experiments were conducted in two different years and an effect due to different populations cannot be excluded.

3.3 *Temora stylifera*

The swimming behaviour of *Temora stylifera* females and males was analysed over 17 experiments an a total of 1,857 three-dimensional (3D) trajectories that lasted complexively $\sim$ 11 hours (Table 3.13). Between 4 and 8 copepods could be followed simultaneously, making possible to explore individual variability.

Females and males spent all the time swimming and only in very rare occasions they were observed sinking or jumping. Swimming propels the copepod forward while creating a feeding current and it was usually performed with the ventral side of the body and the appendages oriented upward. The body was slightly obliquely oriented along the swimming direction.

The swimming paths were made of consecutive loops in the plane (Fig. 3.21), with a few changes of travelling direction (Fig. 3.22). All the loops were performed in a clockwise direction (seen from the top) and rarely interrupted by jumps (Fig. 3.23, 3.24, 3.25).

Table 3.13: General information on *Temora stylifera* swimming trajectories recorded during 17 experiments.

Exp	Date	Gender	ind. L^{-1}	Food	Recording time	N. trajectories	N. points	Cumulative trajectory duration	Max trajectory duration	Max N. simultaneous trajectories
15	30 Sep '08	F	25	Yes	20' 20"	82	27,158	30' 11"	3' 08"	5
16	30 Sep '08	M	25	Yes	20' 20"	96	19,927	22' 08"	1' 26"	4
17	30 Sep '08	F	50	Yes	20' 20"	85	31,767	35' 18"	1' 56"	6
18	30 Sep '08	M	50	Yes	20' 20"	170	42,857	47' 37"	1' 41"	6
19	7 Oct '08	M	25	Yes	20' 20"	79	21,884	24' 19"	2' 41"	4
20	7 Oct '08	M	25	No	20' 20"	45	10,494	11' 40"	1' 00"	4
21	7 Oct '08	F	25	Yes	20' 20"	101	28,424	31' 35"	1' 26"	5
22	7 Oct '08	F	25	No	20' 20"	52	19,226	21' 22"	1' 20"	3
23	14 Oct '08	F	25	Yes	20' 20"	120	52,443	58' 16"	4' 43"	6
24	14 Oct '08	F	25	Yes	20' 20"	114	46,750	51' 57"	3' 08"	6
25	14 Oct '08	F	50	Yes	20' 20"	232	63,494	1h 10' 33"	2' 21"	8
26	15 Oct '08	M	25	Yes	20' 20"	76	23,675	26' 18"	2' 53"	4
27	15 Oct '08	M	25	Yes	20' 20"	95	31,695	35' 13"	4' 36"	5
28	15 Oct '08	M	50	Yes	20' 20"	173	44,265	49' 11"	2' 00"	7
29	21 Oct '08	F	25	No	20' 20"	51	20,811	23' 07"	3' 39"	5
30	21 Oct '08	F	25	No	20' 20"	106	40,748	45' 17"	2' 43"	6
31	21 Oct '08	F	50	No	20' 20"	180	64,541	1h 11' 43"	2' 42"	8
				Total	5h 45' 40"	1,857	590,159	10h 55' 45"		

F = female, M = male.

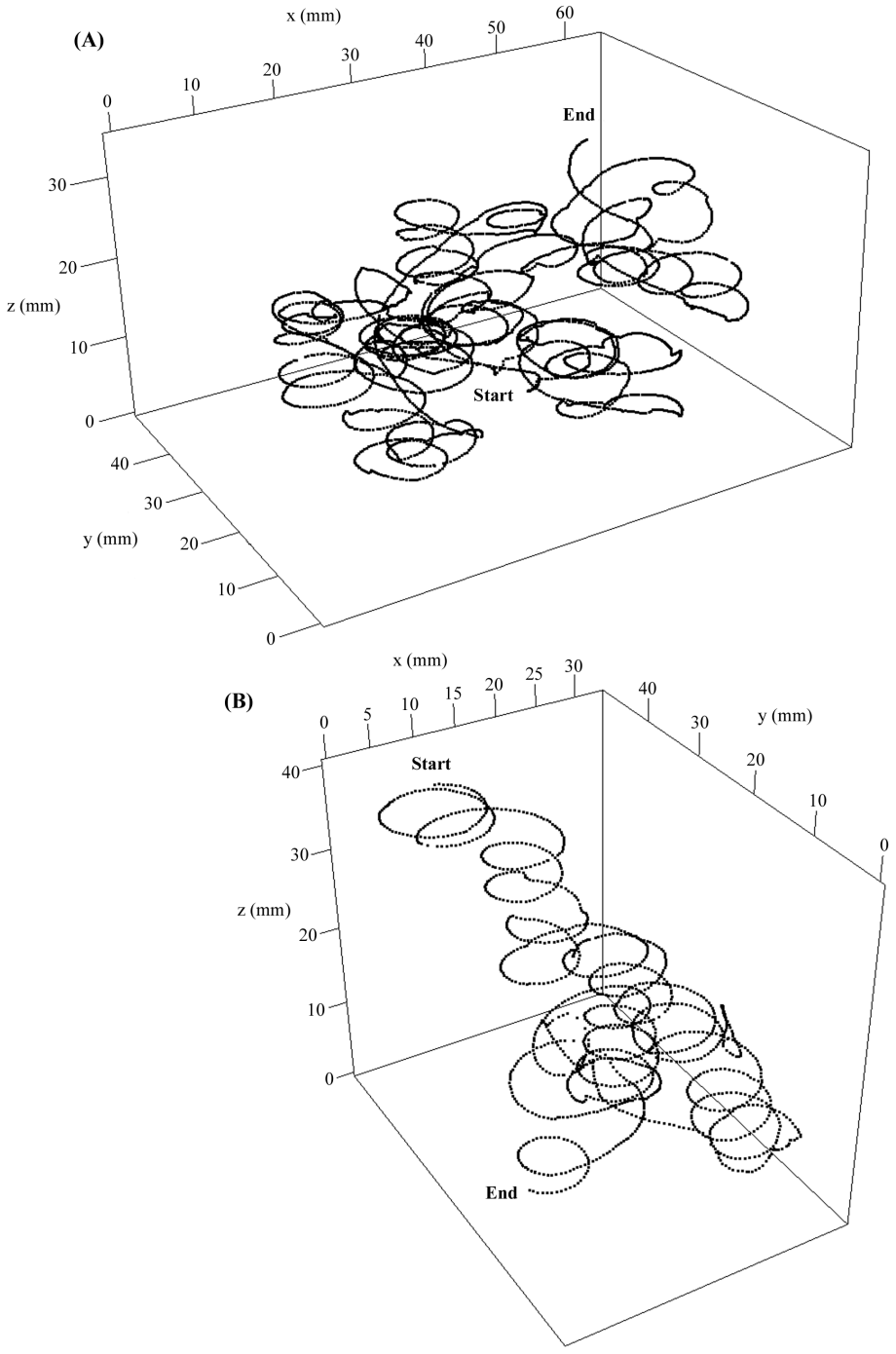

Figure 3.21: Examples of *Temora stylifera* female swimming trajectories in presence of food. Dots represent the copepod positions at 1/15 s intervals. (A) Exp. #23, 288 s; (B) Exp. #24, 104 s. Both panels in lateral view.

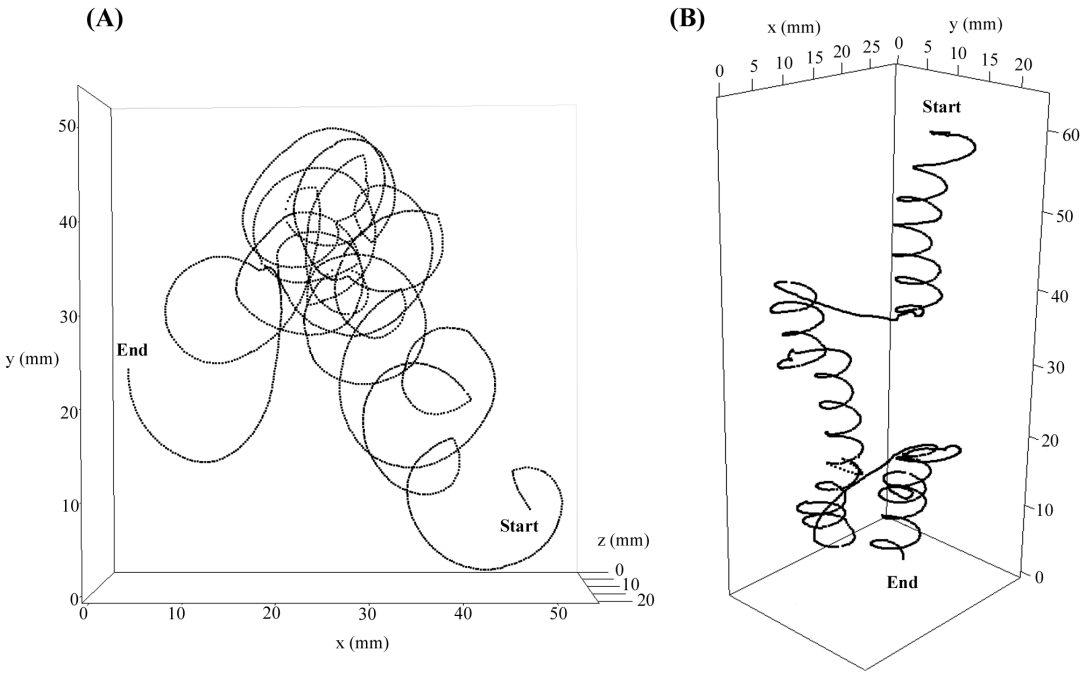

Figure 3.22: Examples of *Temora stylifera* female swimming trajectories in presence of food. Dots represent the copepod positions at 1/15 s intervals. (A) Top view, Exp. #25, 141 s; (B) Lateral view, Exp. #111, 104 s.

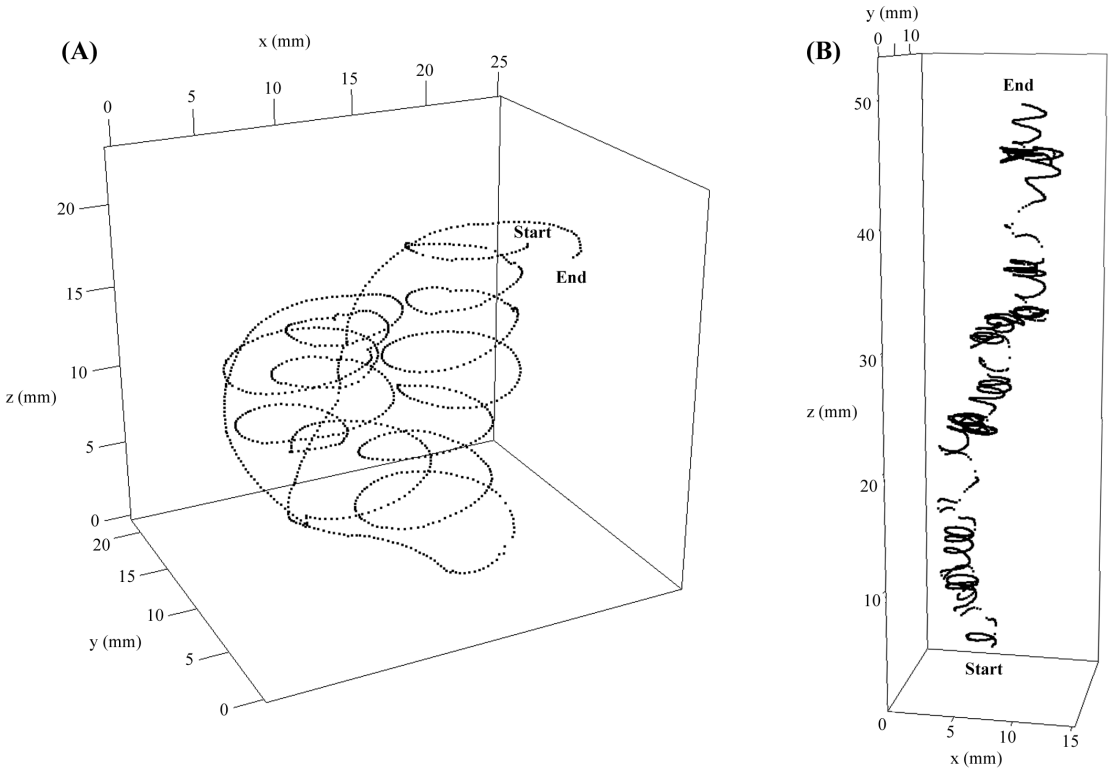

Figure 3.23: Examples of *Temora stylifera* male swimming trajectories in presence of food. Dots represent the copepod positions at 1/15 s intervals. (A) Exp. #16, 70 s; (B) Exp. #26, 73 s. Both panels in lateral view.

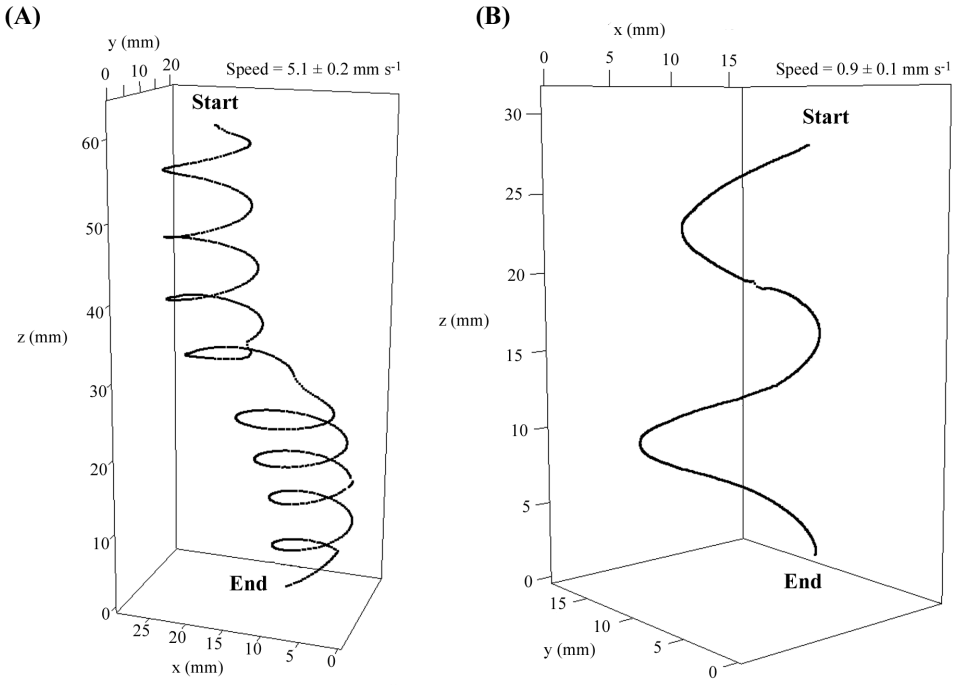

Figure 3.24: Examples of *Temora stylifera* female swimming trajectories. Dots represent the copepod positions at 1/15 s intervals. (A) Exp. #21, 63 s; (B) Exp. #31, 85 s. Both panels in lateral view.

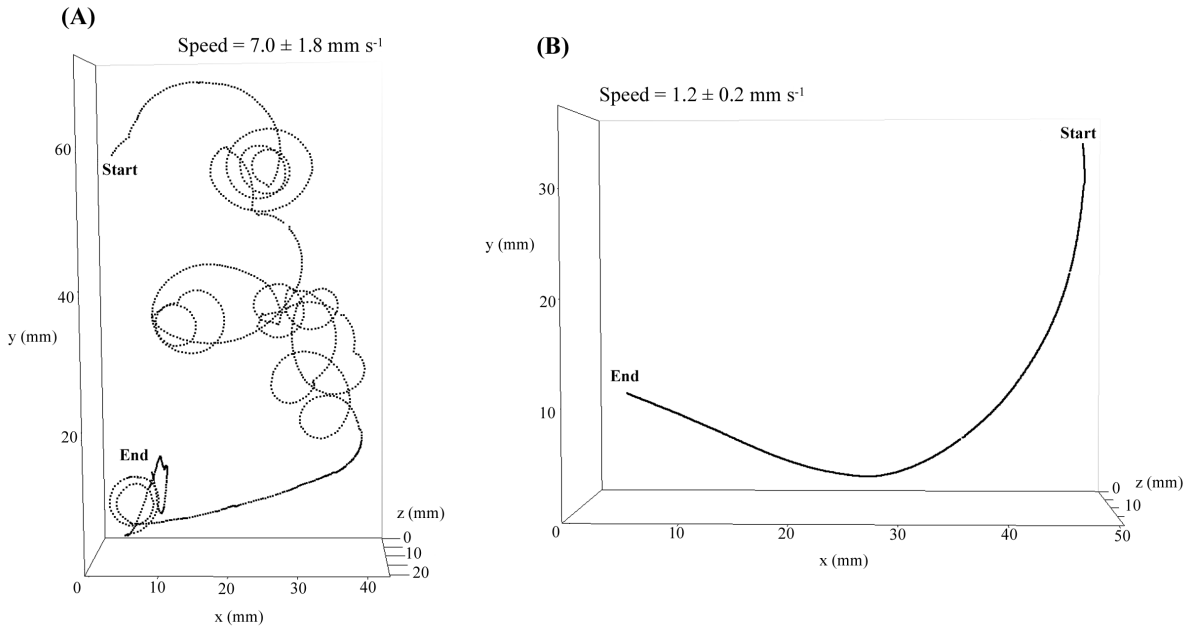

Figure 3.25: Examples of *Temora stylifera* male swimming trajectories. Dots represent the copepod positions at 1/15 s intervals. (A) Exp. #25, 141 s; (B) Exp. #20, 59 s. Both panels in top view.

3.3.1 Females

In presence of food represented by $\sim 4 \times 10^3$ ciliate cells L^{-1} and $\sim 3 \times 10^6$ phytoplankton cells L^{-1}, *Temora stylifera* females spent $\sim 99\%$ swimming (Table 3.14). Jumping and sinking were rare events.

In presence of food the frequency distribution of instantaneous speed had a peak at 4–5 mm s^{-1} (Fig. 3.26, A), while the mean speed was 5.1 ± 1.0 mm s^{-1} (Table 3.14).

Without food the peak in the distribution of instantaneous speed was at 0–1 mm s^{-1} (Fig. 3.26, C) an the speed significantly ($p < 0.001$) decreased to 2.5 ± 0.8 mm s^{-1}. Passing from food condition to without food condition, the NGDR increased significantly ($p < 0.001$) from 0.58 ± 0.06 to 0.75 ± 0.10 while the horizontal component lowered ($p < 0.001$) from 0.93 ± 0.02 to 0.88 ± 0.06.

At different population densities in presence of food, females showed a similar frequency distribution of instantaneous speed (Fig. 3.26, A and B) with the main peak at 4–5 mm s^{-1}, while speed, NGDR and horizontal component were significantly (Table 3.15).

At different population densities in filtered sea water, females showed similar frequency distribution of instantaneous speed (Fig. 3.26, C and D) with the main peak at 0–1 mm s^{-1}, but the speed was lower (1.8 ± 1.7 mm s^{-1}) at 50 ind. L^{-1} than at 25 ind. L^{-1} (2.5 ± 0.8 mm s^{-1}).

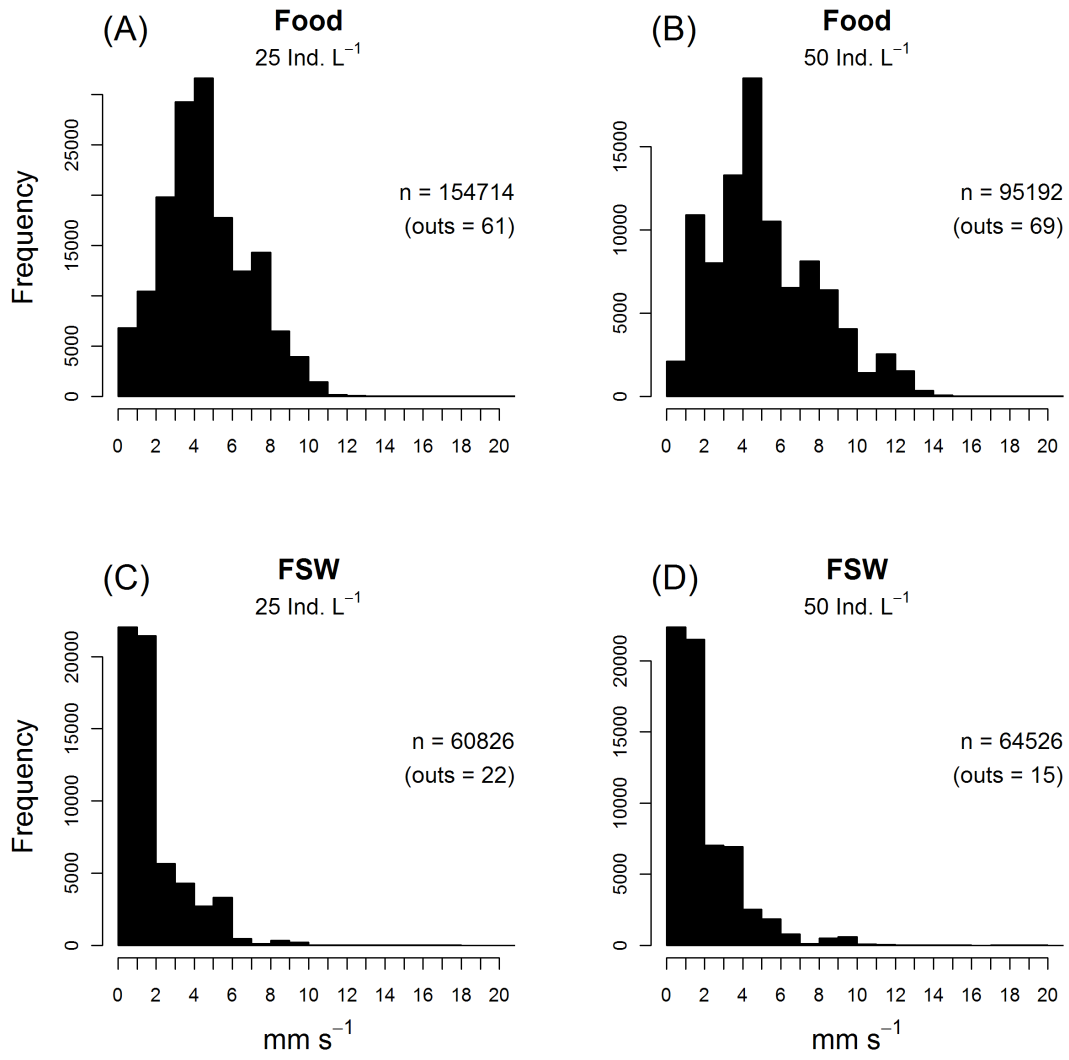

Figure 3.26: Distribution of instantaneous speed (mm s^{-1}) of *Temora stylifera* females. Number of points (n) and corresponding values > 20 mm s^{-1} not reported (outs). (A) Exp. 15, 21, 23, 24; (B) Exp. 17, 25; (C) Exp. 22, 29, 30; (D) Exp. 31.

Table 3.14: *Temora stylifera* experimental food conditions and swimming activity. Food is reported as microzooplankton concentration (cells L^{-1}) and phyto-plankton cell concentration (cells L^{-1}) and quality (FSW = filtered sea water without particles). Swimming behaviour is reported as percentage of time allocation.

		Food condition					
		Microzooplankton	**Phytoplankton**		**Activity occurrence (%)**		
Exp.	**ind. L^{-1}**	**(cells L^{-1})**	**(cells L^{-1})**	**Quality**	**Swimming**	**Sinking**	**Jumping**
Females				$43-48\%$ phyto-			
15, 21, 23, 24	25	$3.7-4.2\times10^3$	$2.7-3.6\times10^6$	flagellates $<5\,\mu$m	98.9 ± 0.8	0.1 ± 0.1	1.0 ± 0.8
				$1.4-1.9\%$ cells $>10\,\mu$m			
				$43-48\%$ phyto-			
17, 25	50	$3.7-4.2\times10^3$	$2.7-3.6\times10^6$	flagellates $<5\,\mu$m	98.3 ± 0.7	0.6 ± 0.8	1.1 ± 0.1
				$1.4-1.9\%$ cells $>10\,\mu$m			
22, 29, 30	25	—	—	—	98.9 ± 1.4	0.9 ± 1.4	0.3 ± 0.1
31	50	—	—	—	99.4	0.3	0.3
Males				$43-48\%$ phyto-			
16, 19, 26, 27	25	$3.7-4.2\times10^3$	$2.7-3.6\times10^6$	flagellates $<5\,\mu$m	98.5 ± 1.6	0.3 ± 0.4	1.2 ± 1.5
				$1.4-1.9\%$ cells $>10\,\mu$m			
				$43-48\%$ phyto-			
18, 28	50	$3.7-4.2\times10^3$	$2.7-3.6\times10^6$	flagellates $<5\,\mu$m	98.3 ± 1.7	0.0 ± 0.0	1.7 ± 1.7
				$1.4-1.9\%$ cells $>10\,\mu$m			
20	25	—	—	—	99.4	0.0	0.6

Table 3.15: *Temora stylifera* swimming speed (mean ± SD) computed averaging all instantaneous speed values in all trajectories. Net to Gross Displacement Ratio (NGDR ± SD) was estimated as mean value for each individual track at the smallest resolution (1/15 s). Horizontal Component (HC ± SD) was computed as mean value for each individual track. Explored Volume (EV ± SD).

			Food condition					
			Microzooplankton	**Phytoplankton**	**Speed**	**NGDR**	**HC**	**EV**
	Experiment	**ind. L^{-1}**	**(cells L^{-1})**	**(cells L^{-1})**	**(mm s^{-1})**	**(adim.)**	**(adim.)**	**(ml h^{-1})**
Females	15, 21, 23, 24	25	$3.7 - 4.2 \times 10^3$	$2.7 - 3.6 \times 10^6$	5.1 ± 1.0	0.58 ± 0.06	0.93 ± 0.02	4.4 ± 0.7
	17, 25	50	$3.7 - 4.2 \times 10^3$	$2.7 - 3.6 \times 10^6$	5.5 ± 1.1	0.53 ± 0.04	0.90 ± 0.01	5.0 ± 0.7
	22, 29, 30	25	—	—	2.5 ± 0.8	0.75 ± 0.10	0.88 ± 0.06	2.4 ± 0.5
	31	50	—	—	1.8 ± 1.7	0.79 ± 0.19	0.90 ± 0.13	2.1 ± 1.5
Males	16, 19, 26, 27	25	$3.7 - 4.2 \times 10^3$	$2.7 - 3.6 \times 10^6$	5.2 ± 1.1	0.72 ± 0.05	0.92 ± 0.01	4.5 ± 1.3
	18, 28	50	$3.7 - 4.2 \times 10^3$	$2.7 - 3.6 \times 10^6$	5.3 ± 1.7	0.68 ± 0.10	0.91 ± 0.01	4.7 ± 1.7
	20	25	—	—	4.0 ± 1.8	0.86 ± 0.17	0.89 ± 0.11	3.2 ± 1.5

3.3.2 Males

In presence of the same natural particle assemblage as for females, *Temora stylifera* males showed the same behaviour of continuous swimming in $\sim 99\%$ of the time (Table 3.14).

The frequency distribution of instantaneous speed in presence of food had a peak at 5–6 mm s^{-1} (Fig. 3.27, A) and the speed was 5.2 ± 1.1 mm s^{-1}; in filtered sea water the distribution had two peaks, at 1–2 mm s^{-1} and at 3–4 mm s^{-1} (Fig. 3.27, C), and the speed significantly ($p < 0.001$) decreased to 4.0 ± 1.8 mm s^{-1}. The NGDR was significantly ($p < 0.001$) lower in presence of food (0.75 ± 0.05) then in filtered sea water (0.86 ± 0.17).

At different population densities, males showed similar frequency distribution of instantaneous speed (Fig. 3.27, A and B) with the main peak at 4–5 mm s^{-1} and similar mean speed, horizontal component and explored volume (Table 3.15). The NGDR was lower ($p < 0.001$) at higher population density (Table 3.15).

3.3.3 Synthesis

Both genders of *Temora stylifera* spent $\sim 99\%$ of the time swimming at ~ 5 mm s^{-1}, and only rarely sank or jumped. Swimming speed was higher ($p < 0.001$) in males than in females in any experimental conditions (Table 3.15). Passing from food to filtered sea water the speed decreased, more in females than in males.

NGDR increased when in absence of food, with the male having higher values ($p < 0.001$) than females. Different population density do not affect the swimming activity of *T. stylifera* females and males.

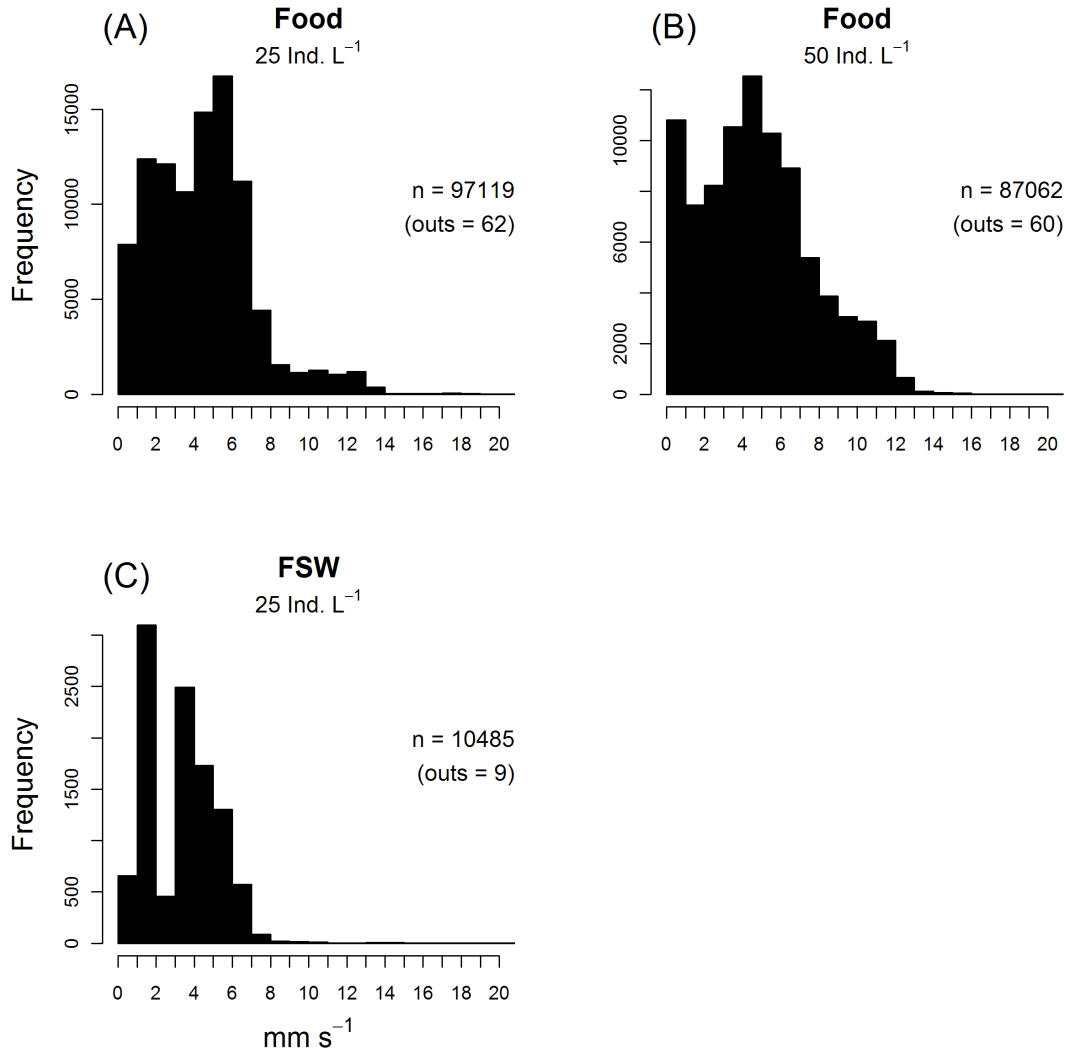

Figure 3.27: Distribution of instantaneous speed (mm s^{-1}) of *Temora stylifera* males. Number of points (n) and corresponding values > 20 mm s^{-1} not reported (outs). (A) Exp. 16, 19, 26, 27; (B) Exp. 18, 28; (C) Exp. 20.

3.4 *Paracalanus parvus*

The swimming behaviour of *Paracalanus parvus* was analysed in the course of 6 experiments that allowed to acquire 2,248 three-dimensional (3D) trajectories lasting $\sim$ 18 hours complexively (Table 3.16). For each experiment, a large number of trajectories were longer than 4 min, providing an extensive dataset suitable for statistical treatment.

3.4.1 Females

Paracalanus parvus females moved by: (1) swimming, (2) sinking and (3) jumping. Swimming was due to the rhythmic high frequency motion of cephalic appendages, which propel the copepod forward while creating a feeding current. The most frequently observed swimming path was a continuos looping with forward displacement (Fig. 3.28, A). At variable frequency, *P. parvus* females stopped swimming and sunk (Fig. 3.28, B). Sinking could be alternated by short upward swim creating a different kind of trajectory (Fig. 3.28, C, D). Jumping was a fast ($\sim$ 1/10 s) displacement ($\geqslant$ 8 mm) that *P. parvus* females performed quite rarely under undisturbed hydrodynamic conditions (Table 3.17).

In presence of food particles represented mainly by small phytoplankton species and very few ($\sim$ 8%) larger ($>$ 10μm) cells, the predominant motion behaviour of *P. parvus* females was represented by swimming (86.7%), followed by sinking (11.4%) and by rare jumping (Table 3.17). Swimming duration was very variable, while sinking duration was $\sim$ 1 s and jumping $\sim$ 1/10 s (Table 3.17). In filtered sea water, swimming and jumping were reduced while sinking increased from 11.4% to 21.2%. The swimming duration decreased significantly ($p < 0.001$), and sinking duration increase ($p < 0.001$).

In presence of high food particles concentration (Exp. #40) *P. parvus* females spent 43.2% of the time sinking and 0.3% jumping (Table 3.17). Swimming duration was significantly ($p < 0.001$) lower. Both the total and the active speed decreased significantly ($p < 0.001$). The NGDR, the horizontal component of the trajectories and the explored volume reduced ($p < 0.001$) to lower values.

The frequency distribution of instantaneous speed of *P. parvus* females, in both conditions, had a clear peak (Fig. 3.29), respectively at 2.5–3 mm s^{-1} and at 2–2.5 mm s^{-1}. Sinking had the speed peak at 1–1.5 mm s^{-1} in both cases. Speeds higher than 6 mm s^{-1} were rarely observed in both experimental conditions.

In filtered sea water condition both the total and the active speed decreased significantly ($p < 0.001$) when copepod were recorded. The NGDR and the horizontal component of the trajectories changed slightly in absence of food, while the explored volume decreased significantly ($p < 0.001$).

At different population density (30, 60, 90 ind. L^{-1}), *P. parvus* females did not change their swimming activity. The swimming occurrence increased from 54–56% at lower density to 65.5% at the highest density and sinking was consequently reduced. The lower time spent swimming at 90 ind. L^{-1} was related of the significantly higher ($p < 0.001$) swimming duration (Table 3.17). The frequency distribution of instantaneous speed of *P. parvus* females showed a main peak at 1–1.5 mm s^{-1} that was partially due to sinking speeds in all three density conditions (Fig. 3.30, A–C).

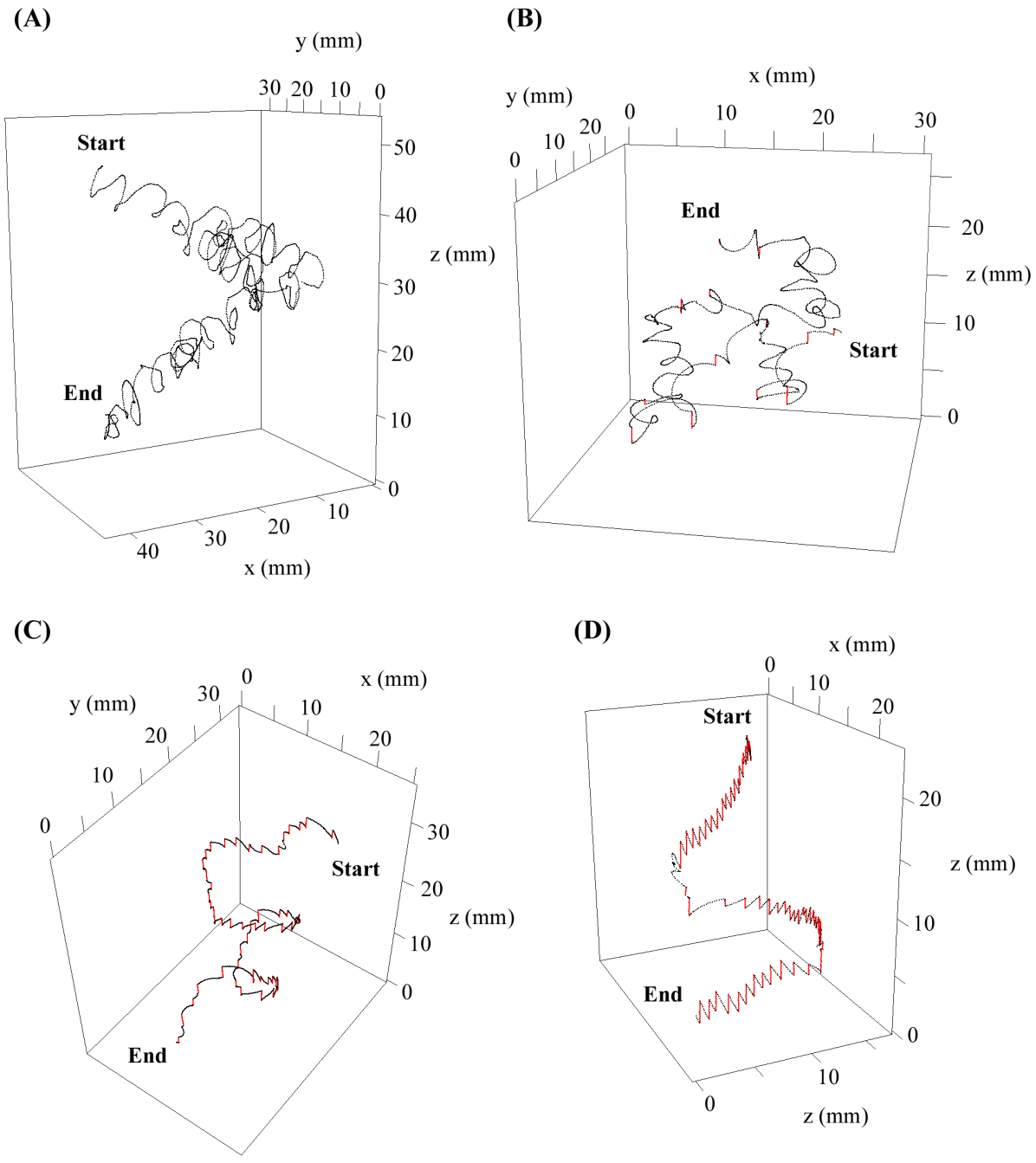

Figure 3.28: Examples of *Paracalanus parvus* females swimming trajectories. Dots represent the copepod positions at 1/15 s intervals. Swimming state in black and sinking state in red. (A) Exp. #36, food, 161 s; (B) Exp. #37, FSW, 121 s; (C) Exp. #37, FSW, 141 s; (D) Exp. #37, FSW, 122 s.

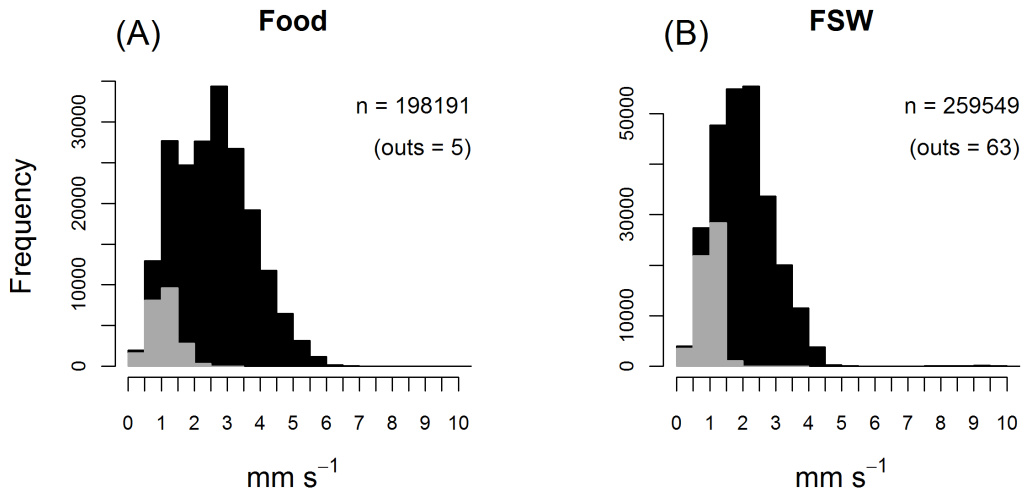

Figure 3.29: Distribution of instantaneous speed (mm s^{-1}) of *Paracalanus parvus* females during swimming (black) and sinking (grey) states in presence of food (A, Exp. #36) and in filtered sea water (FSW) (B, Exp. #37). Number of points (n) and corresponding values > 10 mm s^{-1} not reported (outs).

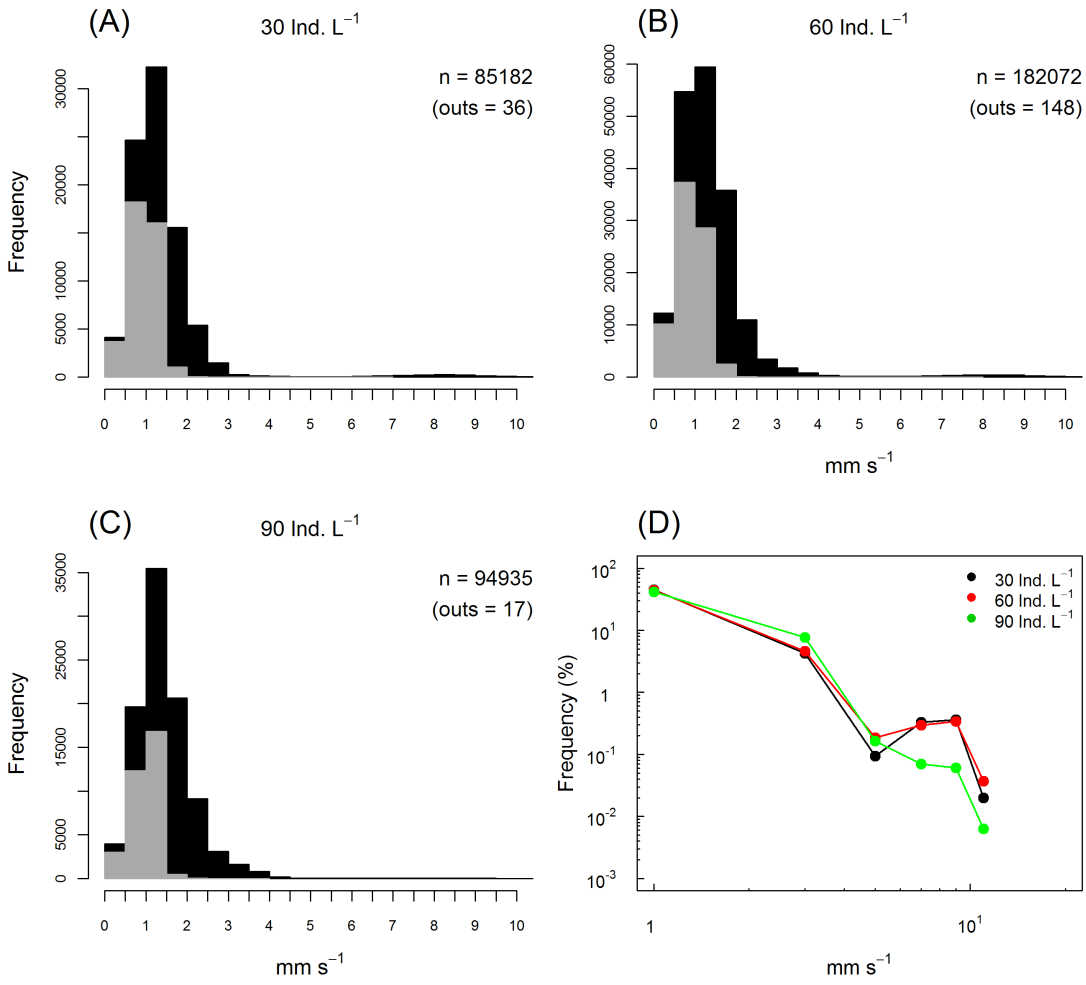

Figure 3.30: Distribution of instantaneous speed (mm s^{-1}) of *Paracalanus parvus* females during swimming (black) and sinking (grey) states at different population density (ind. L^{-1}) (Exp. #39–41) (A–C). Number of points (n) and corresponding values $>$ 10 mm s^{-1} not reported (outs). Polygon frequency distribution of instantaneous speed (mm s^{-1}) in Exp. #39 (black), Exp. #40 (red) and Exp. #41 (green) (D).

Table 3.16: General information on *Paracalanus parvus* swimming trajectories recorded during 6 experiments.

Exp	Date	Gender	ind. L^{-1}	Food	Recording time	N. trajectories	N. points	Cumulative trajectory duration	Max trajectory duration	Max N. simultaneous trajectories
36	15 Jul '09	F	60	Yes	1h 07' 20"	480	198,196	3h 40' 13"	4' 07"	8
37	16 Jul '09	F	60	No	1h 07' 20"	637	259,612	4h 48' 27"	4' 33"	11
38	17 Jul '09	M	60	Yes	1h 27' 40"	406	146,990	2h 43' 19"	2' 41"	8
39	28 Jul '09	F	30	Yes	33' 40"	166	85,218	1h 34' 41"	5' 52"	9
40	28 Jul '09	F	60	Yes	33' 40"	356	182,220	3h 22' 28"	6' 24"	10
41	28 Jul '09	F	90	Yes	16' 20"	203	94,952	1h 45' 30"	4' 42"	11
				Total	5h 06' 00"	2,248	967,188	17h 54' 38"		

F = female, M = male.

Table 3.17: *Paracalanus parvus* experimental food conditions and swimming activity. Food is reported as microzooplankton concentration (cells L^{-1}) and phyto-plankton cell concentration (cells L^{-1}) and quality (FSW = filtered sea water without particles). Swimming behaviour is reported as occurrence (percentage of time allocation) and duration (s) of the three states: swimming (Sw), sinking (Sk), and jumping (Jp). Swimming durations is assumed as the time interval between 2 consecutive sinking events.

		Food condition			**Activity**					
		Microzoo	**Phytoplankton**		**Occurrence (%)**			**Duration ± SD (s)**		
Exp.	**ind. L^{-1}**	**(cells L^{-1})**	**(cells L^{-1})**	**Quality**	**Sw**	**Sk**	**Jp**	**Sw**	**Sk**	**Jp**
Females				∼ 60% phyto-						
36	60	3.4×10^3	6.6×10^6	flagellates $< 5\,\mu$m	86.7	11.4	1.9	3.1 ± 6.9	1.1 ± 1.0	0.10 ± 0.06
				∼ 8% cells $> 10\,\mu$m						
37	60	—	—	FSW	78.6	21.2	0.2	1.9 ± 5.6	1.3 ± 0.5	0.10 ± 0.05
				∼ 26% *Skeletonema*						
39	30			*menzelii**	54.2	45.7	0.1	1.0 ± 0.8	0.9 ± 0.4	0.13 ± 0.09
				∼ 25% phyto-						
40	60	1.4×10^4	6.1×10^7	flagellates $< 5\,\mu$m	56.5	43.2	0.3	1.0 ± 0.8	0.8 ± 0.3	0.11 ± 0.07
41	90			∼ 8% cells $> 10\,\mu$m	65.5	34.3	0.2	1.3 ± 1.0	0.8 ± 0.3	0.09 ± 0.04
Males				∼ 60% phyto-						
38	60	3.4×10^3	6.6×10^6	flagellates $< x\,\mu$m	95.5	0	4.5	—	—	0.12 ± 0.07
				∼ 8% cells $> 10\,\mu$m						

* 4–5 μm.

Table 3.18: *Paracalanus parvus* swimming speed (mean ± SD) computed averaging all instantaneous speed values in all trajectories (Total) or excluding sinking events (Active). Net to Gross Displacement Ratio (NGDR ± SD) was estimated as mean value for each individual track at the smallest resolution (1/15 s). Horizontal Component (HC ± SD) was computed as mean value for each individual track. Explored Volume (EV ± SD).

			Food	**Speed ± SD (mm s^{-1})**		**NGDR**	**HC**	**EV**
	Exp.	**ind. L^{-1}**	**(cells L^{-1})**	**Total**	**Active**	**(adim.)**	**(adim.)**	**(ml h^{-1})**
Females	36	60	6.6×10^6	2.5 ± 0.9	2.7 ± 0.9	0.43 ± 0.19	0.66 ± 0.13	1.1 ± 0.4
	37	60	—	2.1 ± 0.7	2.3 ± 0.8	0.48 ± 0.19	0.63 ± 0.18	0.9 ± 0.4
	39	30	6.1×10^7	1.5 ± 0.8	1.9 ± 1.4	0.37 ± 0.19	0.47 ± 0.13	0.5 ± 0.4
	40	60	6.1×10^7	1.6 ± 1.0	2.0 ± 1.6	0.34 ± 0.16	0.46 ± 0.10	0.6 ± 0.4
	41	90	6.1×10^7	1.5 ± 0.5	1.7 ± 0.8	0.37 ± 0.18	0.52 ± 0.13	0.6 ± 0.2
Males	38	60	6.6×10^6	2.6 ± 2.4	2.6 ± 2.4	0.53 ± 0.22	0.68 ± 0.17	1.3 ± 1.1

3.4.2 Males

Paracalanus parvus males did not sink like females and their motion was characterised by: (1) slow swimming, (2) fast swimming and (3) jumping. Slow swimming was due to frequent appendages movements that allowed the copepod to progress in a slow (0.5–1 mm s^{-1}) looping path (Fig. 3.31, A). Fast swimming was characterized by up to ten times faster speed within a looping path (Fig. 3.31, B). The same male could switch repetitively between slow to fast swim (Fig. 3.32). Also for males, the jumping activity was observed rarely (Table 3.17).

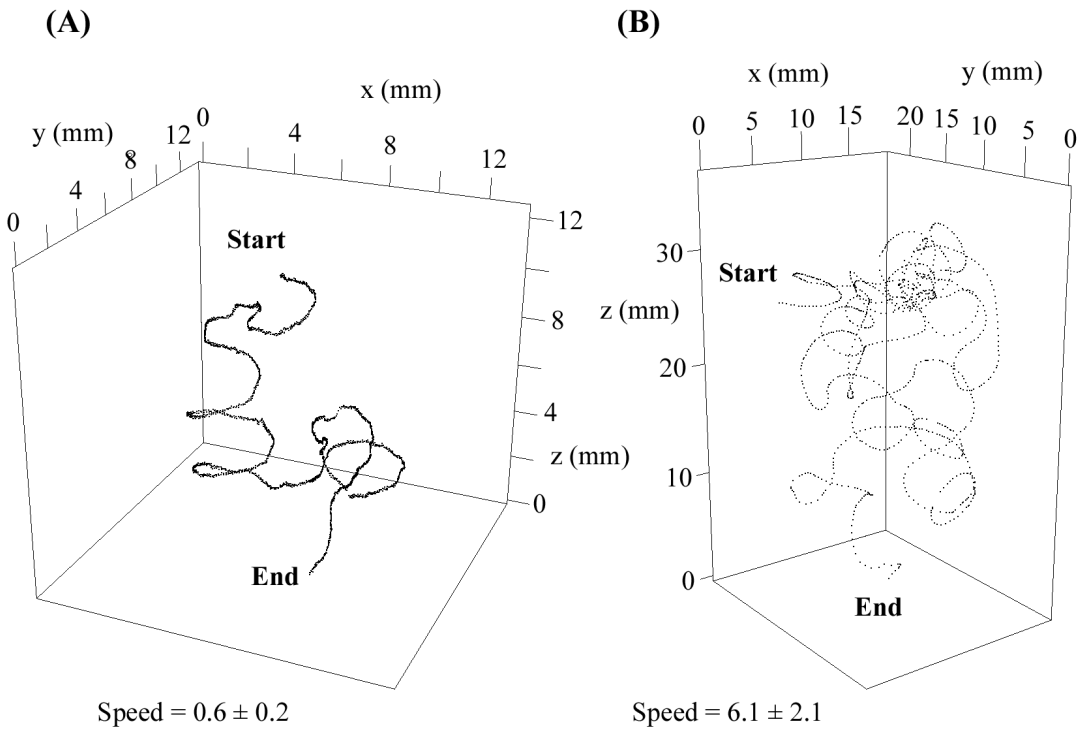

Figure 3.31: Examples of *Paracalanus parvus* males swimming trajectories. Dots represent the copepod positions at 1/15 s intervals. (A) Exp. #38, 69 s; (B) Exp. #38, 161 s.

In presence of food particles represented mainly by small phytoplankton species and a very few ($\sim$ 8%) larger ($>$ 10μm) cells, the motion behaviour of *Para-*

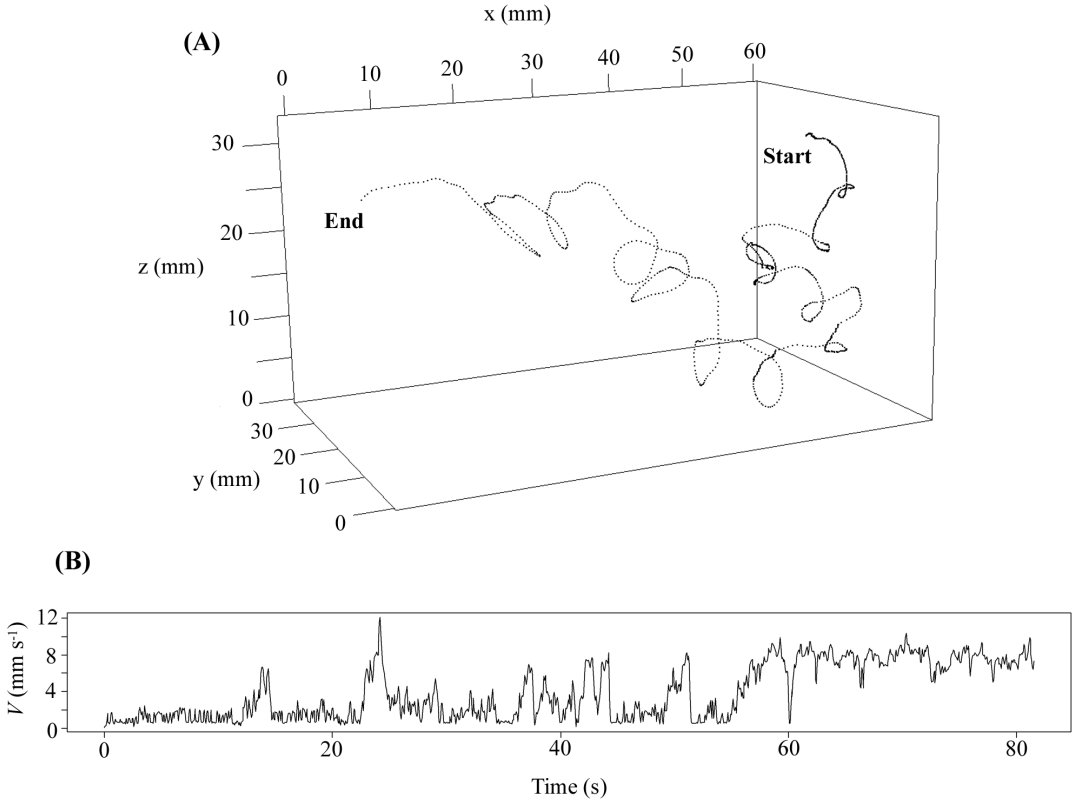

Figure 3.32: Examples of *Paracalanus parvus* males swimming trajectories (A) and relative 3D speed (B). Dots represent the copepod positions at 1/15 s intervals. Exp. #38, 82 s.

calanus parvus males was represented by 95.5% of swimming and 4.5% of jumps of 0.12 ± 0.07 s durations. The instantaneous speed distribution had a major peak at 0.5–1 mm s^{-1} followed by a step decrease with a long tail up to 15 mm s^{-1} (Fig. 3.33).

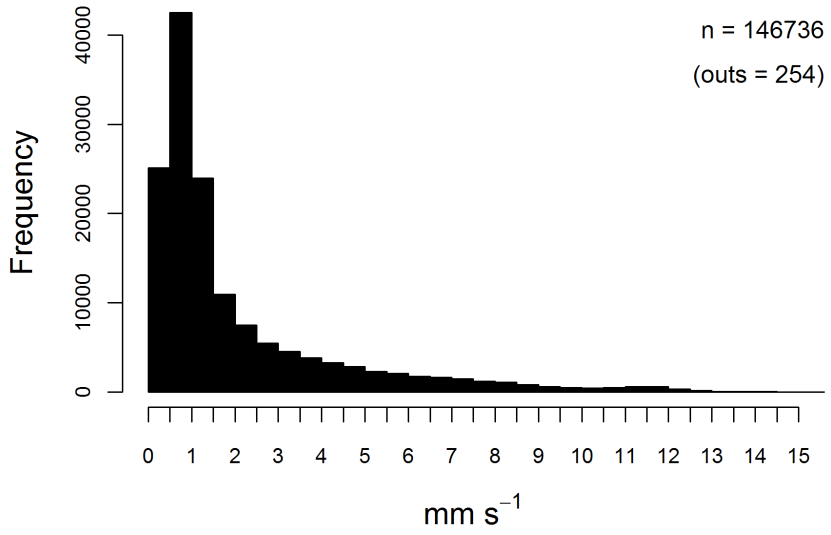

Figure 3.33: Distribution of instantaneous speed (mm s^{-1}) of *Paracalanus parvus* males during swimming (black) and sinking (grey) states in presence of food (Exp. #38). Number of points (n) and corresponding values > 15 mm s^{-1} not reported (outs).

3.4.3 Gender comparison

Females and males of *Paracalanus parvus* behave significantly different within the same conditions. Males moved continuously, jumped more than females and also for slightly longer time (Fig. 3.34, A), while females spent also time in sinking. The mean swimming speed was significantly different. Notwithstanding the mean values are similar (Fig. 3.34, B), the speed distribution differed between the genders (Fig. 3.35). Females active speed distribution resemble to a Gaussian shape with consequently lower standard deviation (2.7 ± 0.9 mm s^{-1}), while males presented a distribution with longer-tailed and a mean of 2.6 ± 2.4 mm s^{-1}. The NGDR and explored volume were significantly higher in males ($p < 0.001$).

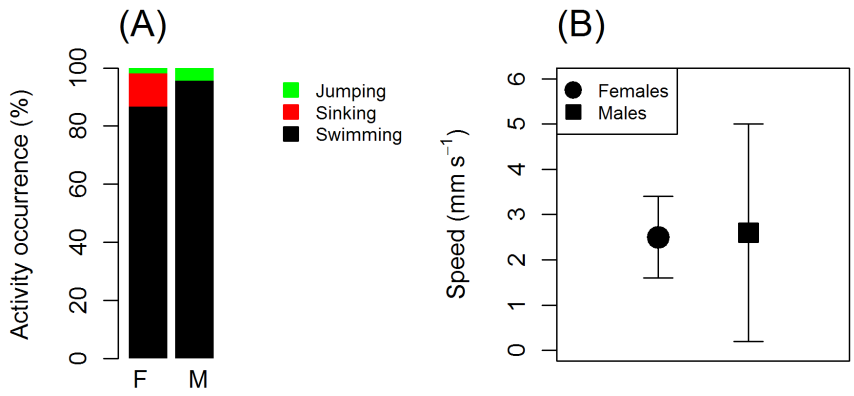

Figure 3.34: (A) Activity duration (swimming, sinking, jumping) in *Paracalanus parvus* females and males in presence of food. (B) Mean swimming speed ± SD. Exp. #36 and 38. F = females, M = males.

3.4.4 Synthesis

Paracalanus parvus females swam differently in function of food. In filtered sea water or in higher food concentration, females reduced their swimming and jumping activity while increased their sinking. At different population density, females did not change significantly their swimming behaviour. Moreover, females differed on many aspects from males swimming behaviour. For example males did not sink but jumped more frequently than females. Females presented a Gaussian shape distribution of instantaneous speed because swam at regular average speed. Males' speed distribution was more tail-shaped toward higher speeds because they modulate the speed passing from slow swimming to fast swimming while progressing in the same path.

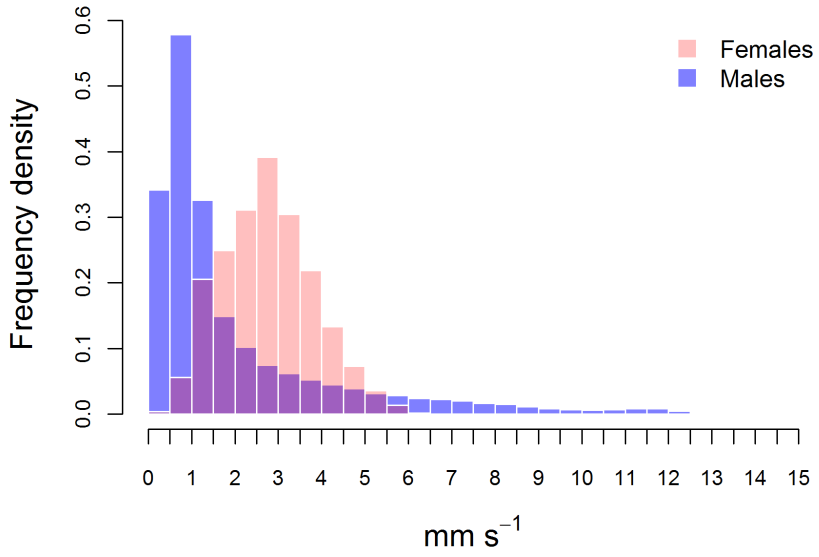

Figure 3.35: Density distribution of active swimming instantaneous speed (mm s^{-1}) of *Paracalanus parvus* females (pink) and males (light blue) in presence of food. Exp. #36 and 38.

3.5 *Clausocalanus furcatus* females

The swimming behaviour of *Clausocalanus furcatus* adult females was analysed in 4 experiments with a total duration of 4 hours and 56 minutes, which provided 1,689 3D trajectories (Table 3.19).

The swimming activity of *C. furcatus* was characterised by continuous convoluted looping movements with frequent and fast turns, interrupted by periods in which the copepod stops and sinks for a while. The straight swimming is performed at average speed of ~ 10 mm s^{-1} (Fig. 3.36).

In most cases the trajectories appeared to be composed by the repetition of simple patterns. The pattern shown in Fig. 3.36 was observed mainly in natural food conditions. In this case, *C. furcatus* described trajectories characterised by short straight segments of very similar length connected by sharp and fast turns. The regularity of this behaviour appear also in the 3D speed plot that shows a rapid (~ 10 mm s^{-1}) and almost rectilinear movement interrupted, at regular time intervals, by sharp deceleration followed by an acceleration (Fig. 3.36, A–C). The copepod kept swimming with the same pattern for up to 4 min while crossing from right to left the entire field of view (of the optical system) (Fig. 3.36, D). The copepod moved in roughly parallel lines for a while before changing direction, and remained in an area before passing to different one.

A different swimming pattern appeared mainly in filtered sea water, but it was also observed in the experiments with food (Fig. 3.37). The pattern consisted regular alternation of swimming and sinking phases (Fig. 3.37, A) while progressing in space along a regular circle (Fig. 3.37, B). This motion track was composed of a single repetitive module (swim upward and sink) that was displaced along a higher level designed path. In the velocity plots, two different periodicities can be observed (Fig. 3.37, C, D). The first periodicity was due to the up movement (~ 7 mm s^{-1}) and sink (~ 1 mm s^{-1}), repeated every ~ 5 s. The second periodicity of ~ 1 min was a sinusoidal signal along the x axis.

A third pattern was observed only during the experiments in filtered sea water (Fig. 3.38). This pattern appeared from top like a series of open triangles that span over a relatively large area (Fig. 3.38, A). In 5 min, the copepod crossed the entire field of view avoiding areas previously explored. Also in this case,

C. furcatus swimming behaviour described a repetitive pattern, but the unit module was different from the previous ones. The pattern was composed by two segments linked by a sharp turn and followed by a sinking phase (Fig. 3.38 B and C). The speed diagram allows to differentiate between the different elements that constituted the swimming pattern (Fig. 3.38, D). Others swimming patterns were observed that appeared like variations of the three patterns described above.

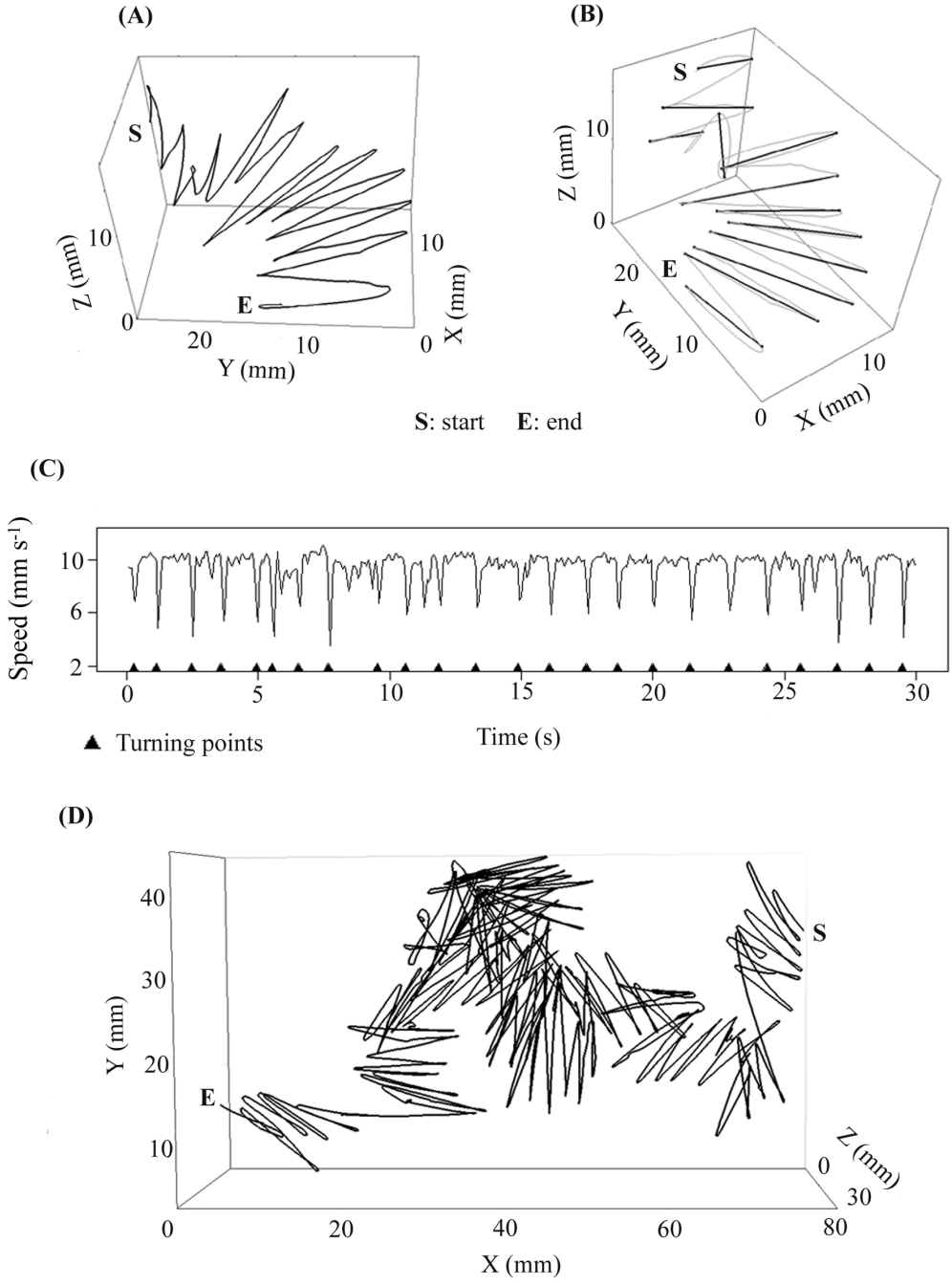

Figure 3.36: Example of *Clausocalanus furcatus* 3D swimming paths in presence of natural particle assemblage (Exp. # 32, 30 s) characterised by round turns between straight segments of roughly equal length, visible in lateral view from different perspectives (A, B). (C) Speed diagram showing the minimum values that correspond to the turning points. (D) Top view of another trajectory presenting the same pattern (Exp. # 42, 4 min).

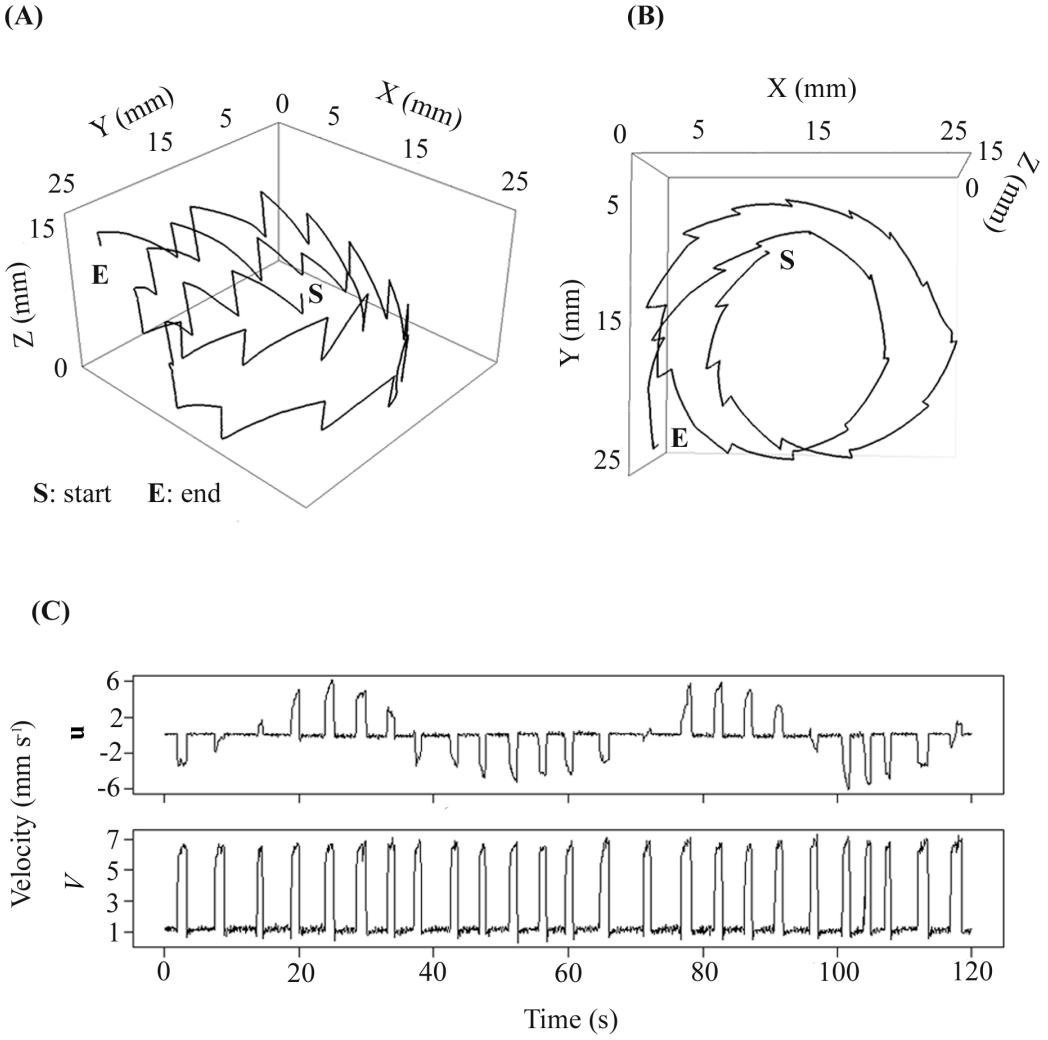

Figure 3.37: Example of *Clausocalanus furcatus* female swimming pattern recorded in filtered sea water. Lateral view (A), top view (B) and (C) diagram of velocity ($\mathbf{u}$) along the x coordinate and 3D speed (V) (Exp. #43, 120 s).

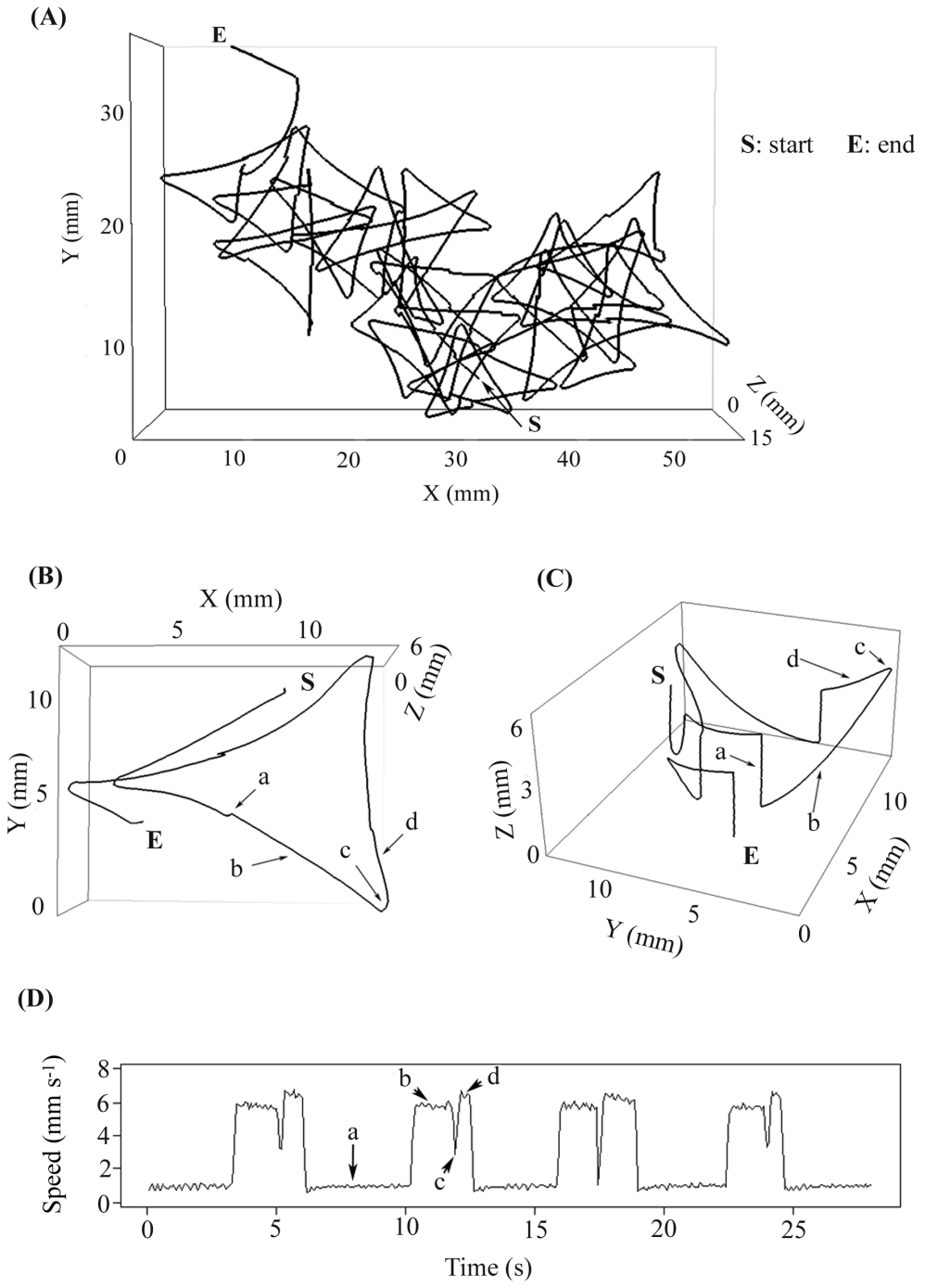

Figure 3.38: Example of *Clausocalanus furcatus* female swimming pattern recorded in filtered sea water. (A) Top view (Exp. #33, 5 min). Particular in top view (B), lateral view (C) and relative speed diagram (D). The pattern is composed by a sinking phase (a), an upward swimming phase (b), a round curve (c) and a further downward swimming (d).

Table 3.19: General information on *Clausocalanus furcatus* swimming trajectories recorded during 4 experiments.

Exp	Date	ind. L^{-1}	Food	Recording time	N. trajectories	N. points	Cumulative trajectory duration	Max trajectory duration	Max N. simultaneous trajectories
32	27 Nov '08	37	Yes	1h 07'	255	91,345	1h 41' 30"	4' 01"	6
33	28 Nov '08	35	No	1h 07'	384	166,203	3h 04' 40"	5' 42"	7
42	30 Sep '09	30	Yes	1h 12'	625	229,084	4h 14' 32"	4' 38"	8
43	1 Oct '09	30	No	1h 30'	425	224,590	4h 09' 33"	4' 38"	9
			Total	4h 56'	1,689	711,222	13h 10' 15"		

3.5.1 Swimming in presence of food

In the two experiments conducted in presence of natural particle assemblages, the food conditions differed in cell concentration (Table 3.20). The *C. furcatus* swimming behaviour was mostly represented by the pattern reported in Fig. 3.36. Similar looping pattern showed the tendency of the copepod to move on planes with relatively costant ($\sim$ 45 deg) inclination (Fig. 3.40, B). The inclination of this plane seems to appear in the speed plot (Fig. 3.39, C), where the values between successive turns (the sharp decelerations), alternate between lower and higher speeds, indicating movement upward and downward, respectively. This pattern was repeated intensively in localised clusters (Fig. 3.40).

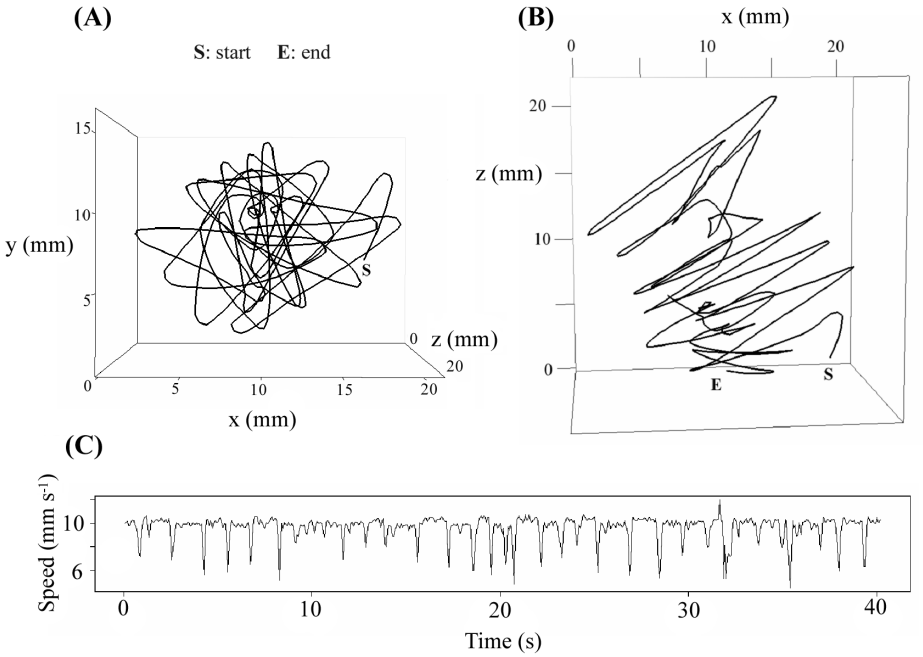

Figure 3.39: Example of *Clausocalanus furcatus* trajectory observed in presence of food (Exp. #32, 40 s). Top view (A), lateral view (B), speed diagram (C).

A swimming path was very similar to the previous one showed. However, a difference in the radius of curvature of turning angles. The trajectory were composed of figures that can be figured out as flower lobes (Fig. 3.40). This progression pattern, made by a series of lobes on a plane, is to explore a cir-

cular area. The wider turning angles might be explained by the fact that the individuals, that performed such pattern, were ovigerous females.

Some trajectories showed the transition between different patterns, e.g. when *C. furcatus* changed from alternating sinking and swimming to a faster looping pattern (Fig. 3.42).

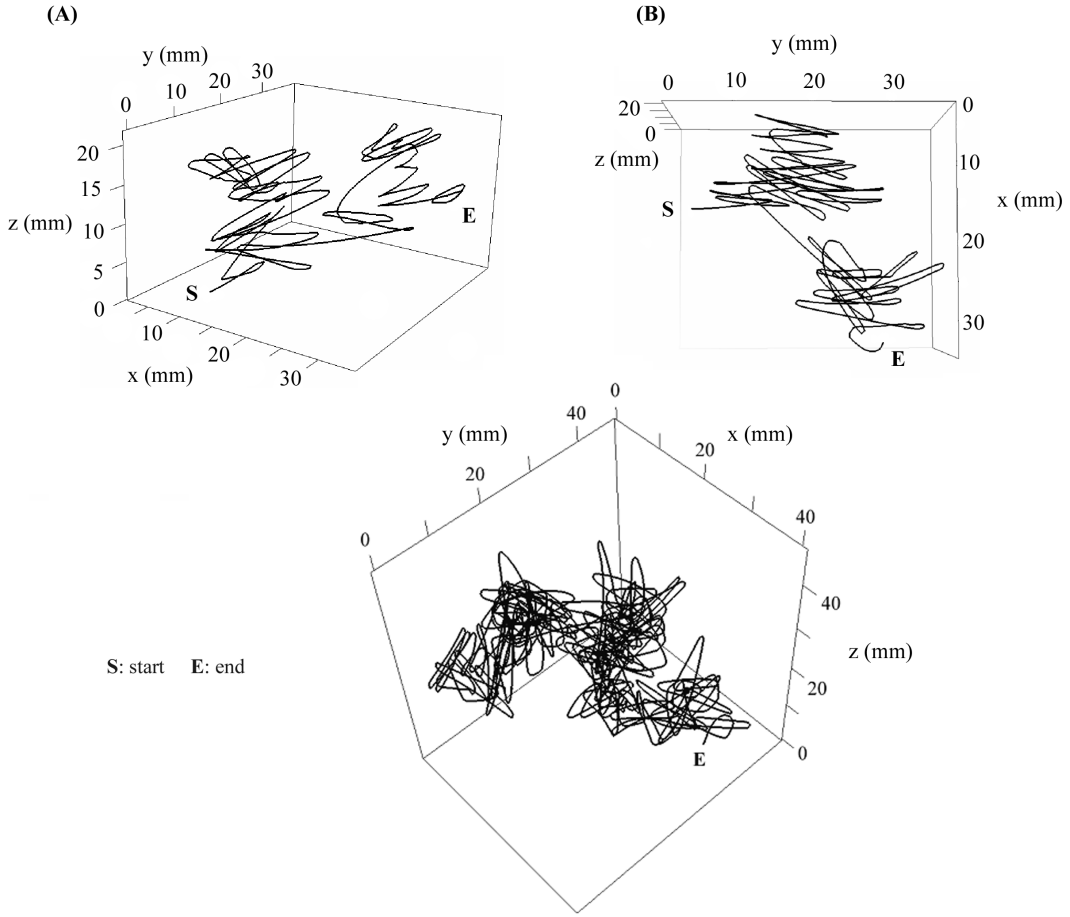

Figure 3.40: Examples of *Clausocalanus furcatus* trajectories recorded observed in presence of food. Lateral view (A) and top view (B), Exp. #42, 60 s. Lateral view (C), Exp. #42, 242 s.

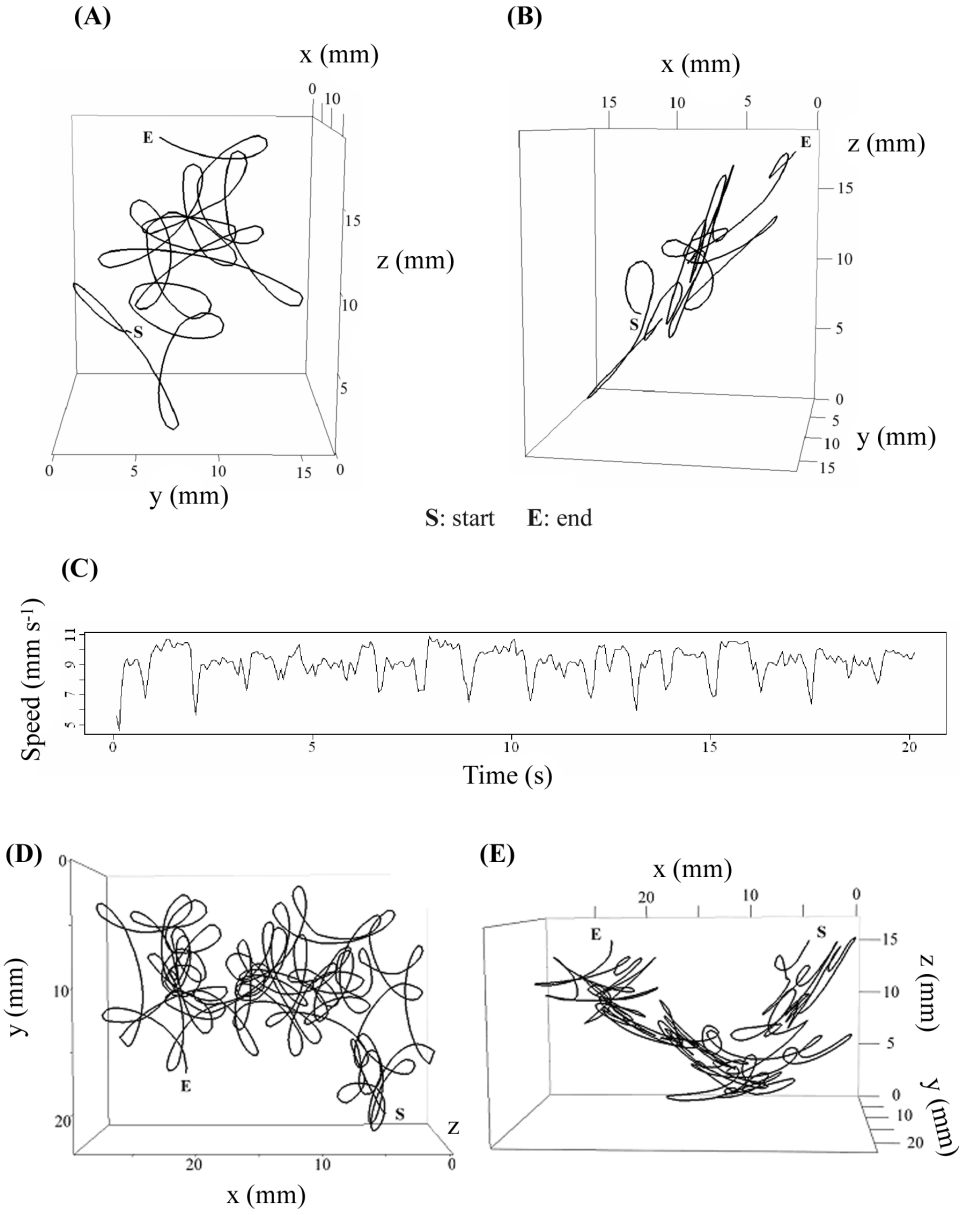

Figure 3.41: Examples of swimming trajectories performed by *Clausocalanus furcatus* ovigerous female in presence of food. Lateral views (A, B) and speed (C), Exp. #32, 20 s. Top view (D), lateral view (E), Exp. #32, 162 s.

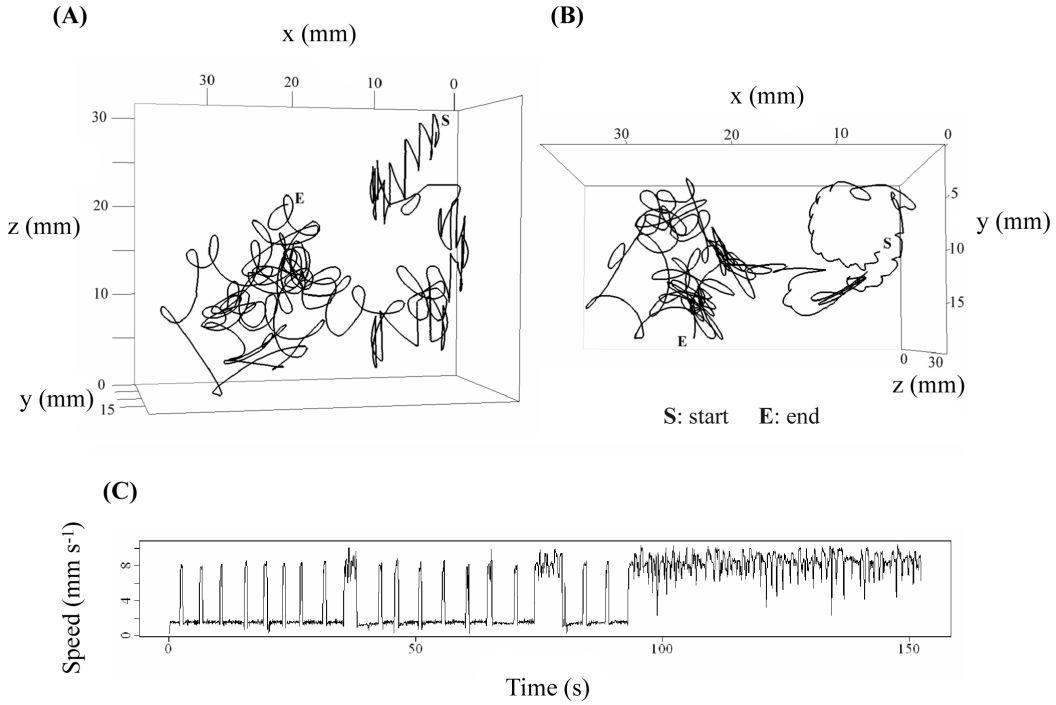

Figure 3.42: Example of swimming trajectory performed by *Clausocalanus furcatus* ovigerous female observed in presence of food (Exp. #32, 160 s). After about 90 s of swim and sink alternation, the copepod suddenly switch to faster pattern. Lateral view (A), top view (B) and speed (C).

3.5.2 Swimming in filtered sea water

The majority of *Clausocalanus furcatus* swimming patterns observed in filtered sea water were characterised by an alternation of swimming and sinking phases. Most patterns resemble to a circular-like path as shown in Fig. 3.37 or can be associated to the triangular-like path as shown in Fig. 3.38.

An interesting example of circular pattern is reported in Fig. 3.43 (A, B) where *C. furcatus* alternated sinking and swimming phases very regularly along a circle before moving to another vertical plane. The remarkable regularity of both swimming and sinking phases are shown also by the z axis coordinate along the curvilinear horizontal component S, ad 3D speed diagram in Fig. 3.43 (C, D).

In one of the most regular pattern observed, *C. furcatus* described an almost perfect circle, with a radius larger than the pattern previous showed, while progressing in space through an alternation of swimming and sinking (Fig. 3.44, A and B). The velocity plots of x and y coordinates (Fig. 3.44, C and D) show a sinusoidal signal in the horizontal velocity while the velocity along the z coordinate (Fig. 3.44, E) shows the periodicity due to the hop and sink behaviour.

Variants of circular-like up and sink patterns , with an upward helical shape, are shown in Fig. 3.45 and 3.46.

In the trajectory reported in Fig. 3.47 (A, B), the copepod moved along a series of quite regular circles of constant radius, at different heights. Regular circular arcs made while swimming upwards at constant speed (5–6 mm s^{-1}) were followed by passive sinking at regular intervals (Fig. 3.47, C).

A single individual could perform different patterns in the same path, as shown by Fig. 3.48.

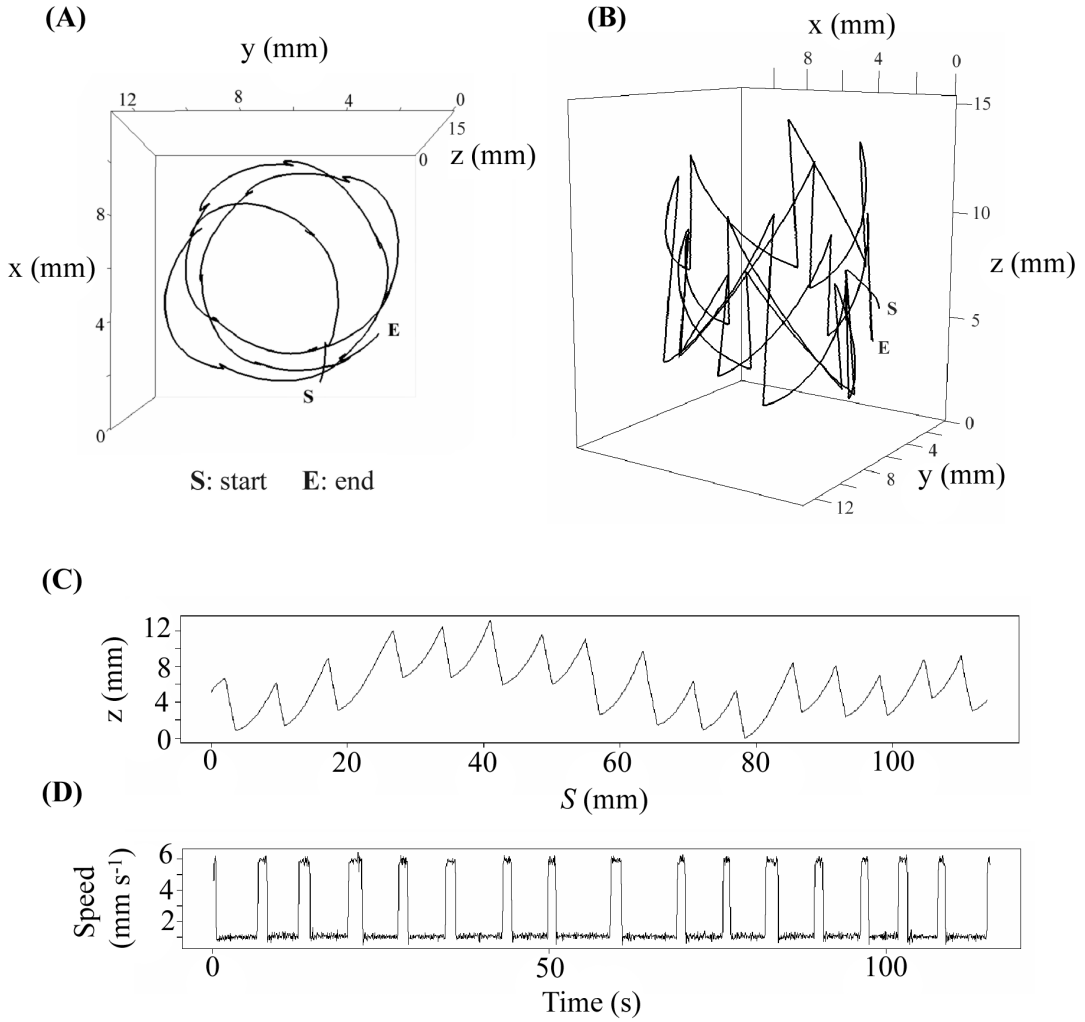

Figure 3.43: Example of *Clausocalanus furcatus* trajectory observed in filtered sea water (Exp. #33, 120 s). Top view (A), lateral view (B), vertical coordinate along the horizontal curvilinear coordinate (C), speed (D).

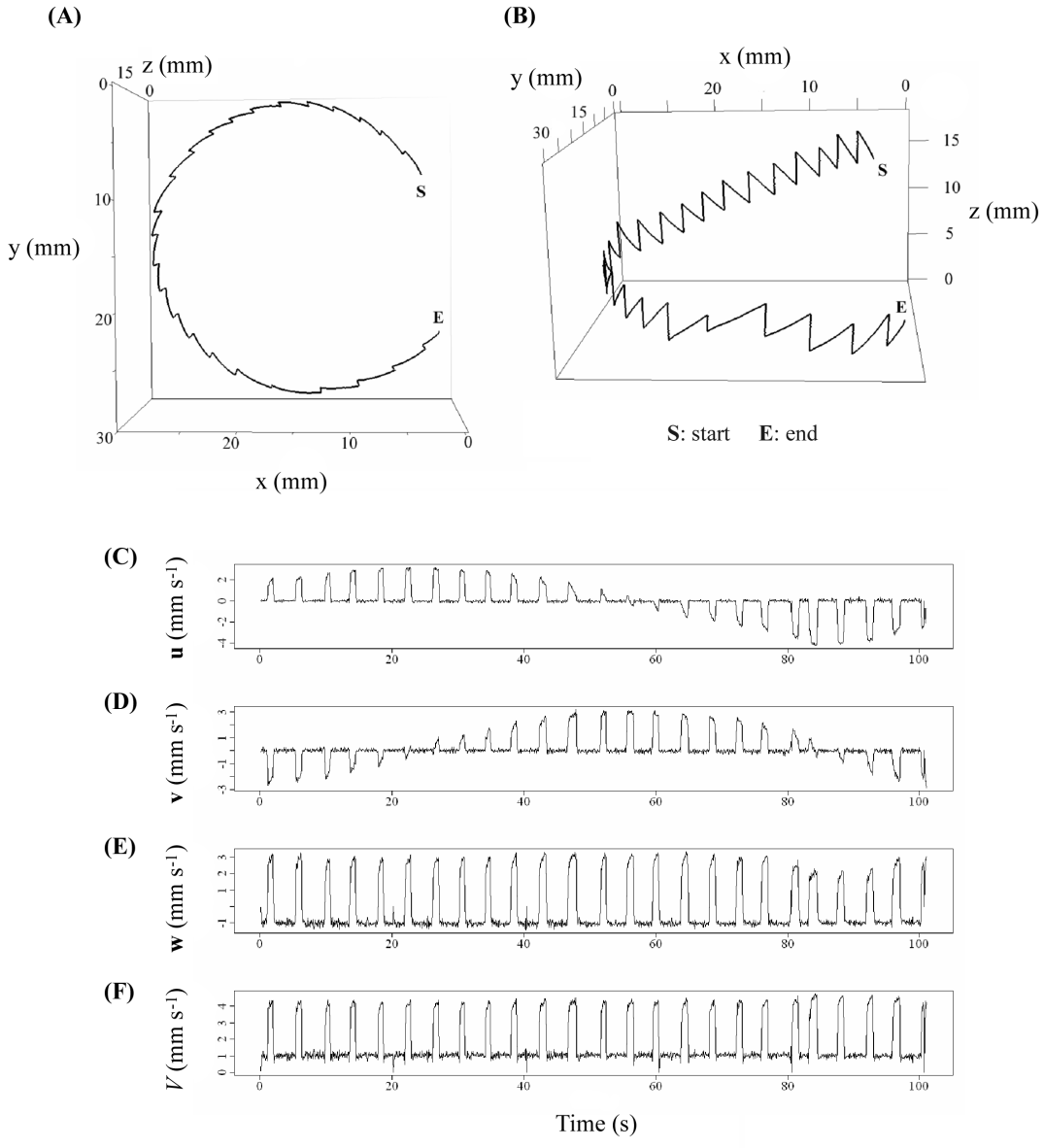

Figure 3.44: Example of *Clausocalanus furcatus* trajectory observed in filtered sea water (Exp. #33, 102 s). Top view (A), lateral view (B), velocity along the x axis (C), velocity along the y axis (D), velocity along the z axis (E), 3D speed (F).

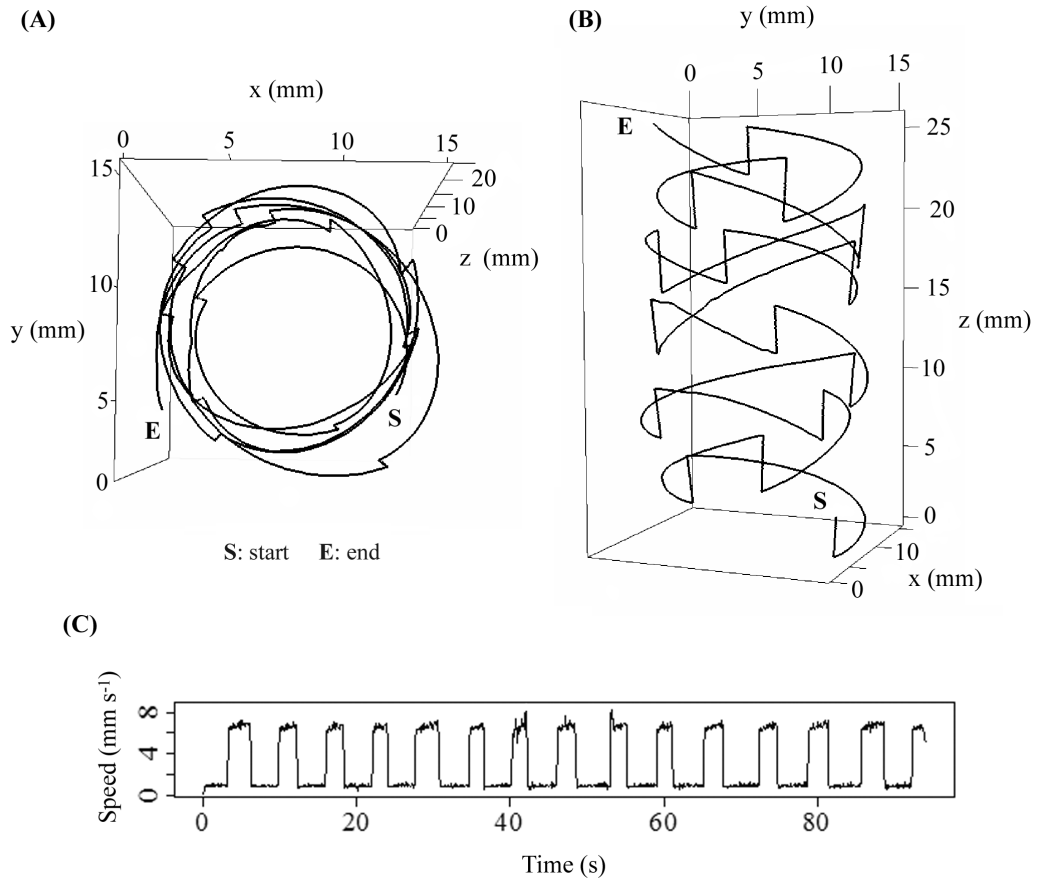

Figure 3.45: Example of *Clausocalanus furcatus* trajectory observed in filtered sea water (Exp. #43, 95 s). Top view (A),lateral view (B), speed (C).

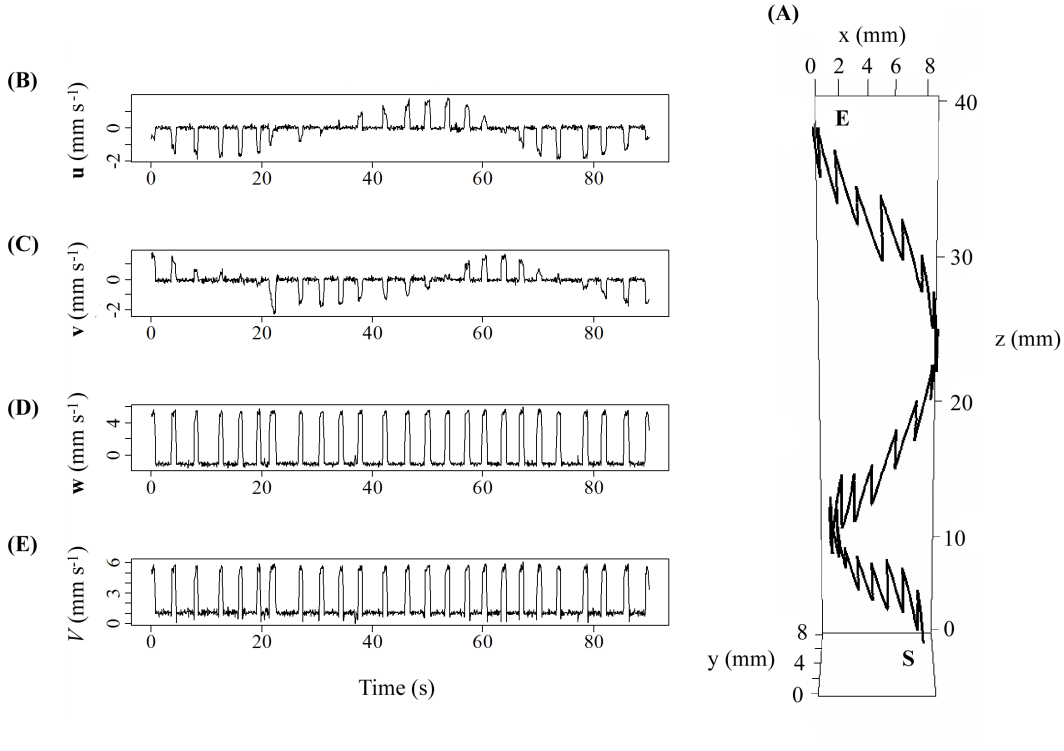

Figure 3.46: Example of *Clausocalanus furcatus* trajectory observed in filtered sea water (Exp. #43, 98 s). Lateral view (A), velocity along the x axis (B), velocity along the y axis (C), velocity along the z axis (D), 3D speed (E).

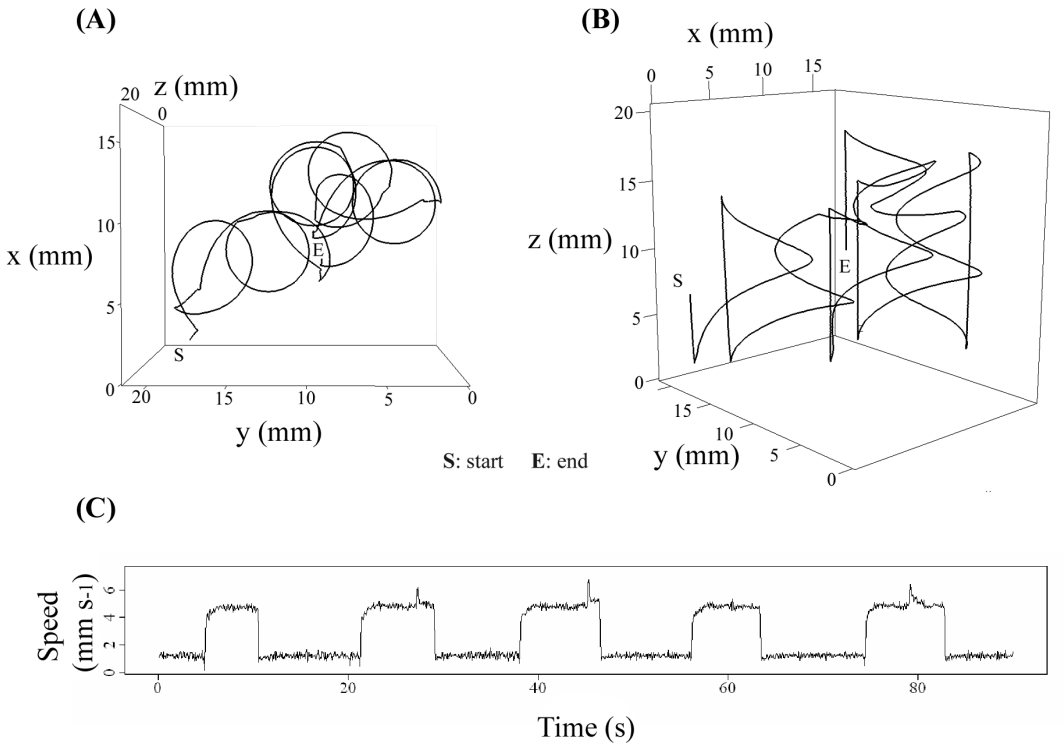

Figure 3.47: Example of *Clausocalanus furcatus* trajectory observed in filtered sea water (Exp. #33, 72 s). Top view (A),lateral view (B), speed (C).

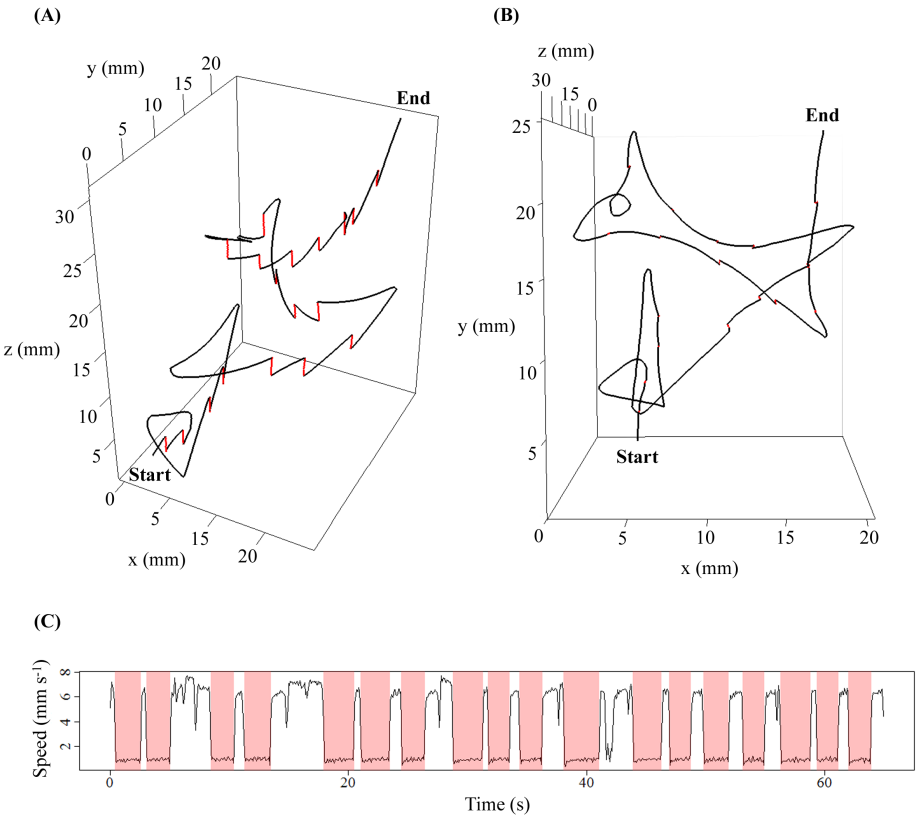

Figure 3.48: Example of *Clausocalanus furcatus* trajectory observed in filtered sea water (Exp. #43, 65 s). Top view (A),lateral view (B), speed (C). Swimming state in black and sinking state in red.

3.5.3 Synthesis

Clausocalanus furcatus females swimming was characterised by fast convoluted looping pattern in presence of food and a more regular swim and sink pattern in absence of food supply. The most striking aspect of the patterns is a substantial regularity, with the repetition of identical elements at almost constant time intervals, that contribute to the creation of a global pattern. Moreover, a single individual can perform more than one pattern during the swimming activity.

The swimming behaviour appeared to be strongly affected by different food conditions. The more the food particles and the more fast and convoluted the pattern. The time spent swimming was higher than sinking in presence of food and lower in filtered sea water (Table 3.20).

The distribution of instantaneous speed of *C. furcatus* showed a major peak at 1–2 mm s^{-1}, mainly dominated by sinking speeds in both food conditions (Fig. 3.49). A second peak was recorded at 9–10 mm s^{-1} or 10–12 mm s^{-1} in presence of food and at 5–6 mm s^{-1} 6–7 mm s^{-1} without food.

Both active and total mean speed of *C. furcatus* was significantly higher ($p < 0.01$) with food than without food (Table 3.21). In presence of food NGDR was lower and the horizontal component was higher than without food. The explored volume was always higher in presence of food (Table 3.21).

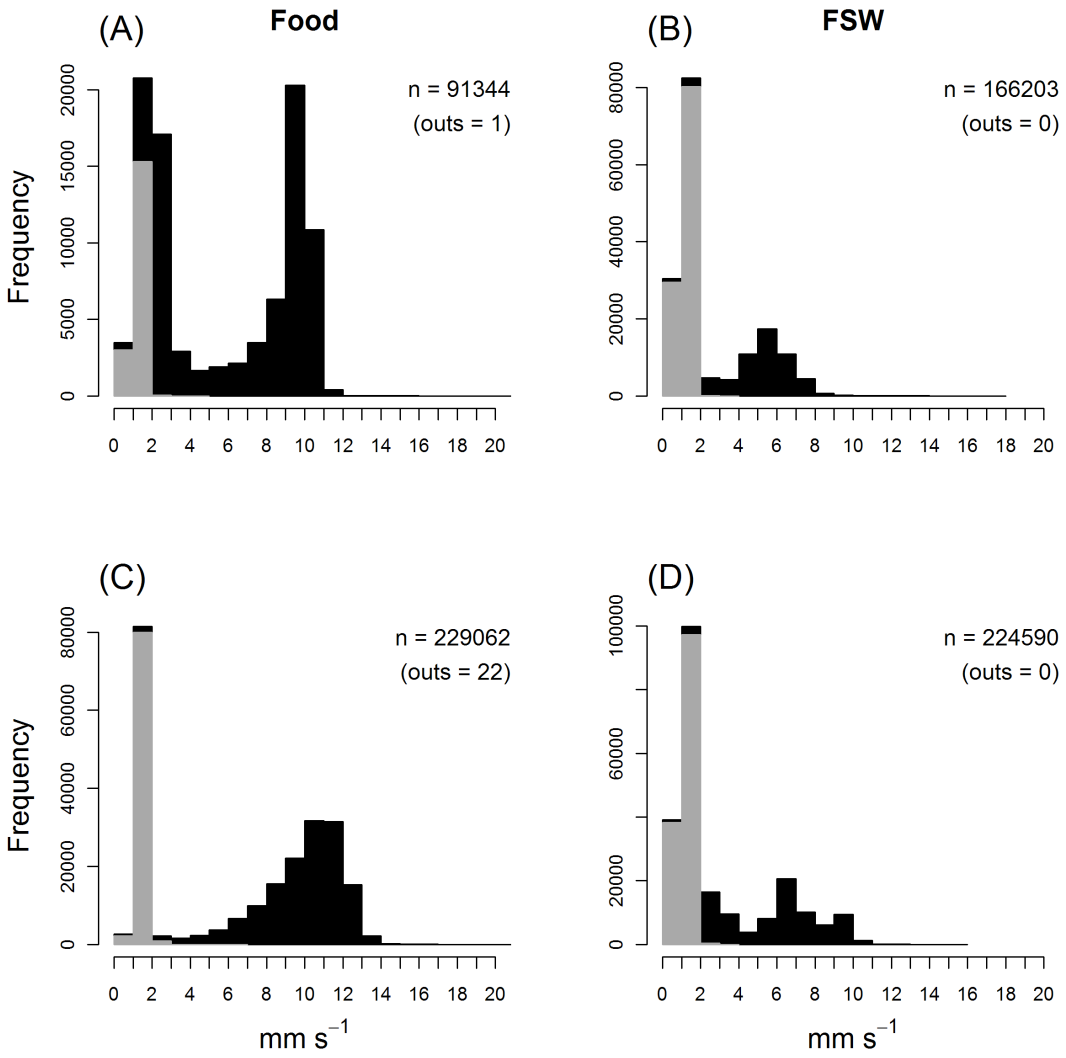

Figure 3.49: Distribution of instantaneous speed (mm s^{-1}) of *Clausocalanus furcatus* females during swimming (black) and sinking (grey) in presence (left panel) and absence (right panel) of food. Number of points (n) and corresponding values $>$ 20 mm s^{-1} not reported (outs). (A) Exp. #32; (B) Exp. #33; (C) Exp. #42; (D) Exp. #43.

Table 3.20: *Clausocalanus furcatus* experimental conditions and swimming activities. Food is reported as cells concentration (cells L^{-1}) and phytoplankton quality (FSW = filtered sea water without particles). Activity is reported as time allocated (%) in swimming or sinking state and respective mean duration (s).

		Food condition			**Activity**			
		Microzooplankton	**Phytoplankton**		**Occurrence (%)**		**Duration ± SD (s)**	
Exp.	**ind. L^{-1}**	**(cells L^{-1})**	**(cells L^{-1})**	**Quality**	**Swimming**	**Sinking**	**Swimming**	**Sinking**
32	37	2.8×10^3	5.0×10^5	∼ 78% phyto-flagellates $< 5\,\mu$m ∼ 3% cells $> 10\,\mu$m	79.9	20.1	1.9 ± 4.0	2.1 ± 1.3
33	35	—	—	FSW	34.0	66.0	2.0 ± 1.9	4.2 ± 2.8
42	30	3.3×10^3	5.0×10^6	∼ 57% phyto-flagellates $< 5\,\mu$m ∼ 15% cells $> 10\,\mu$m	63.8	36.2	2.2 ± 3.1	3.4 ± 1.5
43	30	—	—	FSW	39.5	60.5	1.2 ± 2.4	3.5 ± 1.4

* Not colonial ($\sim 5 \times 10\ \mu$m).

Table 3.21: *Clausocalanus furcatus* swimming speed (mean ± SD) computed averaging all instantaneous speed values in all trajectories (Total) or excluding sinking events (Active). Net to Gross Displacement Ratio (NGDR ± SD) was estimated as mean value for each individual track at the smallest resolution (1/15 s). Horizontal Component (± SD) was computed as mean value for each individual track. Explored Volume (EV ± SD).

			Speed ± SD (mm s^{-1})		**NGDR**	**Horizontal Component**	**Explored Volume**
Exp.	**ind. L^{-1}**	**Food**	**Total**	**Active**	**(adim.)**	**(adim.)**	**(L d^{-1})**
32	37	Yes	5.3 ± 3.3	6.4 ± 3.0	0.41 ± 0.23	0.67 ± 0.26	2.4 ± 1.6
33	35	No	2.5 ± 1.1	5.0 ± 1.3	0.50 ± 0.21	0.39 ± 0.17	0.9 ± 0.6
42	30	Yes	7.4 ± 3.4	9.3 ± 1.9	0.29 ± 0.17	0.61 ± 0.27	3.4 ± 1.8
43	30	No	3.0 ± 1.9	5.7 ± 1.8	0.41 ± 0.21	0.45 ± 0.27	1.2 ± 1.0

3.6 Species comparison

Swimming behaviour was significant different in the five copepod species under study. The swimming paths for both genders had the general tendency to evolve in successive loops but with completely different spatial and temporal scales. *Centropages typicus* moved in loops of similar diameter both in the horizontal and vertical planes, with a slight predominance for the vertical displacement. *Temora stylifera* moved along wider loops in a clockwise direction (from top view) and exclusively in the horizontal plane. *Paracalanus parvus* trajectories were more variable because the loops varied in size and did not show a preferential plane. *Clausocalanus furcatus* showed the most convoluted looping paths with fast turns. Only *Acartia clausi* did not display loops but slow swimming or hovering, frequently interrupted by fast jumps, mainly in upward direction. Jumping was the characteristic mode of *A. clausi* behaviour because it was the main displacement component.

Swimming activity was compared in four of the five target copepod species, excluding *A. clausi* that moves in a jerkier mode. The comparison of male swimming behaviour could be attempted for four out of the five target species, *i.e.*, *Centropages typicus*, *Acartia clausi*, *Paracalanus parvus* and *Temora stylifera*. *Clausocalanus furcatus* males were not recorded because of their rare occurrence in our samples.

In filtered sea water, *i.e.*, absence of food particles, *T. stylifera* and *P. parvus* females spent most of the time swimming ($\sim$ 99% and 80%, respectively) while *C. typicus* and *C. furcatus* females reduced the swimming activity to $\sim$ 40% of the time (Fig. 3.50).

In presence of phytoplankton (10^6 cells L^{-1}) *T. stylifera* females did not change its behaviour ($\sim$ 99% swimming) while *P. parvus* females slightly increased its activity up to 85%. An increase of the swimming activity was observed for *C. typicus* (from 10 to 30%) and *C. furcatus* (from 20 to 30%) females in presence of food particles.

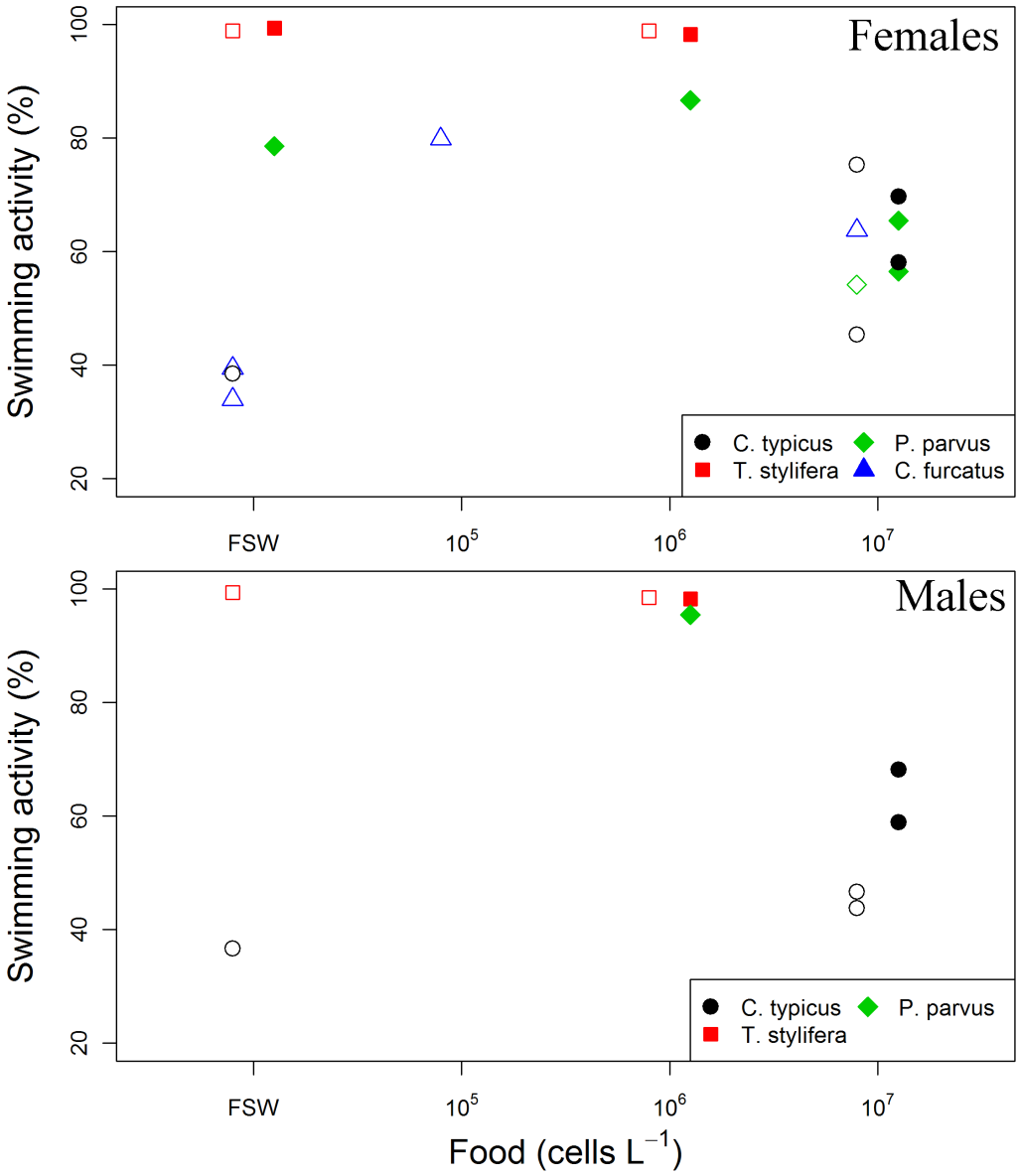

Figure 3.50: Time allocated (%) in swimming activity by females (upper panel) and males (lower panel) of target copepod species (*Centropages typicus*, black; *Temora stylifera*, red; *Paracalanus parvus*, green; *Clausocalanus furcatus*, blue). Low population density (< 50 Ind. L^{-1}) is represented by open symbols and high population density (> 50 Ind. L^{-1}) is represented by filled symbols). FSW = filtered sea water.

Differences in the concentrations of food particles in the medium influenced the swimming activity of *C. furcatus* and *P. parvus* females, which decreased the time allocated when passing from 10^5 to 10^6 cells per litre. Like for females, *T. stylifera* and *P. parvus* males spent $\sim$ 100% of the time swimming in presence of food particles and the behaviour of *T. stylifera* males did not change, also in filtered sea water.

At low population density (20 Ind. L^{-1}), *C. typicus* showed slightly higher swimming activity in presence of food particles ($\sim$ 75%, than in filtered water 38%). At high population density, in presence of food particles, the swimming activity of *C. typicus* increased ($\sim$ 10–20%). Differences in population density did not seem to influence the swimming activity of *P. parvus* and *T. stylifera* females.

The motion of *A. clausi* males did not present swimming, comparable with the other species, because it was characterized by frequent jumps.

Table 3.22 to 3.25 illustrate that the duration of swimming was equal in *T. stylifera* males and females (both conditions). It was also equal for *P. parvus* females over population density. The duration of swimming was increased at high food particle concentration and population density in *C. typicus*. *Paracalanus parvus* presented a threshold along with food particle concentrations.

The speed was observed to increase in both gender for *C. typicus* and *T. stylifera* and in *C. furcatus* females with the increase of food particle concentrations in the medium (Fig. 3.51). Differently, *P. parvus* showed a slight decrease of the swimming speed while *A. clausi* showed no behaviour changes. An increase of speed was also observed in *C. typicus* males and *T. stylifera* females with the increase of population density.

Like for females, in presence of food *T. stylifera* and *C. typicus* males showed a slight increase in swimming speed, whereas *A. clausi* males did not change behaviour (Fig. 3.51).

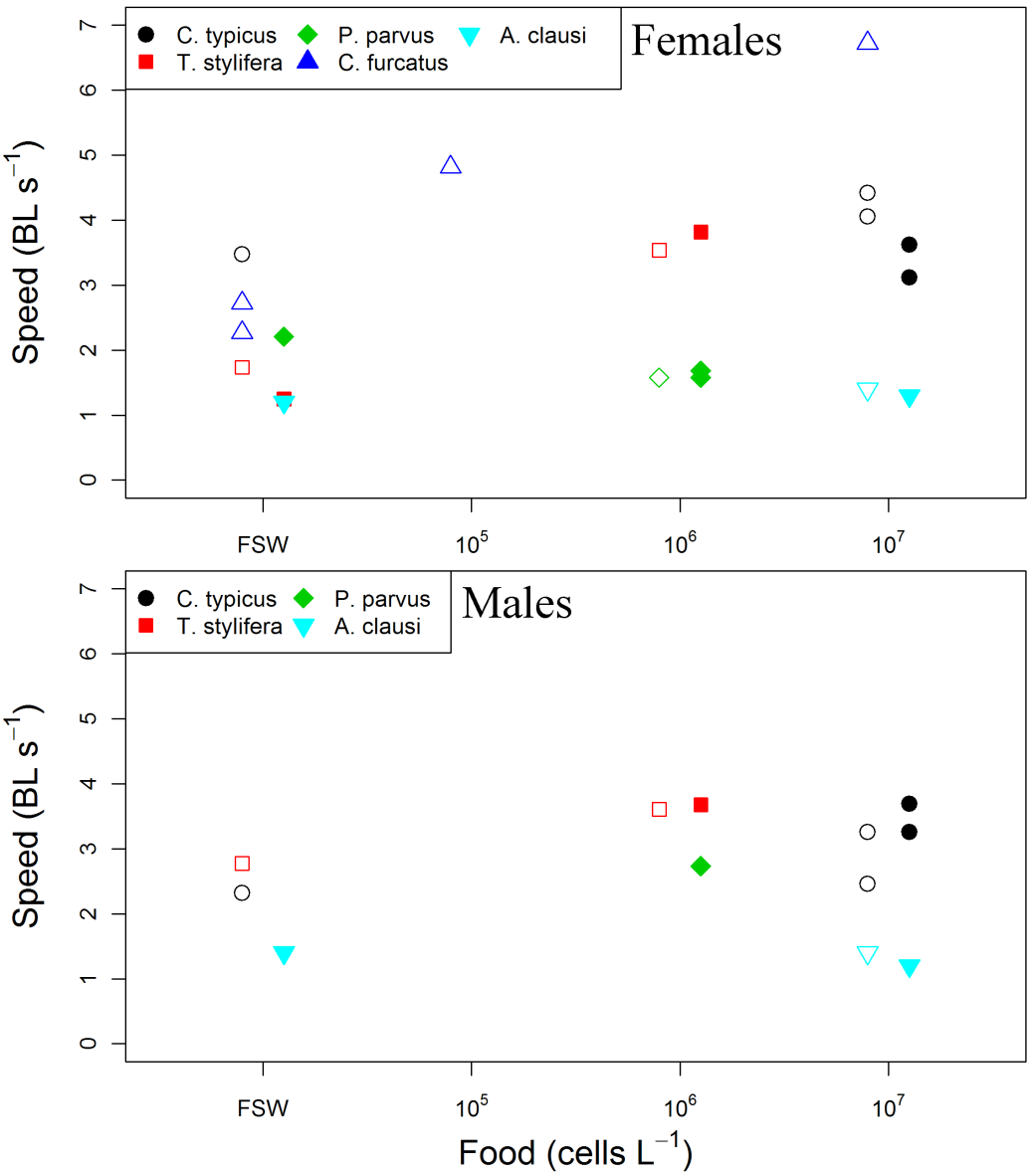

Figure 3.51: Swimming speed as body length per second (BL s^{-1}) of females (upper panel) and males (lower panel) of target copepod species (*Centropages typicus*, black; *Temora stylifera*, red; *Paracalanus parvus*, green; *Clausocalanus furcatus*, blue; *Acartia clausi*, light blue). Low population density (< 50 Ind. L^{-1}) is represented by open symbols and high population density (> 50 Ind. L^{-1}) is represented by filled symbols). FSW = filtered sea water.

Table 3.22 to 3.25 illustrate that no speed variations at high food particle concentration were monitored in *A. clausi* (both conditions and genders), *T. stylifera* males and *P. parvus* females under high population density. An increase of the speed was monitored in *T. stylifera* females (both conditions), *T. stylifera* males (food concentration), *C. typicus* and *C. furcatus* females (food concentration) and *C. typicus* males (both conditions). However, the speed was decreased in *C. typicus* females in population density and *P. parvus* females in food concentration conditions.

Temora stylifera, *P. parvus*, and *C. furcatus* females presented a decrease of NGDR along with the increase of food particles in the medium and population density (Fig. 3.52). On the contrary, the NGDR in *C. typicus* and *A. clausi* females did not change in different food conditions (Fig. 3.52).

With the increase of food particles in the filtered seawater, the NGDR slightly decreased in *T. stylifera* males while increase in *C. typicus* and did not change in *A. clausi* males (Fig. 3.52).

Table 3.22 to 3.25 illustrate that the NGDR was non-significantly different over high food concentration in *C. typicus* females (both conditions), *P. parvus* females (population density) and *A. clausi* males (food concentrations). The NGDR was increased significantly only in *C. typicus* males (both conditions) and *A. clausi* (both gender in population density). However, the NGDR was negatively impacted for *T. stylifera* both genders (both conditions) and *A. clausi*, *P. parvus* and *C. furcatus* females (food concentration).

The volume of water explored while swimming increased with the increase of food particle concentration in *C. typicus*, *C. furcatus* and *T. stylifera* females (Fig. 3.53). *Paracalanus parvus* and *A. clausi* females presented a slight but non significant variation of the explored volume in absence or presence of food particles.

The explored volume of *T. stylifera* and *C. typicus* males increased with the food particle concentration, while it decreased in *A. clausi* males (Fig. 3.53).

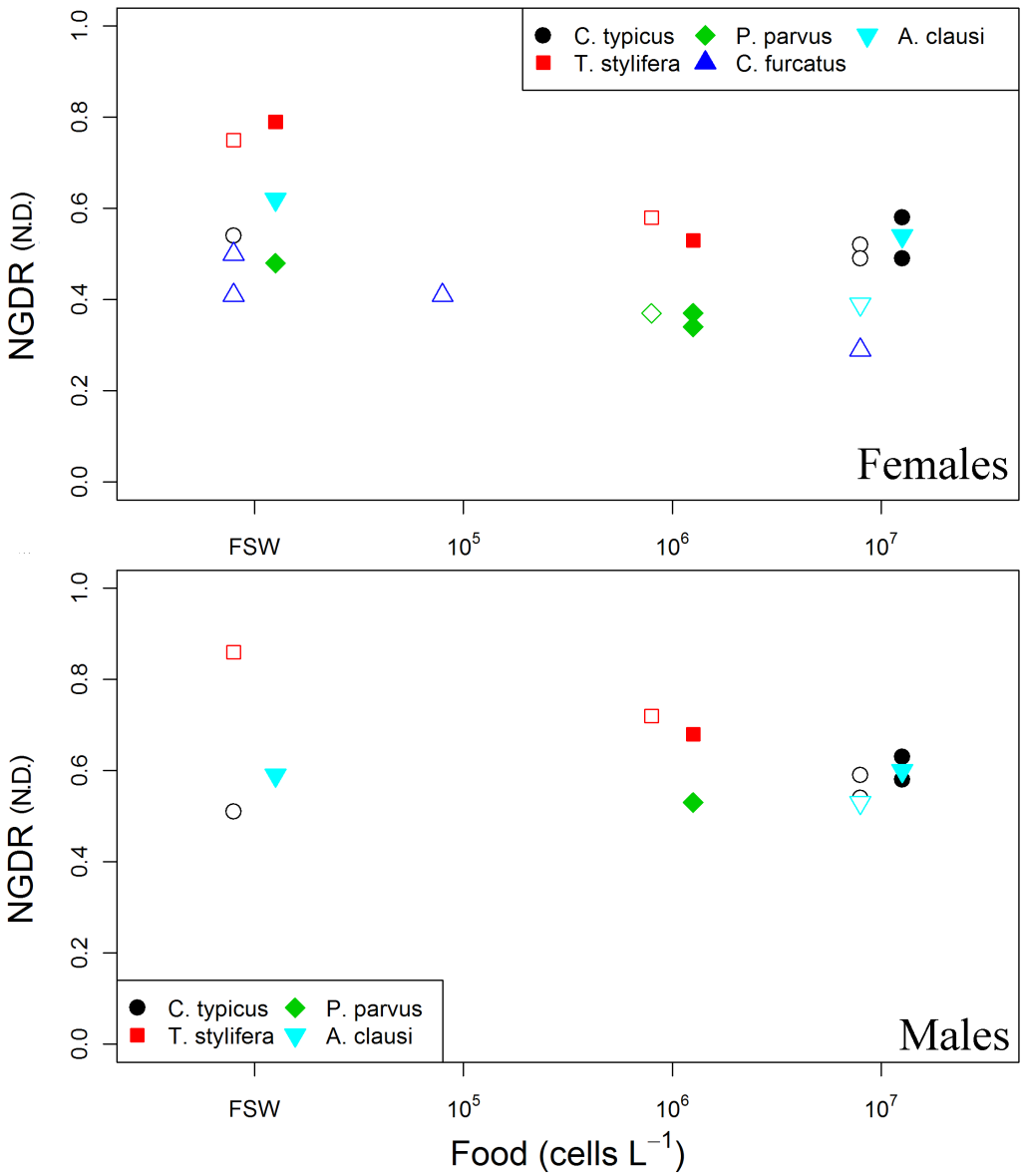

Figure 3.52: Net to Gross Displacement Ratio (N.D.) of females (upper panel) and males (lower panel) of target copepod species (*Centropages typicus*, black; *Temora stylifera*, red; *Paracalanus parvus*, green; *Clausocalanus furcatus*, blue; *Acartia clausi*, light blue). Low population density (< 50 Ind. L^{-1}) is represented by open symbols and high population density (> 50 Ind. L^{-1}) is represented by filled symbols). FSW = filtered sea water.

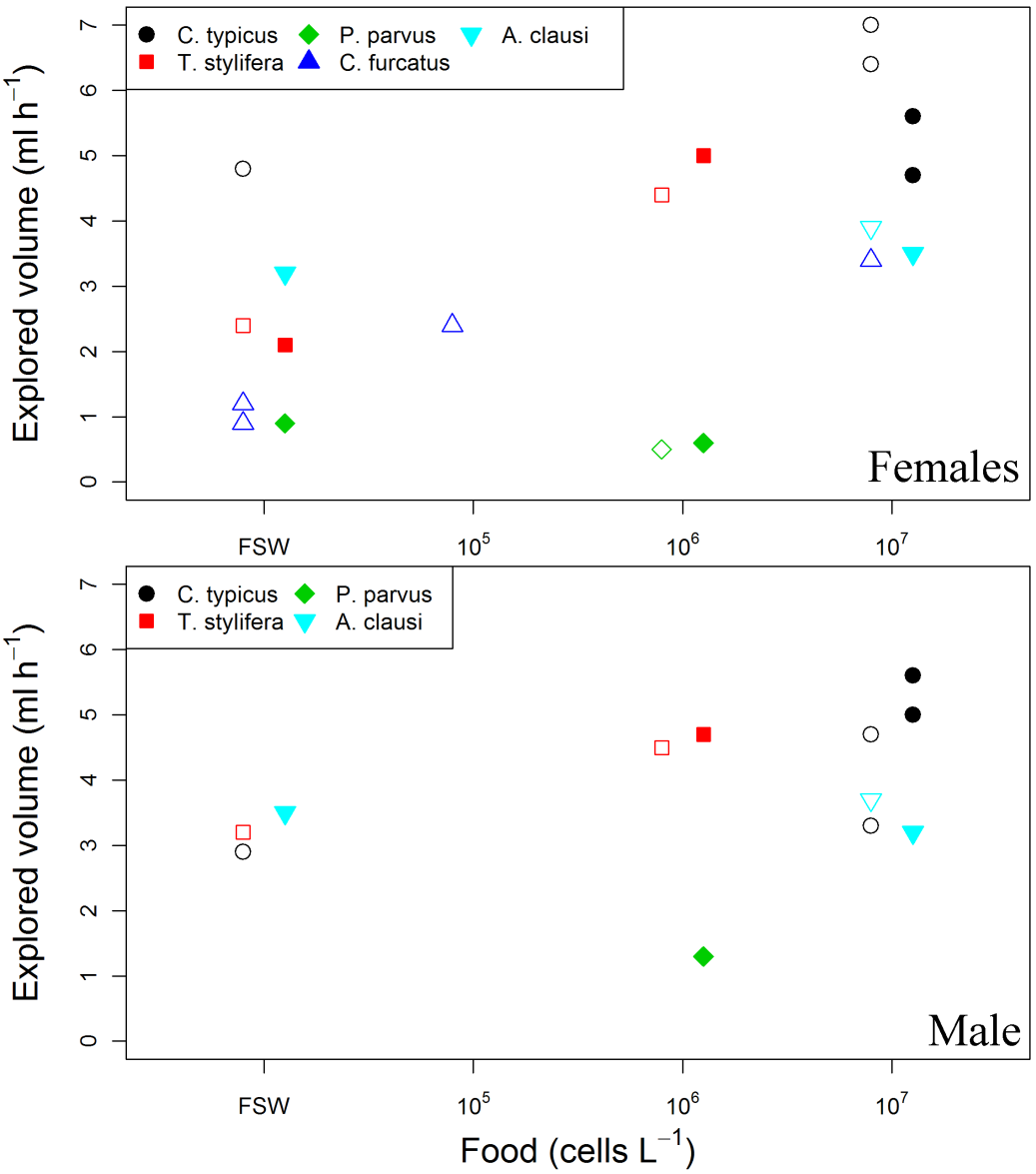

Figure 3.53: Explored Volume (ml h^{-1}) by females (upper panel) and males (lower panel) of target copepod species (*Centropages typicus*, black; *Temora stylifera*, red; *Paracalanus parvus*, green; *Clausocalanus furcatus*, blue; *Acartia clausi*, light blue). Low population density (< 50 Ind. L^{-1}) is represented by open symbols and high population density (> 50 Ind. L^{-1}) is represented by filled symbols). FSW = filtered sea water.

Table 3.22 to 3.25 illustrate that the explored volume was unchanged for *A. clausi* females (food concentration) and *P. parvus* females (population density). It was increasing for *T. stylifera* (both genders and conditions), *C. typicus* females (food concentration) and males (both conditions) and *C. furcatus* females (food concentration). It was decreasing for *A. clausi* males (both conditions), and in *A. clausi* and *C. typicus* females (population density).

In synthesis, the direct comparison of swimming behaviour showed:

1. The swimming pattern of females and males were similar under both conditions.

2. Almost all the copepod species were stimulated at high food particle concentrations and high population density.

3. The swimming duration was increased in *Centropages typicus*, *Clausocalanus furcatus* and *Paracalanus parvus* (food concentration) while was maintained constant in *Temora stylifera*.

4. The speed activity was increased in *Centropages typicus* (food concentration), *Temora stylifera* and *Clausocalanus furcatus*, slightly decreased in *Paracalanus parvus* and maintained constant in *Acartia clausi*.

5. The NDGR was decreased in *Temora stylifera*, *Paracalanus parvus* and *Clausocalanus furcatus* while constant in *Centropages typicus* and *Acartia clausi*.

6. The explored volume while swimming was increased in *Centropages typicus*, *Temora stylifera* and *Clausocalanus furcatus*, but slightly decreased in *Paracalanus parvus* and *Acartia clausi*.

Table 3.22: Comparison of swimming duration, speed, Net to Gross Displacement Ratio (NGDR) and Explored Volume (EV) of females for the five target species along the food gradient (*i.e.*, from no food to higher food concentration). Increase (+), decrease (−) and increase followed by a decrease ($\bigwedge$) along the gradient.

Species	Swimming occurrence	Speed	NGDR	Explored volume
Centropages typicus	+	+	=	+
Acartia clausi	n.a.	=	−	=
Temora stylifera	=	+	−	+
Paracalanus parvus	$\bigwedge$	−	−	−
Clausocalanus furcatus	$\bigwedge$	+	−	+

Table 3.23: Comparison of swimming duration, speed, Net to Gross Displacement Ratio (NGDR) and Explored Volume (EV) of males for the five target species along the food gradient (*i.e.*, from no food to higher food concentration). Increase (+), decrease (−) and increase followed by a decrease ($\bigwedge$) along the gradient.

Species	Swimming occurrence	Speed	NGDR	Explored volume
Centropages typicus	+	+	+	+
Acartia clausi	n.a.	=	=	−
Temora stylifera	=	+	−	+
Paracalanus parvus	n.a.	n.a.	n.a.	n.a.
Clausocalanus furcatus	n.a.	n.a.	n.a.	n.a.

Table 3.24: Comparison of swimming duration, speed, Net to Gross Displacement Ratio (NGDR) and Explored Volume (EV) of females for the five target species along the population density gradient (*i.e.*, from low to higher Ind. L^{-1}). Increase (+), decrease (−) and increase followed by a decrease ($\bigwedge$) along the gradient.

Species	Swimming occurrence	Speed	NGDR	Explored volume
Centropages typicus	$\bigwedge$	−	=	−
Acartia clausi	n.a.	=	+	−
Temora stylifera	=	+	−	+
Paracalanus parvus	=	=	=	=
Clausocalanus furcatus	n.a.	n.a.	n.a.	n.a.

Table 3.25: Comparison of swimming duration, speed, Net to Gross Displacement Ratio (NGDR) and Explored Volume (EV) of males for the five target species along the population density gradient (*i.e.*, from low to higher Ind. L^{-1}). Increase (+), decrease (−) and increase followed by a decrease ($\bigwedge$) along the gradient.

Species	Swimming occurrence	Speed	NGDR	Explored volume
Centropages typicus	$\bigwedge$	+	+	+
Acartia clausi	n.a.	=	+	−
Temora stylifera	=	=	−	+
Paracalanus parvus	n.a.	n.a.	n.a.	n.a.
Clausocalanus furcatus	n.a.	n.a.	n.a.	n.a.

Chapter 4

Discussion

The present thesis focused on behavioural diversity in copepods by analysing five calanoid species that are very common and abundant in Mediterranean waters. They were recorded with a video equipment to assess their swimming performances in a three-dimensional (3D) space, in different trophic conditions. The discussion of the experimental results will focussed on the species and then on their comparison.

Copepod behaviour is triggered by the gain (feeding) and losses of energy (swimming, jumping, speed and so on), the environmental conditions (food supply, population density, hydrodynamic currents and so on) and the risk of predations (Alcaraz *et al.*, 2007).

The behaviour of Centropages typicus species has been recently reviewed by Alcaraz *et al.* (2007) who compared the duration behaviour of *C. typicus* with that of *C. hamatus* and *C. velificatus*. The review highlighted a high degree of plasticity and adaptive capacity in this genus.

Centropages typicus swimming behaviour may be affected by gender, food (quality and quantity), physical environmental parameters and conspecific density. These factors will be discussed in the following.

The behaviour of *C. typicus* does not differ among genders considering the absence and presence of food supply. However, drastically differ in presence of high conspecific population density. Tiselius and Jonsson (1990) monitored that *C. typicus* is a slow moving or stationary suspension feeder, as confirmed by this

thesis results. Males and females behave similarly under high food of particles concentration. However, with the increase of population density, the swimming pattern of the female changes, as demonstrated by a reduction of the speed and the volume explored.

Food quantity and quality both influence swimming behaviour of *C. typicus*. The results, presented in the thesis, showed that the swimming behaviour of *C. typicus* was increased in both gender in presence of high concentration of food particles. Those results are conformed to Caparroy *et al.* (1998) and Calbet *et al.* (1999). On the other hand, the food quality depends on the prey characteristics such as its body size or its motility. Tiselius and Jonsson (1990) showed that *C. typicus* feeds principally on non motile prey. Caparroy *et al.* (1998) demonstrate that *C. typicus* can also feed on motile preys when they become the principal food resource. Feeding on motile prey conducts to an increase of the swimming duration (Caparroy *et al.*, 1998). The results of the present thesis seem to contradict Caparroy *et al.* (1998). Changes in the composition of the natural phytoplankton diet from numerical predominance of flagellates (mainly phytoflagellates $< 5\mu$m) to diatoms (*e.g.*, *Skeletonema* species) lead to a small, but significant, extension of the swimming phase. Feeding on diatoms might require a wider screening of the environment for encountering and acquiring more cells to feed in and therefore, results in an extended period of swimming. However, flagellates species, although being motile cells, might be too small for efficient capture by *C. typicus*.

Cowles and Strickler (1983) further demonstrated different prey belonging to the same genus may affect differently the swimming duration of *C. typicus*. In fact, feeding on *Prorocentrum micans*, *C. typicus* swimming phase was increased, while feeding on *Gymnodinum nelsoni* the *C. typicus* swimming phase was decreased (Cowles and Strickler, 1983). In the present thesis, feeding on natural assemblages (phytoflagellates $< 5\mu$m), a significant increase of the swimming duration was recorded at high food concentration such as a decrease of the sinking phase. Cowles and Strickler (1983) interpret the sinking behaviour as a mechanism for scanning chemical and physical signals present in the surrounding environment.

Hydrodynamic conditions were not tested in the present thesis since the experiments were performed in undisturbed calm conditions. Caparroy *et al.* (1998)

showed that an increase of the turbulence in the environment lead to a facilitated cruising behaviour and higher clearance rate.

The population density affects swimming behaviour of *C. typicus* of the female gender since they showed a significant reduction in their speed, the jump frequency and the volume explored with increase of the conspecific individuals in the experimental volume. On the contrary, males maintained the same parameters constant. Probably females strategy is to avoid to encountering other females and not competing for mating, while males continue searching for female cues. Interesting, along with population density gradient, the only variation observed in those patterns was at the intermediate population density of 50 Ind. L^1. At this density the duration of swimming was stimulated in females and the sink duration, the volume explored and the speed intensity in males. This result indicates the presence of a population density threshold that triggers female swimming behaviour. The existence of this threshold has not been investigated in the thesis but should be taken into account for future experiments.

A possible explanation is to link the threshold to the mate-finding behaviour. Apart from feeding, *C. typicus* search for mates. Males and females possess different mate-finding behaviour: while the females produce pheromonal trails (Bagoien and Kiørboe, 2005a), the males shift their swimming pattern to a zigzag mode and a restricted explored volume to accurately screen the path (Bagoien and Kiørboe, 2005a), detect, track, pursue the trail and catch the females. However, females and males are able to produce trails, which in some species do not chemically differ among genders (Doall *et al.*, 1998; Goetze, 2008). The increase of copepod abundance in the medium may stimulate both genders as the increase in chemical odours. The hypothesis is that the female possess a lower threshold and therefore are inhibited faster than males.

Acartia clausi presents motion behaviour very different from that of the four target calanoids. It is characterised by hovering, long period of sinking and short but fast and frequent jumps, as also reported by Tiselius and Jonsson (1990). The species creates a local feeding current during the sinking and the hovering phase of its behaviour (Leising and Franks, 2002).

The behaviour among both females and males does not differ in presence or absence of food supply. The time spent in sinking, hovering and jumping are con-

stant over the two conditions, as expected by previous study (Leising and Franks, 2002). The results of the present thesis showed a higher time allocated to sink ($\sim$ 72–77%) than hover ($\sim$ 20–24%) and even than jump ($\sim$ 3%). Food supply does not stimulate the behaviour of *A. clausi*. However, females presented a far higher complexity in their behaviour than males under high food concentration. The restricted volume screen by female may be link to the foraging strategy Leising and Franks (2002).

The population density influences the behaviour of the two genders in presence of food. In females, the duration of sinking, hovering and jumping was constant at low and high conspecific concentration. However, sinking, hovering and pattern complexity (NGDR) were higher at high individuals concentration. It might be hypothesised that at high density, *A. clausi* spends more time feeding because its displacement is more restricted and complex. Males are always in activity, creating feeding current whatever the population density; as showed by a constant of the duration of jumping, the speed and the explored volume. The feeding strategy of *A. clausi* is mainly raptorial on ciliated but it can change in suspension feeding in presence of micro flagellates (Jonsson and Tiselius, 1990). Experiments conducted in the present thesis at 50 Ind. L^{-1} in a mixture of $\sim$ 46% phytoflagellates showed that *A. clausi* spent more time hovering and sinking, which is compatible with a suspension feeding behaviour as reported by Jonsson and Tiselius (1990).

Temora stylifera exhibit the same motion behaviour represented for about 99% of swimming, and rare and short jumps and sinking, over both genders. The swimming pattern is composed of consecutive clock-wise loops, with rare direction shifts and mainly developed in the horizontal plane. This pattern has been only recorded over this species in the thesis. Direct pattern comparison between *T. stylifera* and a close related species *T. longicornis* (recurrent species studied in literature) was not possible as the *T. longicornis* swimming pattern was not previously assessed.

However, studied on congeneric *T. longicornis* reported that males exhibits a higher velocity pattern than females (Doall *et al.*, 1998; Weissburg *et al.*, 1998). This strategy has been elaborated to pursue and reach the female along the trail leaving by her. A male is able to detect a trail at least 10 second old, to track it

over long distances and to distinguished between heterospecific species through the swimming behaviour (Doall *et al.*, 1998; Weissburg *et al.*, 1998).

Food concentration stimulates the speed reaction of *T. stylifera* in both females and males suggesting that swimming is closely related to feeding behaviour as suspension feeder, as reported for *T. longicornis* (Tiselius and Jonsson, 1990; Kiørboe, 2008b). Results also indicate that food stimulate the cruiser behaviour. The impact of food concentration on motion behaviour has also been reported on T. longicornis (van Duren and Videler, 1995), which moved at low speed at low food concentration, at higher speed at intermediate food concentration, and at low speed at very high concentration (up to 10^7 cells L^{-1}). The authors associated the behaviour of *T. longicornis* with the optimal foraging theory, *i.e.*, speed increases with food until a threshold of food concentrations, over which increasing speed does not allow to acquire more food.

van Duren and Videler (1995) also showed that the velocity of males was always higher than the females, whatever the food conditions tested, and associated this result to the seeking strategy. On the contrary, in *T. stylifera*, observed in the present study, showed no significant differences between males and females in the speed over the gradient of food concentration. The theory has to be considered and is probably related to the different mating strategies among and between species.

Goetze and Kiørboe (2008) indicate that male of the same species can follow the male trail. Morevover, males can not often distinguish between females/males trails before chemo and hydro-mechanical tactical contact (Doall *et al.*, 1998; Goetze and Kiørboe, 2008). So, an increase of the number of trails in the medium may acts as a stimulus for seeking mates in the mono-gender batches. However, *T. stylifera* females and males did not seem to react to the population density, indicating that, contrary to *C. typicus*, the population density does not act as a mate-finding stimulus in mono-gender batches. However, the stimulation may occur when the two genders are both present in the same batch, indicating that mate-finding stimulus is gender and density-specific. When females detect males by chemo-sensory they indicate their presence by jumps van Duren and Videler (1996).

4. DISCUSSION

Very few studies have been focused on *Paracalanus parvus*. So far, Paffenhöfer (1984) linked the copepod sensitivity in different developmental stages to algal chemistry. *Paracalanus parvus* exhibit a long swimming patter interrupted by jumps. The swimming phases recorded in the present study are divided in two categories: the slow and the fast regimes associated with the swimming in the loop patterns. In general, *P. parvus* is considered as slow moving or suspension feeder (Tiselius and Jonsson, 1990). The present results showed that, in presence of small phytoflagellates, the swimming phase and the jumps in females are increased to the reduction of sinking phase. Males, that did not present sinking phases, showed a less complex swimming pattern and explore higher volume of water. The explored volume of males are ca. twice the female one, because males are always active while females presented sinking phases. It might be that the males do not sink in order to smell the trail of females.

The swimming behaviour of *Clausocalanus furcatus* is composed by a series of small convoluted loops, interrupted by jumps and occasional by sink, as identified by Mazzocchi and Paffenhöfer (1999), through two-dimensional (2D) analysis. The strategy described is to explore rapidly small volumes of water. *C. furcatus* predatory horizon is confined to a small frontal region of the anterior end of the copepod (Uttieri *et al.*, 2008).

The present study is the first that analysed the behaviour of *C. furcatus* in 3D space. It confirmed the patterns found by Mazzocchi and Paffenhöfer (1999) but also showed that, in absence of food particles, the sinking can be a major component of *C. furcatus* behaviour.

Clausocalanus furcatus swimming patterns were highly diverse and influenced by food conditions. Swimming patterns were very regular and characterised by the high speed and the regularity of alternation between swimming and sinking phases. The swimming patterns were classified in 3 categories: (1) straight and short segments of very similar length connected by sharp and fast turns; (2) regular alternation of swimming and sinking progressively along a regular circle; and (3) series of open triangles that span over a relatively large area, composed with a pattern of sharp turns and phases of sinking. In presence of food, *C. furcatus* females present the swimming pattern 1 with the tendency to swim faster, to perform more complex and convoluted patterns and explore a larger

volume of water. In absence of food, the swimming patterns were patterns 2 and 3. It can be hypothesised that these two patterns imply less energy expenditures and might be adapted for exploring a large water volume avoiding returning in previous explored area.

In synthesis, three swimming behaviours observed in the five species of copepod analysed in the present thesis may be classified according to Tiselius and Jonsson (1990): (1) slow moving or stationary suspension feeder; (2) fast swimming interrupted by sink periods; and (3) motionless interrupted by jumps. *Temora stylifera* and *Paracalanus parvus* belong to the first behavioural category. The two species have in common the major activity of swimming compared to sinking and jumping, which were very rare. *Temora stylifera* exhibited a slow cruising behaviour. The swimming behaviour over the two species, in both genders, was very similar. Individuals of both genders were stimulated by food supply, and responded with a low but significant increase of the swimming speed. *Temora stylifera* presented small or none variations between genders, while P. parvus exhibit a small change in the swimming complexity and the volume explored. Moreover, the males of *P. parvus* do not sink at all.

Centropages typicus and *Clausocalanus furcatus* belong to the second category. Both genders exhibited a high speed swimming interrupted by sinking periods. *Centropages typicus* and *C. furcatus* females were sensitive to food supply showing an increase of the speed and an extension of the swimming duration, threshold dependent for *C. furcatus*.

Acartia clausi is the only one belonging to the third behavioural category and is characterised by long phases of sinking and frequent jumps. It is also the only species not affected by both the gradient of food concentration and population density.

The species under study do not peak in the same seasonal period, with the exception of *C. typicus* and *A. clausi* which overlap in spring-early-summer. *Temora stylifera* and *C. furcatus* peak in autumn, while *P. parvus* is recorded in summer. The wide survival conditions to which the species are confronted over the year indicate a strong plasticity and capacity of adaptation.

The two spring species: *A. clausi* and *C. typicus* belong to two ecological diverse niches. *Acartia* species are typically found in turbid ecosystems (*e.g.*,

coastal waters) with diverse phytoplankton assemblages while *C. typicus* is a more ubiquitous species that extends its occurrence from coastal to open waters where the food concentration is variable and diversified (Calbet *et al.*, 1999). The fast moving and shift of swimming speed help *C. typicus* to adapt its swimming behaviour to the available preys. Phytoplankton communities in open waters of the Gulf of Naples are mainly represented by of motile prey, *i.e.*, dinoflagellates and other flagellates (Zingone *et al.*, 1995). On the other hand, *A. clausi* is motionless, and probably benefits of local turbulences to be transported passively and to increase food particles encounter as for *A. tonsa* (Saiz and Kiørboe, 1995; Caparroy and Carlotti, 1996). Moreover, *A. tonsa* needs to jump in order to track and catch preys (Kiørboe *et al.*, 2009) and find mate Bagoien and Kiørboe (2005b). The present results show also that *A. clausi* jumps also for relocating in the vertical plane.

The two species that co-occur in late-summer-autumn, *C. furcatus* and *T. stylifera*, also differ in the swimming behaviour. Food stimulates both species but they respond differently, *i.e.*, *C. furcatus* by lengthening the sinking phases and *T. stylifera* by small but significant increase of the swimming speed. As a suspension feeder *T. stylifera* prevalently catches non motile prey and is located in the upper 30 meters of the water column at LTER-MC (Di Capua and Mazzocchi, 2004). *Clausocalanus furcatus* swims fast and pursues motile prey. This is in agreement with its ubiquitous distribution (Frost and Fleminger, 1968). Albeit the two species presented different behaviour, they occur along the same period and are therefore subject to the same climatic and environmental conditions. Nevertheless, the two different behaviour strategies allow their co-occurrence. *Clausocalanus furcatus* is currently monitored over small interval over the autumn. *Temora stylifera* is impacted by the temperature (Di Capua and Mazzocchi, 2004) and show a wider occurrence at LTER-MC.

In the Gulf of Naples the thermocline is disrupted in autumn, period during which major mixing occur. This period can be in a way stimulated of *T. Stylifera* and *C. furcatus* because of their plasticity in changing swimming in function of food. *A. clausi* and *C. typicus* can be favourable of different phytoplankton assemblage (e.g., motile flagellates). More experiments are needed to evaluate the hypothesis.

In conclusion, the five examined species that occur all over the year in the coastal area of the Gulf of Naples presented different swimming strategies. Species behaviour can be stimulated dominantly by the food availability. The population density impacts slightly the species behaviour. On four of the five species, few to no differences were seen through genders comparison.

The comparison of species behaviour were only studied during the main species-occurrences. Further experiment can be defined to better screen the swimming behaviour over a peak (*e.g.*, at the beginning, top and fall), to infer the plasticity of each species, and to unrevealing the food preferences of each species. Those experiments, together with the results of the present thesis, may help to better understand the succession of population observed at sea.

References

Abramoff, M., Magalhaes, P., and Ram, S. (2004). Image processing with ImageJ. *Biophotonics International*, *11*, 36–43.

Alcaraz, M., Saiz, E., and Calbet, A. (2007). *Centropages* behaviour: Swimming and vertical migration. *Progress in Oceanography*, *72*, 121–136.

Avancini, M., Cicero, A., Di Girolamo, I., Innamorati, M., Magaletti, E., and Sertorio Zunini, T. (2006). *Guida al Riconoscimento del Plancton dei Mari Italiani. Volume II - Zooplancton Neritico*. Ministero dell'Ambiente, Roma.

Bagoien, E., and Kiørboe, T. (2005a). Blind dating - mate finding in planktonic copepods. I. Tracking the pheromone trail of *Centropages typicus*. *Marine Ecology-Progress Series*, *300*, 105–115.

Bagoien, E., and Kiørboe, T. (2005b). Blind dating - mate finding in planktonic copepods. III. Hydromechanical communication in *Acartia tonsa*. *Marine Ecology-Progress Series*, *300*, 129–133.

Barrientos, Y. (1980). *Ultrastructure of sensory units on the first antennae of calanoid copepods*. Master's thesis University of Ottawa, Canada.

Bianco, G. (2007). *Implementazione di un sistema per lo studio dello zooplancton nello spazio tridimensionale*. Master's thesis Universitá di Napoli Parthenope.

Boxshall, G., and Halsey, S. (2004). *An introduction to copepod diversity*. The Ray Society.

REFERENCES

Bundy, M. H., Gross, T. F., Coughlin, D. J., and Strickler, J. R. (1993). Quantifying copepod searching efficiency using swimming pattern and perceptive ability. *Bulletin of Marine Science*, *53*, 15–28.

Bundy, M. H., Gross, T. F., Vanderploeg, H. A., and Strickler, J. R. (1998). Perception of inert particles by calanoid copepods: behavioral observations and a numerical model. *Journal of Plankton Research*, *20*, 2129–2152.

Bundy, M. H., and Paffenhöfer, G. A. (1996). Analysis of flow fields associated with freely swimming calanoid copepods. *Marine Ecology-Progress Series*, *133*, 99–113.

Buskey, E. J. (1984). Swimming pattern as an indicator of the roles of copepod sensory systems in the recognition of food. *Marine Biology*, *79*, 165–175.

Buskey, E. J., and Hartline, D. K. (2003). High-speed video analysis of the escape responses of the copepod textitAcartia tonsa to shadows. *Biological Bulletin*, *204*, 28–37.

Buskey, E. J., Lenz, P. H., and Hartline, D. K. (2002). Escape behavior of planktonic copepods in response to hydrodynamic disturbances: high speed video analysis. *Marine Ecology-Progress Series*, *235*, 135–146.

Calbet, A., Saiz, E., Irigoien, X., Alcaraz, M., and Trepat, I. (1999). Food availability and diel feeding rhythms in the marine copepods *Acartia grani* and *Centropages typicus*. *Journal of Plankton Research*, *21*, 1009–1015.

Caparroy, P., and Carlotti, F. (1996). A model for *Acartia tonsa*: Effect of turbulence and consequences for the related physiological processes. *Journal of Plankton Research*, *18*, 2139–2177.

Caparroy, P., Perez, M. T., and Carlotti, F. (1998). Feeding behaviour of *Centropages typicus* in calm and turbulent conditions. *Marine Ecology-Progress Series*, *168*, 109–118.

Cowles, T., and Strickler, J. (1983). Characterization of feeding activity patterns in the planktonic copepod *Centropages typicus* Kroyer under various food conditions. *Limnology and Oceanography*, *28*, 106–115.

Di Capua, I., and Mazzocchi, M. (2004). Population structure of the copepods *Centropages typicus* and *Temora stylifera* in different environmental conditions. *ICES Journal of Marine Science*, *61*, 632.

Doall, M. H., Colin, S. P., Strickler, J. R., and Yen, J. (1998). Locating a mate in 3D: the case of *Temora longicornis*. *Philosophical Transactions of the Royal Society of London Series B-Biological Sciences*, *353*, 681–689.

Ducklow, H., Steinberg, D., and Buesseler, K. (2001). Upper ocean carbon export and the biological pump. *Oceanography*, *14*, 50–58.

van Duren, L., and Videler, J. (1995). Swimming behaviour of developmental stages of the calanoid copepod *Temora longicornis* at different food concentrations. *Marine Ecology-Progress Series*, *126*, 153–153.

van Duren, L., and Videler, J. (1996). The trade-off between feeding, mate seeking and predator avoidance in copepods: behavioural responses to chemical cues. *Journal of Plankton Research*, *18*, 805.

van Duren, L., and Videler, J. (2003). Escape from viscosity: the kinematics and hydrodynamics of copepod foraging and escape swimming. *Journal of Experimental Biology*, *206*, 269–279.

Friedman, M., and Strickler, J. (1975). Chemoreceptors and feeding in calanoid copepods (Arthropoda: Crustacea). *Proceedings of the National Academy of Sciences of the United States of America*, *72*, 4185.

Frost, B., and Fleminger, A. (1968). A Revision of the Genus *Clausocalanus* (Copepoda: Calanoida) with Remarks on Distributional Patterns in Diagnostic Characters, .

REFERENCES

Goetze, E. (2008). Heterospecific mating and partial prezygotic reproductive isolation in the planktonic marine copepods *Centropages typicus* and *Centropages hamatus*. *Limnology and Oceanography*, *53*, 433–445.

Goetze, E., and Kiørboe, T. (2008). Heterospecific mating and species recognition in the planktonic marine copepods *Temora stylifera* and *T. longicornis*. *Marine Ecology-Progress Series*, *370*, 185–198.

Huys, R., and Boxshall, G. (1991). *Copepod evolution* volume 159.

Hwang, J. S., and Strickler, R. (2001). Can copepods differentiate prey from predator hydromechanically? *Zoological Studies*, *40*, 1–6.

Ianora, A., and Buttino, I. (1990). Seasonal cycles in population abundances and egg production rates in the planktonic copepods *Centropages typicus* and *Acartia clausi*. *Journal of Plankton Research*, *12*, 473.

Jakobsen, H. H., Halvorsen, E., Hansen, B. W., and Visser, A. W. (2005). Effects of prey motility and concentration on feeding in *Acartia tonsa* and *Temora longicornis*: the importance of feeding modes. *Journal of Plankton Research*, *27*, 775–785.

Jiang, H. S., and Osborn, T. R. (2004). Hydrodynamics of copepods: A review. *Surveys in Geophysics*, *25*, 339–370.

Jiang, H. S., and Paffenhöfer, G. A. (2008). Hydrodynamic signal perception by the copepod oithona plumifera. *Marine Ecology-Progress Series*, *373*, 37–52.

Jonsson, P. R., and Tiselius, P. (1990). Feeding-behavior, prey detection and capture efficiency of the copepod acartia-tonsa feeding on planktonic ciliates. *Marine Ecology-Progress Series*, *60*, 35–44.

Kiørboe, T. (2008a). *A mechanistic approach to plankton ecology*. Princeton University Press.

Kiørboe, T. (2008b). Optimal swimming strategies in mate-searching pelagic copepods. *Oecologia*, *155*, 179–192.

Kiørboe, T. (2010). How zooplankton feed: mechanisms, traits and trade-offs. *Biological Reviews*, (pp. –).

Kiørboe, T., Andersen, A., Langlois, V. J., Jakobsen, H. H., and Bohr, T. (2009). Mechanisms and feasibility of prey capture in ambush-feeding zooplankton. *Proceedings of the National Academy of Sciences of the United States of America*, *106*, 12394–12399.

Kiørboe, T., and Bagoien, E. (2005). Motility patterns and mate encounter rates in planktonic copepods. *Limnology and Oceanography*, *50*, 1999–2007.

Kiørboe, T., Bagoien, E., and Thygesen, U. H. (2005). Blind dating - mate finding in planktonic copepods. II. The pheromone cloud of *Pseudocalanus elongatus*. *Marine Ecology-Progress Series*, *300*, 117–128.

Kiørboe, T., Saiz, E., and Visser, A. (1999). Hydrodynamic signal perception in the copepod *Acartia tonsa*. *Marine Ecology-Progress Series*, *179*, 97–111.

Kiørboe, T., and Visser, A. W. (1999). Predator and prey perception in copepods due to hydromechanical signals. *Marine Ecology-Progress Series*, *179*, 81–95.

Klopfenstein, D., and Vale, R. (2004). The lipid binding pleckstrin homology domain in UNC-104 kinesin is necessary for synaptic vesicle transport in Caenorhabditis elegans. *Molecular biology of the cell*, *15*, 3729.

Legier-Visser, M., Mitchell, J., Okubo, A., and Fuhrman, J. (1986). Mechanoreception in calanoid copepods. *Marine Biology*, *90*, 529–535.

Leising, A., and Franks, P. (2002). Does *Acartia clausi* (Copepoda: Calanoida) use an area-restricted search foraging strategy to find food? *Hydrobiologia*, *480*, 193–207.

Longhurst, A., and Glen Harrison, W. (1989). The biological pump: profiles of plankton production and consumption in the upper ocean. *Progress in Oceanography*, *22*, 47–123.

REFERENCES

Mauchline, J., Blaxter, J. H. S., Southward, A. J., and Tyler, P. A. (1998). *Advances in marine biology - The biology of calanoid copepods - Introduction* volume 33 of *Advances in Marine Biology*.

Mazzocchi, M., and Ribera d'Alcalà, M. (1995). Recurrent patterns in zooplankton structure and succession in a variable coastal environment. *ICES Journal of Marine Science*, *52*, 679.

Mazzocchi, M. G., and Paffenhöfer, G. A. (1999). Swimming and feeding behaviour of the planktonic copepod clausocalanus furcatus. *Journal of Plankton Research*, *21*, 1501–1518.

Michalec, F., Souissi, S., Dur, G., Mahjoub, M., Schmitt, F., and Hwang, J. (2010). Differences in behavioral responses of *Eurytemora affinis* (Copepoda, Calanoida) reproductive stages to salinity variations. *Journal of Plankton Research*, *32*, 805.

Paffenhöfer, G. A. (1984). Food ingestion by the marine planktonic copepod paracalanus in relation to abundance and size distribution of food. *Marine Biology*, *80*, 323–333.

Paffenhöfer, G. A., and Mazzocchi, M. G. (2002). On some aspects of the behaviour of *Oithona plumifera* (Copepoda : Cyclopoida). *Journal of Plankton Research*, *24*, 129–135.

Paffenhöfer, G. A., and Vansant, K. B. (1985). The feeding response of a marine planktonic copepod to quantity and quality of particles. *Marine Ecology-Progress Series*, *27*, 55–65.

Peralba, A., and Mazzocchi, M. G. (2004). Vertical and seasonal distribution of eight *Clausocalanus* species (Copepoda : Calanoida) in oligotrophic waters. *Ices Journal of Marine Science*, *61*, 645–653.

Peterson, W. (2001). Patterns in stage duration and development among marine and freshwater calanoid and cyclopoid copepods: a review of rules, physiological constraints, and evolutionary significance. *Hydrobiologia*, *453*, 91–105.

Poulet, S., and Gill, C. (1988). Spectral analyses of movements made by the cephalic appendages of copepods. *Marine ecology progress series. Oldendorf*, *43*, 259–267.

R Development Core Team (2010). *R: A Language and Environment for Statistical Computing*. R Foundation for Statistical Computing Vienna, Austria. ISBN 3-900051-07-0.

Ramcharan, C. W., and Sprules, W. G. (1989). Preliminary-results from an inexpensive motion analyzer for free-swimming zooplankton. *Limnology and Oceanography*, *34*, 457–462.

Razouls, C., de Bovée, F., Kouwenberg, J., and N., D. (2005-2010). Diversity and geographic distribution of marine planktonic copepods. *Available at http://copepodes.obs-banyuls.fr/en*, *[Accessed November 28, 2010]*.

Ribera d'Alcalá, M., Conversano, F., Corato, F., Licandro, P., Mangoni, O., Marino, D., Mazzocchi, M. G., Modigh, M., Montresor, M., Nardella, M., Saggiomo, V., Sarno, D., and Zingone, A. (2004). Seasonal patterns in plankton communities in a pluriannual time series at a coastal mediterranean site (Gulf of Naples): an attempt to discern recurrences and trends. *Scientia Marina*, *68*, 65–83.

Saiz, E., and Kiørboe, T. (1995). Predatory and suspension-feeding of the copepod *Acartia tonsa* in turbulent environments. *Marine Ecology-Progress Series*, *122*, 147–158.

Seuront, L. (2006). Effect of salinity on the swimming behaviour of the estuarine calanoid copepod *Eurytemora affinis*. *Journal of Plankton Research*, *28*, 805–813.

Strickler, J. (1982). Calanoid copepods, feeding currents, and the role of gravity. *Science*, *218*, 158–160.

Strickler, J. (1985). Feeding currents in calanoid copepods: two new hypotheses. In *Symposia of the Society for Experimental Biology* (p. 459). volume 39.

Strickler, J., and Hwang, J. (1999). Matched spatial filters in long working distance microscopy of phase objects. *Focus on multidimensional microscopy*, (pp. 217–239).

REFERENCES

Strickler, J. R. (1998). Observing free-swimming copepods mating. *Philosophical Transactions of the Royal Society of London Series B-Biological Sciences*, *353*, 671–680.

Strickler, J. R., and Balazsi, G. (2007). Planktonic copepods reacting selectively to hydrodynamic disturbances. *Philosophical Transactions of the Royal Society B-Biological Sciences*, *362*, 1947–1958.

Takahashi, K., and Tiselius, P. (2005). Ontogenetic change of foraging behaviour during copepodite development of *Acartia clausi*. *Marine Ecology-Progress Series*, *303*, 213–223.

Tiselius, P., and Jonsson, P. R. (1990). Foraging behavior of 6 calanoid copepods - observations and hydrodynamic analysis. *Marine Ecology-Progress Series*, *66*, 23–33.

Tiselius, P., and Jonsson, P. R. (1997). Effects of copepod foraging behavior on predation risk: An experimental study of the predatory copepod pareuchaeta norvegica feeding on acartia clausi and a-tonsa (copepoda). *Limnology and Oceanography*, *42*, 164–170.

Titelman, J. (2001). Swimming and escape behavior of copepod nauplii: implications for predator-prey interactions among copepods. *Marine Ecology-Progress Series*, *213*, 203–213.

Titelman, J., and Kiørboe, T. (2003a). Motility of copepod nauplii and implications for food encounter. *Marine Ecology-Progress Series*, *247*, 123–135.

Titelman, J., and Kiørboe, T. (2003b). Predator avoidance by nauplii. *Marine Ecology-Progress Series*, *247*, 137–149.

Uttieri, M., Paffenhöfer, G. A., and Mazzocchi, M. G. (2008). Prey capture in *Clausocalanus furcatus* (Copepoda : Calanoida). The role of swimming behaviour. *Marine Biology*, *153*, 925–935.

Viitasalo, M., Kiørboe, T., Flinkman, J., Pedersen, L. W., and Visser, A. W. (1998). Predation vulnerability of planktonic copepods: consequences of predator foraging strategies and prey sensory abilities. *Marine Ecology-Progress Series*, *175*, 129–142.

Waggett, R. J., and Buskey, E. J. (2007). Calanoid copepod escape behavior in response to a visual predator. *Marine Biology*, *150*, 599–607.

Weissburg, M. J., Doall, M. H., and Yen, J. (1998). Following the invisible trail: kinematic analysis of mate-tracking in the copepod *Temora longicornis*. *Philosophical Transactions of the Royal Society of London Series B-Biological Sciences*, *353*, 701–712.

Yen, J. (1988). Directionality and swimming speeds in predator-prey and male-female interactions of *Euchaeta rimana*, a subtropical marine copepod. *Bulletin of marine science*, *43*, 395–403.

Yen, J. (2000). Life in transition: Balancing inertial and viscous forces by planktonic copepods. *Biological Bulletin*, *198*, 213–224.

Yen, J., Rasberry, K. D., and Webster, D. R. (2008). Quantifying copepod kinematics in a laboratory turbulence apparatus. *Journal of Marine Systems*, *69*, 283–294.

Yen, J., Weissburg, M. J., and Doall, M. H. (1998). The fluid physics of signal perception by mate-tracking copepods. *Philosophical Transactions of the Royal Society of London Series B-Biological Sciences*, *353*, 787–804.

Young, S., and Getty, C. (1987). Visually guided feeding behaviour in the filter feeding cladoceran, *Daphaia magna*. *Animal Behaviour*, *35*, 541–548.

Zingone, A., Casotti, R., d'Alcalà, M., Scardi, M., and Marino, D. (1995). St Martin's Summer: the case of an autumn phytoplankton bloom in the Gulf of Naples (Mediterranean Sea). *Journal of Plankton Research*, *17*, 575.